NITROGEN CYCLING IN OXYGEN DEFICIENT ZONES: INSIGHTS FROM $\delta^{15}N$ AND $\delta^{18}O$ OF NITRITE AND NITRATE

By

Carolyn Buchwald

S.B., Massachusetts Institute of Technology, 2007
Submitted in partial fulfillment of the requirements for the degree of

Doctor of Philosophy
at the
MASSACHUSETTS INSTITUTE OF TECHNOLOGY
and the
WOODS HOLE OCEANOGRAPHIC INSTITUTION

February 2013

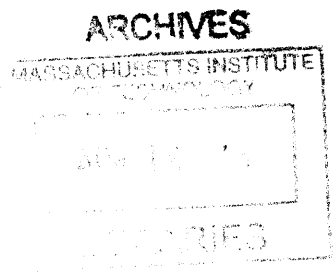

Signature of Author

Joint Program in Oceanography/Applied Ocean Science and Engineering
Massachusetts Institute of Technology
And Woods Hole Oceanographic Institution
September 10, 2012

Certified by

Karen Casciotti
Thesis Supervisor

Certified by

Mak Saito
Thesis Supervisor

Certified by

Bernhard Peucker-Ehrenbrink
Chair, Joint Committee for Chemical Oceanography
Woods Hole Oceanographic Institution

NITROGEN CYCLING IN OXYGEN DEFICIENT ZONES: INSIGHTS FROM $\delta^{15}N$ AND $\delta^{18}O$ OF NITRITE AND NITRATE

By
Carolyn Buchwald

Submitted to the MIT/WHOI Joint Program in Oceanography in partial fulfillment of the requirements for the degree of Doctor of Philosophy in the field of Chemical Oceanography

THESIS ABSTRACT

The stable isotopes, $\delta^{15}N$ and $\delta^{18}O$, of nitrite and nitrate can be powerful tools used to interpret nitrogen cycling in the ocean. They are particularly useful in regions of the ocean where there are multiple sources and sinks of nitrogenous nutrients, which concentration profiles alone cannot distinguish. Examples of such regions are "oxygen deficient zones" (ODZ). They are of particular interest because they are also important hot spots of fixed N loss and production of N_2O, a potent greenhouse gas.

In order to interpret these isotope profiles, the isotope systematics of each process involved must be known so that we can distinguish the isotopic signature of each process. One of the important processes to consider here is nitrification, the process by which ammonium is oxidized nitrite and then to nitrate. This thesis describes numerous experiments using both cultures of nitrifying organisms as well as natural seawater samples to determine the oxygen isotope systematics of nitrification. These experimental incubations show that the accumulation of nitrite has a large effect on the resulting $\delta^{18}O_{NO3}$. In experiments where nitrite does not accumulate, $\delta^{18}O_{NO3}$ produced from nitrification is between -1 to 1‰. These values will be applicable for the majority of the ocean, but the nitrite isotopic exchange will be important in the regions of the ocean where nitrite accumulates, such as the base of the euphotic zone and oxygen deficient zones.

$\delta^{18}O_{NO2}$ was developed as a unique tracer in this thesis because it undergoes abiotic equilibration with water $\delta^{18}O$ at a predictable rate based on pH, temperature and salinity. This rate, its dependencies, and how the $\delta^{18}O_{NO2}$ values can be used as not only biological source indicators but also indicators of age are described. This method was applied to samples from the primary nitrite maximum in the Arabian Sea, revealing that the dominant source and sinks of nitrite are ammonia oxidation and nitrite oxidation with an average age of 37 days.

Finally, using the isotope systematics of nitrification as well as the properties of nitrite oxygen isotope exchange described in this thesis, the final chapter interprets multi-isotope nitrate and nitrite profiles in the Costa Rica Upwelling Dome using a simple 1D model. The nitrite isotopes showed that there were multiple sources of nitrite in the primary nitrite maximum including (1) decoupling of ammonia oxidation and nitrite oxidation, (2) nitrate reduction during assimilation and leakage of nitrite by

phytoplankton. In the oxygen deficient zone and secondary nitrite maximum, there were equal contributions of nitrite removal from nitrite oxidation and nitrite reduction. This recycling of nitrite to nitrate through oxidation indicates that the percentage of reduced nitrate fully consumed to N_2 gas is actually smaller than previous estimates.

Overall, this thesis describes new nitrogen and oxygen isotopic tracers and uses them to elucidate the complicated nitrogen biogeochemistry in oxygen deficient zones.

Thesis supervisors:

Dr. Karen Casciotti
Title: Assistant Professor, Department of Environmental Earth System Science, Stanford University

Dr. Mak Saito
Title: Tenured Associate Scientist, Marine Chemistry and Geochemistry, WHOI

Acknowledgements

The work described in this thesis was funded by the National Science Foundation grants OCE 05-26277 and OCE 09-610998 to KLC, the MIT Presidential Fellowship, the WHOI Coastal Ocean Institute, the WHOI Academic Programs Office, and the MIT Houghton fund.

First and foremost, I would like to thank my advisor Karen Casciotti. During my Phd, she helped me every step of the way. She always had her door open and would answer any questions that I had. Later in my graduate career she transitioned to treating me like a colleague and this helped my gain a lot of confidence as a scientist, which will be important in the years to come.

Next, I want to thank my committee, Mak Saito, Rachel Stanley and Shuhei Ono. They were always there to help with an insightful comment and new perspective. Each of them has made a positive impact on this thesis. When my advisor moved across the country to Stanford, Mak took me into his lab group and made me feel like I still had a home at WHOI. Rachel has been an integral part of my fifth chapter of my thesis and I do not think I could have gotten this chapter done in the time without her.

Throughout my research I have had many helpful collaborators. Within the Casciotti lab, I have worked closely with Matthew McIlvin and have received so much advice and help throughout the years. He has helped me in lab, running samples and taking time points for experiments. I could not have done this thesis without him. I want to thank Alyson Santoro, whom I also set up experiments with and have gone to sea with twice. I could not have asked for a better ship labmate and roommate. Also I want to thank the past Casciotti graduate students: Erin Banning, Caitlin Frame and Dan Rogers. They were always there to give me advice, read manuscripts and watch practice talks when I needed. I want to thank the new Casciotti lab crew, Brian Peters and Matthew Forbes, for all their help while I was at Stanford. I want to also thank Freddy Valois and John Waterbury for providing bacteria for the experiments in the first two chapters of my thesis. I also want to thank all of the chief scientists that I have sailed with over the past 5 years; Doug Capone, Will Berelson, Angie Knapp, Michael Landry, Jim Moffett, Bess Ward and Al Devol. They have helped me be productive at sea and taught me the skills necessary to be a chief scientist in the future.

Lastly, I want to thank all my friends and family who have supported me during graduate school. The chemistry crew Erin Bertrand, Daniel Ohnemus, Stephanie Owens, Kimberly Popendorf, Dreux Chappell, Travis Meador, Eoghan Reeves, Abigail Noble and many more. I have enjoyed taking classes, going to conferences and talking science with all of you. Also, I want to thank all my friends in the joint program, especially Maya Yamato and Jeffery Kaeli, you have been great friends for the past 6 years. I'm so glad we met as summer student fellows in 2006.

And to my family. Thank you for everything. I want to acknowledge my Mom, Dad, Pop and Phylis and all of my siblings (Ben, Allison, Jackie, Greg, Peter, Danny, Alex and Missy). Each one of you has been so supportive and I have loved explaining my research to you over the years.

TABLE OF CONTENTS

Chapter 1

An introduction to the applications of the $\delta^{15}N$ and $\delta^{18}O$ of nitrate and nitrite as tracers of nitrogen cycling in the ocean

Nitrate can be a limiting nutrient in many regions of the ocean, where its supply controls the amount of primary production and subsequent export of carbon from the surface ocean. Consequently, controls on the nitrate inventory, the inputs and outputs of nitrate to the ocean, have been studied extensively. Fixed nitrogen is added from the atmosphere during nitrogen fixation in the surface ocean. It is removed during denitrification and anammox. These removal processes occur in areas of low oxygen, called "oxygen deficient zones" (ODZ's).

There are three main open-ocean ODZ's: the Eastern Tropical North Pacific (ETNP), the Eastern Tropical South Pacific (ETSP), and the Arabian Sea. Although these three areas account for 0.1% of the ocean surface area, they play an important role in controlling the inventory of fixed nitrogen in the ocean (Codispoti et al. 2001). There are several difficulties associated with studying ODZ's. Currently, there is some controversy regarding how much each removal process—denitrification or anammox—contributes to the nitrogen loss in each ODZ (Lam et al. 2009; Ward et al. 2009). Lam, et al. 2009, found that in the Arabian Sea the dominant nitrogen loss was due to anammox, supported by DNA and incubation measurements, while Ward et al. also in the Arabian Sea found that denitrification contributed to the majority of N loss. The current theory is that denitrification, which is fueled by organic matter, is very episodic based on large particulate flux events, while the autrophic process of anammox occurs at a more constant and slow rate. Studies to attribute a percentage loss to each process have relied on short-term incubation measurements and DNA analysis. Drawbacks of these studies include: oxygen contamination during collection; the negative affects on bacteria from bottle containment; and the fact that the studies occur instantaneously while the systems are temporally variable.

To address these drawbacks, our research has utilized stable isotopes as tracers for monitoring biological processes in the ocean. The nitrogen (N) and oxygen (O) isotopes of nitrite and nitrate ($\delta^{15}N_{NO2\text{ or }NO3}$ (‰ vs. atmospheric N_2) = ($^{15}N/^{14}N_{NO2\text{ or }NO3} \div {}^{15}N/^{14}N_{N2}$ -1) · 1000; $\delta^{18}O_{NO2\text{ or }NO3}$ (‰ vs. Vienna Standard Mean Ocean Water) = ($^{18}O/^{16}O_{NO2\text{ or }NO3} \div {}^{18}O/^{16}O_{VSMOW}$ -1) · 1000) can be used together to disentangle the

biological processes present in ODZ's. In order to successfully analyze stable-isotope tracers, an in depth understanding of the isotope systematics for each process and each isotope is required.

The $\delta^{15}N$ of nitrate, which varies little in the deep ocean and between ocean basins (Sigman et al. 2009), can be used for creating a global fixed nitrogen budget (Brandes and Devol 2002; Deutsch et al. 2004). Budgeting exercises using $\delta^{15}N$ have predicted a large net loss of fixed nitrogen from the ocean, which had not been predicted through the use of sedimentary records (Brandes and Devol 2002).

With the development of recent methods for measuring both $\delta^{15}N$ and $\delta^{18}O$, there has been interest in constructing a similar budget as $\delta^{15}N$, but this time using also $\delta^{18}O$. Nitrogen and oxygen atoms are added and removed from the nitrate pool during different processes, Figure 1. Oxygen is added during nitrification and removed during denitrification and assimilation. Therefore in order to construct a nitrogen budget using $\delta^{18}O_{NO3}$, the oxygen isotope systematics of nitrification need to be known. The N and O isotope budgets provide intersecting and complementary views of the N cycle because they record different aspects of the N cycle.

Nitrification oxygen isotope systematics

Microbial nitrification is a two-step process involving first, ammonia oxidation and second, nitrite oxidation. During ammonia oxidation, nitrite is produced with the addition of one oxygen atom from O_2 and one from H_2O (Andersson and Hooper 1983). Ammonia oxidation is carried out by both ammonia-oxidizing bacteria (AOB) and archaea (AOA). Nitrite oxidation incorporates an additional oxygen atom from H_2O to produce nitrate (Dispirito and Hooper 1986; Kumar et al. 1983) and is carried out by nitrite-oxidizing bacteria (NOB). There are a wide array of microbes within each of these groups of microbes that may be involved with nitrification in the ocean. The process of nitrification and associated isotope effects are shown in Figure 2. Previous studies have assumed that the final $\delta^{18}O$ of NO_3^- produced during nitrification could be calculated from this simple stoichiometry ($1/3\ \delta^{18}O_{O2} + 2/3\ \delta^{18}O_{H2O}$), but further experiments

conducted in our lab have proved this to be untrue (Buchwald et al. 2012; Buchwald and Casciotti 2010; Casciotti et al. 2010). There are, indeed, several isotope effects and isotope exchanges that cause the $\delta^{18}O$ of NO_3 to be lower than that calculated neglecting these isotope systematics (Figure 2). For ammonia oxidation there are kinetic isotope effects for the incorporation of O_2 ($^{18}\varepsilon_{k,O2}$) and H_2O ($^{18}\varepsilon_{k,H2O,1}$) and a biotic exchange between nitrite and water (x_{AO}). For nitrite oxidation there may be a kinetic isotope effect for water incorporation ($^{18}\varepsilon_{k,H2O,2}$) and an exchange between nitrite and water (x_{NO}).

Chapter 2 describes for the first time the measurement of these isotope effects in bacterial cultures of NOB. Little biotic exchange (x_{NO}) and large isotope effects were found for the incorporation of water during nitrite oxidation. Chapter 3 describes an extension of this study to co-cultures of AOB or AOA and NOB, as well as field experiments with natural assemblages of nitrifying organisms. During complete nitrification (ammonia to nitrate) with little nitrite accumulation, the amount of overall exchange was extremely low. A major finding of this work was that in artificial bottle experiment conditions, nitrite often accumulated due to slow nitrification rates, and there was a significant amount of abiotic exchange of nitrite oxygen atoms with water, which would cause the $\delta^{18}O_{NO3}$ produced to be artificially high. This will not be a factor in most areas of the ocean since nitrite rarely accumulates. Abiotic exchange will be important in regions where nitrite accumulates, such as in the primary nitrite maximum (PNM) at the base of the euphotic zone and in the secondary nitrite maximum (SNM) in oxygen deficient zones.

Abiotic exchange of nitrite oxygen atoms

Abiotic exchange rate of oxygen atoms between nitrite and water is a function of pH, temperature and salinity of the water. By determining the relationship between these parameters and the rate of abiotic exchange, this information can be used to determine the age of nitrite based on its $\delta^{18}O_{NO2}$ value. The original purpose of determining the rate of exchange was to correct abiotic exchange from nitrification isotope systematics

experiments, but the rate of exchange can also be used in the interpretation of oceanic nitrite. Equation 1 can be used to calculate the average age of a nitrite pool in the ocean.

$$\delta^{18}O_{NO2,t} = \left(\delta^{18}O_{NO2,b} - \left(\delta^{18}O_{H2O} + {}^{18}\varepsilon_{eq}\right)\right) \times e^{-kt} + \left(\delta^{18}O_{H2O} + {}^{18}\varepsilon_{eq}\right) \quad (1)$$

In order to calculate the age, one must first determine the biotic endmember or pre-equilibrated nitrite value ($\delta^{18}O_{NO2,b}$). Using the $\delta^{15}N_{NO2}$, one can determine the $\delta^{18}O_{NO2,b}$ because it does not undergo equilibration and therefore, will only record the biological processes that have produced and consumed that nitrite. Once the sinks and sources are determined using the isotope effects for these processes for ^{18}O, the $\delta^{18}O_{NO2,b}$ can be predicted. The greatest uncertainty exists in determining the value of the $\delta^{18}O_{NO2,b}$ through this method.

The second parameter in Equation 1 is the equilibrium isotope effect ($^{18}\varepsilon_{eq}$) between water and nitrite. This parameter will determine the final equilibrated value of the nitrite. The equilibrium isotope effect is dependent on temperature. Chapter 4 provides a method for determining the relationship between $^{18}\varepsilon_{eq}$ and temperature.

Lastly the rate constant k, is the final parameter needed to calculate the age. Chapter 4 discusses abiotic experiments, which were performed to determine k values at a large range of temperatures (4 to 37°C) and pH values (6.7 to 8.2). Taken all together this information can be used to calculate nitrite turnover time in the ocean and will be extremely helpful in interpreting the nitrogen cycling processes and rates in the PNM and SNM.

Isotope profiles of nitrite and new tracers: $\Delta(15,18)$ and $\Delta\delta^{15}N$

Isotope profiles in the ocean record the processes that have affected the species being measured. In order to accurately interpret the isotope profiles it is important to know the isotope fractionation associated with all processes which add and remove the

species being studied. The $\delta^{15}N_{NO3}$ has been used in oxygen deficient regions in the ocean to determine where and how much denitrification (Brandes et al. 1998; Cline and Kaplan 1975; Voss et al. 2001) and nitrogen fixation (Carpenter et al. 1997; Liu et al. 1996) have occurred. Areas that are heavily influenced by denitrification will have very enriched values of $\delta^{15}N_{NO3}$, because there is an isotope effect for denitrification of ~25‰ (Brandes et al. 1998; Voss et al. 2001). However, the stable isotope enrichment of $\delta^{15}N$ due to denitrification can be masked by nitrogen fixation activity in the overlying water (Brandes et al. 1998; Sigman et al. 2005).

In order to separate nitrogen fixation from denitrification, a study by Sigman et al (2005) proposed the use of a new tracer $\Delta(15,18) = (\delta^{15}N_{NO3} - \delta^{15}N_{NO3,deep}) - {}^{15}\varepsilon/{}^{18}\varepsilon^{*}(\delta^{18}O_{NO3} - \delta^{18}O_{NO3.deep})$. This tracer represents a nitrate isotope anomaly generated from the production of nitrate with either an unexpectedly low $\delta^{15}N$ value or unexpectedly high $\delta^{18}O$ value. It is useful because while effects of denitrification and nitrogen fixation counteract each other in both $\delta^{15}N_{NO3}$ and $\delta^{18}O_{NO3}$, the oxygen isotopes will be affected differently. Using both isotopes together will allow for better separation of these two processes.

If denitrification is the only process operating to remove nitrate, the $\delta^{15}N_{NO3}$ and $\delta^{18}O_{NO3}$ of the remaining nitrate pool will fall on a line with a slope equal to one, because the isotope effects for denitrification for ^{15}N and ^{18}O are identical (Granger et al. 2004; Granger et al. 2008; Sigman et al. 2005). When the isotope values deviate from this line, this indicates that there are other processes at work, which are affecting the removal of nitrate.

Sigman et al. (2005) propose that nitrogen fixation and nitrite reoxidation cause these deviations. Nitrogen fixation leads to the input of nitrate with low $\delta^{15}N$ (Capone et al. 1997; Hoering and Ford 1960; Minagawa and Wada 1986), causing a negative $\Delta(15,18)$ anomaly. The effects of nitrite reoxidation were not well understood. It has been assumed that the $\delta^{18}O_{NO3}$ added during nitrite reoxidation adds nitrite with a $\delta^{18}O$ value of 0‰, because of complete exchange with water of this value. However, in laboratory experiments, we have not measured such complete exchange as has been assumed

(Casciotti et al. 2010). Besides, even if there were complete exchange the $\delta^{18}O_{NO3}$ would be ~14‰ instead of 0‰ because of an equilibrium isotope effect between nitrite and water (Casciotti and McIlvin, 2007; Buchwald and Casciotti, submitted).

Even if the effects of nitrite reoxidation were known, it may be impossible to separate the effects of nitrogen fixation and nitrite reoxidation with only $\Delta(15,18)$. For example, a deviation from the 1:1 line could result from an increased $\delta^{18}O$ for nitrite reoxidation or the depletion of $\delta^{15}N$ during nitrogen fixation and therefore cannot be separated without an additional tracer. Nitrite isotopes may be the answer to separating these processes. Since the development of nitrite isotope measurement methods (McIlvin and Altabet 2005), we have been working towards integrating nitrate and nitrite isotopic measurements (Casciotti and McIlvin 2007; Casciotti 2009).

The most striking finding from the use of nitrite isotopes was that the $\delta^{15}N_{NO2}$ values were very low and much different from the higher $\delta^{15}N_{NO3}$. This term was defined as $\Delta\delta^{15}N = \delta^{15}N_{NO3} - \delta^{15}N_{NO2}$. This difference could be as much as 35‰ in the middle of the oxygen minimum zone, which is surprising because it is a larger difference than the isotope effect for nitrate reduction, indicating other processes are involved. The mechanisms leading to variations in $\Delta\delta^{15}N$ have yet to be fully understood, but could be attributed in part to nitrite reoxidation with an inverse isotope effect (Buchwald and Casciotti 2010; Casciotti 2009).

Global fixed nitrogen budget using nitrate isotopes

The profiles of $\delta^{15}N_{NO3}$ have also been used to predict the amount and location of assimilation, nitrogen fixation and denitrification that occur throughout the water column, specifically in ODZ's (Brandes et al. 1998; Casciotti and McIlvin 2007; Cline and Kaplan 1975; Voss et al. 2001). While $\delta^{15}N_{NO3}$ measurements have been useful, there are complicating factors that make their interpretation difficult such as concurrent denitrification and nitrogen fixation. Recent methods have been developed to measure both the $\delta^{15}N$ and $\delta^{18}O$ of nitrate (Casciotti et al. 2002; Sigman et al. 2001) and nitrite

(Casciotti et al. 2007; McIlvin and Altabet 2005). Already the use of both isotopes has provided helpful insights (Casciotti and McIlvin 2007; Casciotti 2009; Sigman et al. 2005; Wankel et al. 2007), but these insights rely on certain assumptions about nitrification, which may or may not be correct.

The $\delta^{15}N$ of deep water nitrate records the history of processes that consume and produce nitrate. Nitrogen is added during nitrogen fixation and removed during denitrification. Brandes and Devol (2002) determined the relative rates of sedimentary and water column denitrification, assuming a steady state deep water $\delta^{15}N_{NO3}$ value of 5‰ (Sigman et al. 2000), $\delta^{15}N$ for nitrogen fixation of 0‰ and ^{15}N isotopes effects ($^{15}\varepsilon$ (‰)=($^{14}k/^{15}k - 1$)*1000) of 25‰ and 0‰ for water column and sedimentary denitrification, respectively. These researchers found that sedimentary denitrification must account for 80% of all denitrification. If that were the case then a water column denitrification rate of 75 Tg N/yr would mean a sedimentary denitrification rate of greater than 280 Tg N/yr. Given that the highest estimates of global nitrogen fixation rates are only 135 Tg N/yr (Deutsch et al. 2007), this method predicts a large net loss of fixed nitrogen every year. Deutsch et al (2004) modified the previous approach by restricting denitrification to areas of the ocean with low oxygen and estimated sedimentary denitrification fluxes of 190 Tg N/yr, which still predicts a net loss of fixed N, but moves closer to creating a balanced budget.

Now with methods available to measure the $\delta^{18}O$ in NO_3^-, a fixed nitrogen budget can be created using the $\delta^{18}O_{NO3}$. Nitrogen and oxygen atoms are added and removed from the nitrate pool during different processes as shown in Figure 1. Oxygen is added during nitrification and removed during denitrification and assimilation. Previous assumptions about the $\delta^{18}O_{NO3}$ produced by nitrification were calculated using the biochemically-based nitrification stoichiometry of $\delta^{18}O_{NO3}$ =1/3 $\delta^{18}O_{O2}$ + 2/3 $\delta^{18}O_{H2O}$ and assuming no isotope effects (Andersson and Hooper 1983; Dispirito and Hooper 1986; Kumar et al. 1983). This approach yields an estimate of about 7.8‰ for the $\delta^{18}O$ of nitrate produced by nitrification. However, deep water nitrate has a $\delta^{18}O$ value of 1.5‰ to 2.5‰, and since removal processes will only further enrich the $\delta^{18}O$ value there would

be no way to create a balanced budget with a starting $\delta^{18}O_{NO3}$ value of 7.8‰. Chapters 2 and 3 discuss research that led to the determination of the nitrification $\delta^{18}O$ signature and the isotope systematics of nitrification that can be used in a fixed N budget.

Questions addressed in this thesis

Chapter 2 and 3 provide a discussion of a number of systematic experiments which resulted in a comprehensive understanding of nitrification isotope systematics. This thesis research has led to the determination of the many of isotope effects depicted in Figure 2. In Chapter 2, the isotope effect for nitrite selection ($^{18}\varepsilon_{k,NO2}$) and the incorporation isotope effect for water ($^{18}\varepsilon_{k,H2O,2}$) during nitrite oxidation in three species of nitrite- oxidizing bacteria were measured. The research also led to the discovery that there was little to no biotic exchange of oxygen atoms (x_{NO}) during nitrite oxidation.

Chapter 3 discusses the progress of research towards determining the $\delta^{18}O_{NO3}$ produced through nitrification in the ocean by conducting co-culture experiments and field incubations. These experiments measured the incorporation isotope effects during ammonia and nitrite oxidation, and determined that when coupled with nitrite oxidation with little accumulation of nitrite, there was very little biotic exchange of oxygen atoms during ammonia oxidation, as had been seen in single culture incubations of AOB.

This chapter also includes a discussion of the first oxygen isotope experiments with AOA. The research determined that they have similar oxygen isotope effects as AOB and low amounts of exchange, most likely from abiotic processes. Through these same experiments, it was discovered that the accumulation of nitrite as an intermediate would significantly affect the final value of the $\delta^{18}O_{NO3}$, due to an abiotic exchange of oxygen atoms. While this will not have importance in most areas of the ocean, it could have large implications in those areas where nitrite accumulates such as the primary nitrite maximum and in ODZs.

Chapter 4 discusses further investigation into controls on the rate of abiotic equilibration of nitrite and oxygen atoms. As a result, the research proved that nitrite

oxygen isotopes can now be used as a new tracer for nitrite cycling in the ocean. Abiotic equilibration of nitrite oxygen atoms allows us to use the isotopes of nitrite as not only a tracers of sources and cycling but also as a "clock" which can record the turnover time or average age of the nitrite in the ocean.

Finally, Chapter 5 contains a full analysis of the isotopic distribution in an ODZ in the Costa Rica Dome using the isotope effects and exchange parameters previously measured in this thesis (Chapters 2, 3 and 4) and elsewhere. By applying the techniques and equations developed through this doctoral research to a specific area of the ocean, the sources, sinks and relative rates of these processes through out the water column could now be identified over long space and time scales without manipulation or perturbation of the system.

References

Andersson, K. K. and A. B. Hooper. 1983. O_2 and H_2O are each the source of one O in NO_2^- produced from NH_3 by *Nitrosomonas* - N-15-NMR evidence. FEBS Lett. **164:** 236-240, doi:10.1016/0014-5793(83)80292-0.

Brandes, J. A. and A. H. Devol. 2002. A global marine-fixed nitrogen isotopic budget: Implications for Holocene nitrogen cycling. Global Biogeochem. Cycles. **16:** 1-14, doi:10.1029/2001GB001856.

Brandes, J. A., A. H. Devol, T. Yoshinari, D. A. Jayakumar and S. W. A. Naqvi. 1998. Isotopic composition of nitrate in the central Arabian Sea and eastern tropical North Pacific: A tracer for mixing and nitrogen cycles. Limnol. Oceanogr. **43:** 1680-1689.

Buchwald, C., A. E. Santoro, M. R. McIlvin and K. L. Casciotti. 2012. Oxygen isotopic composition of nitrate and nitrite produced by nitrifying cocultures in and natural marine assemblages. **57:** 1361-1375.

Buchwald, C. and K. L. Casciotti. 2010. Oxygen isotopic fractionation and exchange during bacterial nitrite oxidation. Limnol. Oceanogr. **55:** 1064-1074, doi:10.4319/lo.2010.55.3.1064.

Capone, D. G., J. P. Zehr, H. W. Paerl, B. Bergman and E. J. Carpenter. 1997. Trichodesmium, a globally significant marine cyanobacterium. Science. **276:** 1221-1229, doi:10.1126/science.276.5316.1221.

Carpenter, E. J., H. R. Harvey, B. Fry and D. G. Capone. 1997. Biogeochemical tracers of the marine cyanobacterium Trichodesmium. **44:** 27-38, doi:10.1016/S0967-0637(96)00091-X.

Casciotti, K. L. and M. R. McIlvin. 2007. Isotopic analyses of nitrate and nitrite from reference mixtures and application to Eastern Tropical North Pacific waters. Mar. Chem. **107:** 184-201, doi:10.1016/j.marchem.2007.06.021.

Casciotti, K. L., D. M. Sigman, M. G. Hastings, J. K. Bohlke and A. Hilkert. 2002. Measurement of the oxygen isotopic composition of nitrate in seawater and freshwater using the denitrifier method. Anal. Chem. **74:** 4905-4912, doi:10.1021/ac020113w.

Casciotti, K. L. 2009. Inverse kinetic isotope fractionation during bacterial nitrite oxidation. Geochim. Cosmochim. Acta. **73:** 2061-2076, doi:10.1016/j.gca.2008.12.022.

Casciotti, K. L., J. K. Boehlke, M. R. McIlvin, S. J. Mroczkowski and J. E. Hannon. 2007. Oxygen isotopes in nitrite: Analysis, calibration, and equilibration. Anal. Chem. **79:** 2427-2436, doi:10.1021/ac061598h.

Casciotti, K. L., M. McIlvin and C. Buchwald. 2010. Oxygen isotopic exchange and fractionation during bacterial ammonia oxidation. Limnol. Oceanogr. **55:** 753-762, doi:10.4319/lo.2009.55.2.0753.

Cline, J. D. and I. R. Kaplan. 1975. Isotopic fractionation of dissolved nitrate during denitrification in the eastern tropical North Pacific Ocean. **3:** 271-299.

Codispoti, L. A., J. A. Brandes, J. P. Christensen, A. H. Devol, S. W. A. Naqvi, H. W. Paerl and T. Yoshinari. 2001. The oceanic fixed nitrogen and nitrous oxide budgets: Moving targets as we enter the anthropocene? **65:** 85-105.

Deutsch, C., D. M. Sigman, R. C. Thunell, A. N. Meckler and G. H. Haug. 2004. Isotopic constraints on glacial/interglacial changes in the oceanic nitrogen budget. Global Biogeochem. Cycles. **18:** GB4012, doi:10.1029/2003GB002189.

Deutsch, C., J. L. Sarmiento, D. M. Sigman, N. Gruber and J. P. Dunne. 2007. Spatial coupling of nitrogen inputs and losses in the ocean. Nature. **445:** 164-167, doi:10.1038/nature05392.

Dispirito, A. A. and A. B. Hooper. 1986. Oxygen-Exchange between Nitrate Molecules during Nitrite Oxidation by Nitrobacter. J. Biol. Chem. **261:** 10534-10537.

Granger, J., D. M. Sigman, J. A. Needoba and P. J. Harrison. 2004. Coupled nitrogen and oxygen isotope fractionation of nitrate during assimilation by cultures of marine phytoplankton. Limnol. Oceanogr. **49:** 1763-1773.

Granger, J., D. M. Sigman, M. F. Lehmann and P. D. Tortell. 2008. Nitrogen and oxygen isotope fractionation during dissimilatory nitrate reduction by denitrifying bacteria. Limnol. Oceanogr. **53:** 2533-2545, doi:10.4319/lo.2008.53.6.2533.

Hoering, T. C. and H. T. Ford. 1960. The isotope effect in the fixation of nitrogen by Azotobacter. **82:** 376-378.

Kumar, S., D. J. D. Nicholas and E. H. Williams. 1983. Definitive N-15 NMR evidence that water serves as a source of O during nitrite oxidation by Nitrobacter-Agilis. FEBS Lett. **152:** 71-74, doi:10.1016/0014-5793(83)80484-0.

Lam, P., G. Lavik, M. M. Jensen, J. van de Vossenberg, M. Schmid, D. Woebken, D. Gutierrez, R. Amann, M. S. M. Jetten and M. M. M. Kuypers. 2009. Revising the nitrogen cycle in the Peruvian oxygen minimum zone. Proc. Natl. Acad. Sci. U. S. A. **106:** 4752-4757, doi:10.1073/pnas.0812444106.

Liu, K. K., M. J. Su, C. R. Hsueh and G. C. Gong. 1996. The nitrogen isotopic composition of nitrate in the Kuroshio Water northeast of Taiwan: Evidence for nitrogen fixation as a source of isotopically light nitrate. Mar. Chem. **54:** 273-292, doi:10.1016/0304-4203(96)00034-5.

McIlvin, M. R. and M. A. Altabet. 2005. Chemical conversion of nitrate and nitrite to nitrous oxide for nitrogen and oxygen isotopic analysis in freshwater and seawater. Anal. Chem. **77:** 5589-5595, doi:10.1021/ac050528s.

Minagawa, M. and E. Wada. 1986. Nitrogen isotope ratios of red tide organisims in the East China Sea: a characterization of biological nitrogen fixation. **19:** 245-259.

Sigman, D. M., M. A. Altabet, D. C. McCorkle, R. Francois and G. Fischer. 2000. The delta N-15 of nitrate in the Southern Ocean: Nitrogen cycling and circulation in the ocean interior. **105:** 19599–19614, doi:10.1029/2000JC000265.

Sigman, D. M., K. L. Casciotti, M. Andreani, C. Barford, M. Galanter and J. K. Bohlke. 2001. A bacterial method for the nitrogen isotopic analysis of nitrate in seawater and freshwater. Anal. Chem. **73:** 4145-4153, doi:10.1021/ac010088e.

Sigman, D. M., J. Granger, P. J. DiFiore, M. M. Lehmann, R. Ho, G. Cane and A. van Geen. 2005. Coupled nitrogen and oxygen isotope measurements of nitrate along the eastern North Pacific margin. Global Biogeochem. Cycles. **19:** GB4022, doi:10.1029/2005GB002458.

Sigman, D. M., P. J. DiFiore, M. P. Hain, C. Deutsch, Y. Wang, D. M. Karl, A. N. Knapp, M. F. Lehmann and S. Pantoja. 2009. The dual isotopes of deep nitrate as a constraint on the cycle and budget of oceanic fixed nitrogen. **56:** 1419-1439, doi:10.1016/j.dsr.2009.04.007.

Voss, M., J. W. Dippner and J. P. Montoya. 2001. Nitrogen isotope patterns in the oxygen-deficient waters of the Eastern Tropical North Pacific Ocean. **48:** 1905-1921, doi:10.1016/S0967-0637(00)00110-2.

Wankel, S. D., C. Kendall, J. T. Pennington, F. P. Chavez and A. Paytan. 2007. Nitrification in the euphotic zone as evidenced by nitrate dual isotopic composition: Observations from Monterey Bay, California. Global Biogeochem. Cycles. **21:** GB2009, doi:10.1029/2006GB002723.

Ward, B. B., A. H. Devol, J. J. Rich, B. X. Chang, S. E. Bulow, H. Naik, A. Pratihary and A. Jayakumar. 2009. Denitrification as the dominant nitrogen loss process in the Arabian Sea. Nature. **461:** 78-82, doi:10.1038/nature08276.

Figures

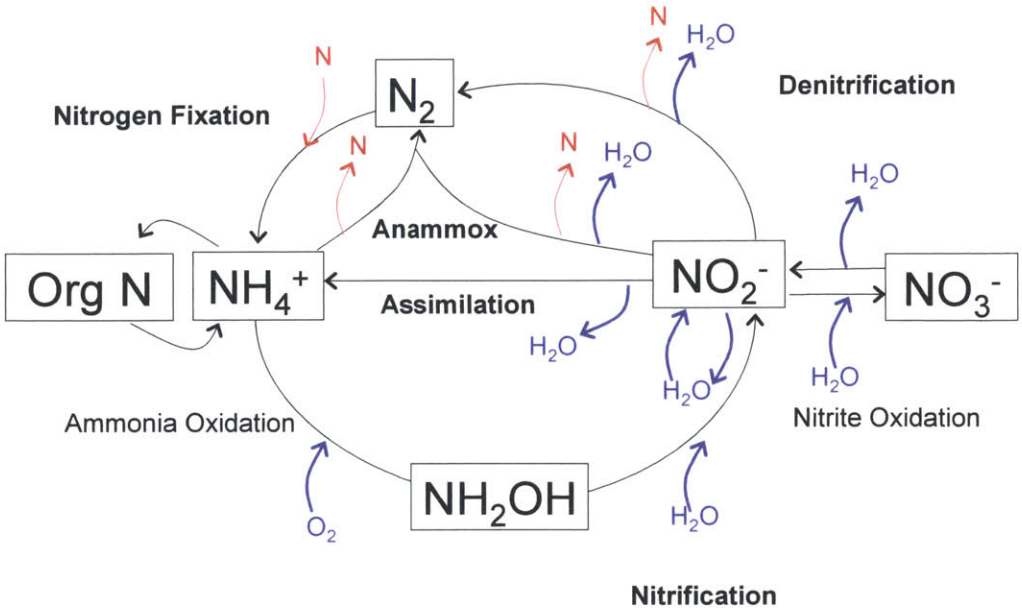

Figure 1. Diagram of the microbial nitrogen cycle, showing where N (red) and O (blue) are added and removed.

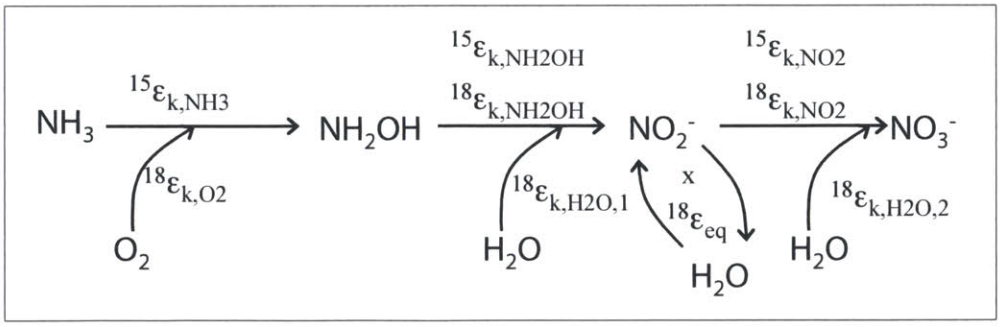

Figure 2. Nitrification pathway showing the isotope effects for each step.

Chapter 2

Oxygen isotopic fractionation and exchange during bacterial nitrite oxidation

Carolyn Buchwald and Karen L. Casciotti

This chapter was originally published in Limnology and Oceanography and is reprinted here with their permission.

Buchwald, C. and K. L. Casciotti. 2010. Oxygen isotopic fractionation and exchange during bacterial nitrite oxidation. *Limnol. Oceanogr.* **55:** 1064-1074.

Limnol. Oceanogr., 55(3), 2010, 1064–1074

doi:10.4319/lo.2010.55.3.1064

Oxygen isotopic fractionation and exchange during bacterial nitrite oxidation

Carolyn Buchwald[a,*] and Karen L. Casciotti[b]

[a] Massachusetts Institute of Technology/Woods Hole Oceanographic Institution Joint Program in Chemical Oceanography, Woods Hole Oceanographic Institution, Woods Hole, Massachusetts

[b] Marine Chemistry and Geochemistry Department, Woods Hole Oceanographic Institution, Woods Hole, Massachusetts

Abstract

We elucidate the controls on the $\delta^{18}O$ values of microbially produced nitrate by tracking the $\delta^{18}O$ of nitrite and nitrate during bacterial nitrite oxidation, which is the final step of the nitrification process. Aside from the $\delta^{18}O$ values of the nitrite and water substrates, three factors can affect the $\delta^{18}O$ value of nitrate produced during nitrite oxidation: (1) a kinetic isotope effect for nitrite oxidation ($^{18}\varepsilon_{k,NO_2}$), (2) a kinetic isotope effect for water incorporation by nitrite oxidoreductase ($^{18}\varepsilon_{k,H_2O,2}$), and (3) microbially mediated exchange of oxygen atoms between nitrite and water (x_{NOB}). These parameters were quantified through batch culture experiments with species from three genera of marine nitrite-oxidizing bacteria: *Nitrococcus*, *Nitrobacter*, and *Nitrospira*. Experiments conducted with ^{18}O-labeled water showed that less than 3% of the oxygen atoms in nitrite were exchanged with water and that $^{18}\varepsilon_{k,H_2O,2}$ ranged from +12.8‰ to +18.2‰. With the use of these parameters and the previously measured values of the $\delta^{18}O$ of nitrite produced by ammonia-oxidizing bacteria, the $\delta^{18}O$ of newly produced nitrate in the ocean was estimated to fall between −8.3‰ to −0.7‰, which is within the range necessary for balancing a deep ocean nitrate $\delta^{18}O$ budget.

Introduction

Isotopic constraints on the global nitrogen budget—Nitrate (NO_3^-) is a limiting nutrient in many areas of the ocean, and its supply from deep water in part controls the productivity and subsequent carbon export from the surface ocean (Eppley and Peterson 1979). Understanding the controls on the oceanic nitrate inventory is therefore critical because of the implications for carbon storage in the ocean. Sources of fixed (bioavailable) nitrogen to the ocean include biological nitrogen fixation, atmospheric deposition, and continental runoff; the major sinks of fixed nitrogen from the ocean include denitrification and anaerobic ammonia oxidation (anammox) in marine sediments and suboxic water columns, as well as burial of organic nitrogen (Brandes and Devol 2002; Gruber 2004). Despite efforts to determine the magnitude of these sources and sinks of fixed nitrogen, the oceanic budget is still poorly constrained.

Nitrogen isotopic analyses of nitrate ($\delta^{15}N_{NO_3}$ [‰ vs. air] = $\{(^{15}R_{NO_3}/^{15}R_{air}) - 1\} \times 1000$, where $^{15}R = {}^{15}N:{}^{14}N$ and air refers to the standard atmospheric N_2) have provided the basis of several efforts to understand the balance of fixed nitrogen sources and sinks (Brandes and Devol 2002; Deutsch et al. 2004). However, this approach predicts a net fixed nitrogen loss from the ocean of 100–270 Tg N yr^{-1} (Codispoti et al. 2001; Brandes and Devol 2002; Deutsch et al. 2004), whereas other approaches predict a balanced budget (Gruber and Sarmiento 1997; Gruber 2004). It is important to note that even those studies that predict a balanced budget have uncertainty of ~ 30% in the total source and sink fluxes.

Difficulty in resolving the $\delta^{15}N$ budget has prompted the use of nitrate $\delta^{18}O$ values ($\delta^{18}O_{NO_3}$ [‰ vs. VSMOW] = $\{(^{18}R_{NO_3}/^{18}R_{VSMOW}) - 1\} \times 1000$, where $^{18}R = {}^{18}O:{}^{16}O$ and VSMOW refers to the standard Vienna Standard Mean Ocean Water) to constrain the marine fixed nitrogen budget (Sigman et al. 2009). The $\delta^{18}O$ value of deep ocean nitrate is controlled by a different set of processes than the $\delta^{15}N$ value (Fig. 1). Oxygen atoms are removed from the nitrate pool during assimilation and denitrification and are added during nitrification (Fig. 1). The $\delta^{18}O$ of deep ocean nitrate is fairly constant at about +1.5‰ to +2.5‰ (Sigman et al. 2005, 2009; Casciotti et al. 2008). For the $\delta^{18}O$ of deep ocean nitrate to be maintained in steady state, the $\delta^{18}O$ signature of the nitrification source must balance the flux-weighted $\delta^{18}O$ value of loss fluxes. To use the deep ocean nitrate $\delta^{18}O$ values to determine the relative effects of competing processes on the nitrate pool, the isotope effects associated with each source and sink process must be known.

A kinetic isotope effect ($^{15}\varepsilon_k$, $^{18}\varepsilon_k$) describes the ratio of the rates at which the heavy (^{15}N, ^{18}O) vs. light (^{14}N, ^{16}O) isotopes react in a given process. For example, $^{15}\varepsilon_k(‰) = (^{14}k:{}^{15}k - 1) \times 1000$ and $^{18}\varepsilon_k(‰) = (^{16}k:{}^{18}k - 1) \times 1000$, where k is the first-order rate constant for reaction of each isotopic species, indicated by superscripts 14 and 15 for nitrogen isotopes and 16 and 18 for oxygen isotopic species. The reduction of nitrate during water column denitrification and assimilation fractionates nitrate nitrogen and oxygen isotopes equally, leaving behind nitrate that is enriched in both ^{15}N and ^{18}O (Granger et al. 2004, 2008).

Given that the kinetic isotope effects for denitrification are nearly identical for both ^{18}O and ^{15}N, we would expect $^{18}\varepsilon_k$ for water column and sedimentary denitrification to be approximately +25‰ and 0‰, respectively. Lehmann et al. (2004) have also provided empirical evidence for a small $^{18}\varepsilon_k$ for sedimentary denitrification. The N and O isotope effects from assimilation are also identical and estimated to be approximately +5‰ (Granger et al. 2004). Consumption

* Corresponding author: cbuchwald@whoi.edu

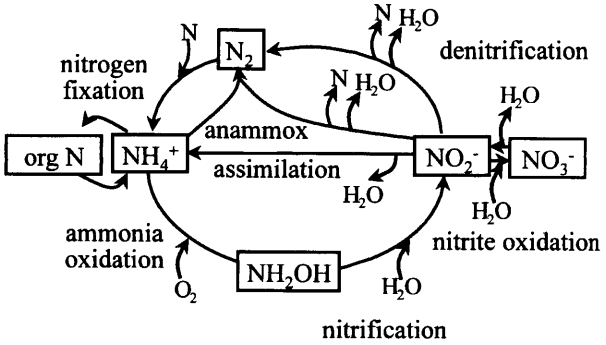

Fig. 1. Overview of microbial nitrogen cycle showing where nitrogen and oxygen atoms are added and removed from fixed nitrogen pools.

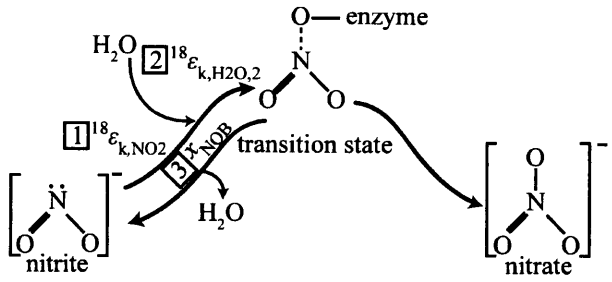

Fig. 2. Mechanism for nitrite oxidation, after Friedman et al. (1986), showing where isotope fractionation and exchange of oxygen occurs. The isotope effects associated with nitrite oxidation are labeled with numbers: (1) a kinetic isotope effect for nitrite oxidation ($^{18}\varepsilon_{k,NO_2}$), (2) a kinetic isotope effect for water incorporation ($^{18}\varepsilon_{k,H_2O,2}$), and (3) exchange between oxygen atoms in nitrite and water (x_{NOB}).

of nitrate by these processes should therefore increase the $\delta^{18}O$ value of the residual nitrate by removing nitrate with a low $\delta^{18}O$ value relative to average deep ocean values. When organic nitrogen is rematerialized, new oxygen atoms enter the nitrate pool through the process of nitrification (Fig. 1). Given that nitrate in the deep ocean has a $\delta^{18}O$ value of +1.5‰ to +2.5‰, the $\delta^{18}O$ of nitrate produced from nitrification must therefore be less than +1.5‰ to +2.5‰ to maintain $\delta^{18}O_{NO_3}$ in steady state.

Constraints on the $\delta^{18}O$ signature of newly produced nitrate—The established biochemical pathway for nitrification indicates that one oxygen atom comes from O_2 and the other two oxygen atoms come from water (Fig. 1; Andersson and Hooper 1983; Kumar et al. 1983; DiSpirito and Hooper 1986). If this simple stoichiometry determines the $\delta^{18}O$ value of nitrate produced by nitrification, then Eq. 1 can be used to calculate this value:

$$\delta^{18}O_{NO_3} = \frac{1}{3}(\delta^{18}O_{O_2}) + \frac{2}{3}(\delta^{18}O_{H_2O}) \quad (1)$$

With values of +23.5‰ to +36‰ for the $\delta^{18}O$ of O_2 ($\delta^{18}O_{O_2}$; Bender 1990) and 0‰ for the average $\delta^{18}O$ of seawater ($\delta^{18}O_{H_2O}$; Epstein and Mayeda 1953), the above equation predicts deep ocean nitrate $\delta^{18}O$ values of +7.8‰ to +12‰. Because this result is higher than the measured deep ocean nitrate value (+1.5‰ to +2.5‰), and given that consumption processes will further enrich the nitrate $\delta^{18}O$ value, factors beyond this simple stoichiometric relationship must come into play. We now know that isotope effects are associated with oxygen atom incorporation, as well as exchange of oxygen atoms between nitrite and water during ammonia oxidation that cause the $\delta^{18}O$ of newly produced nitrite (NO_2^-) to be lower than the stoichiometrically calculated value (Casciotti et al. 2010). In that study, it was determined that the nitrite produced through ammonia oxidation in seawater should have a $\delta^{18}O$ value of −3.3‰ to +5.3‰. The current study examines the hypothesis that there are additional isotope effects for nitrite oxidation to nitrate that might also lower the $\delta^{18}O$ of microbially produced nitrate relative to the simple stoichiometry commonly assumed (Eq. 1).

Biochemistry of nitrite oxidation—During nitrite oxidation, the enzyme nitrite oxidoreductase extracts an oxygen atom from water and then binds nitrite, forming an intermediate, or transition state (Friedman et al. 1986). The intermediate then either completes the oxidation to nitrate or back-reacts to nitrite by losing an oxygen atom (Fig. 2). During this process, three steps can affect the resulting $\delta^{18}O$ value in nitrate: (1) a kinetic isotope effect for nitrite oxidation ($^{18}\varepsilon_{k,NO_2}$), (2) a kinetic isotope effect for water incorporation ($^{18}\varepsilon_{k,H_2O,2}$; the subscript 2 represents the second water incorporated during nitrification, with the first occurring during ammonia oxidation), and (3) exchange of oxygen atoms between nitrite and water (x_{NOB} = the fraction of nitrite oxygen atoms that have been exchanged with water atoms before conversion to nitrate). $^{18}\varepsilon_{k,NO_2}$ should only play a role in setting $\delta^{18}O_{NO_3}$ in situations in which nitrite utilization is incomplete, such as in water column primary or secondary nitrite maxima. $^{18}\varepsilon_{k,H_2O,2}$ determines the $\delta^{18}O$ value at which the new oxygen atom from water is added. When this isotope effect is positive or "normal," $H_2{}^{16}O$ is preferentially added to the nitrite over $H_2{}^{18}O$. Exchange of oxygen atoms between nitrite and water (x_{NOB}) occurs when the decomposition of the transition state results in loss of an oxygen atom from the original nitrite and retention of the oxygen atom from water (Fig. 2), which may also occur with an isotope effect (*see* below).

This study presents experiments in which the isotope effects and oxygen atom exchange associated with bacterially-mediated nitrite oxidation were measured. This is important because these values can be used to calculate an expected $\delta^{18}O$ value for the nitrate produced from nitrification, which can then be used to interpret the distribution of $\delta^{18}O_{NO_3}$ in the ocean and to create a fixed nitrogen budget using oxygen isotopes.

Methods

Maintenance of bacteria—All bacterial cultures used in this study were kindly provided by John Waterbury and Frederica Valois. *Nitrococcus mobilis* was originally isolated from the Pacific Ocean off the Galapagos Archipelago

Table 1. Summary of nitrite oxidation experiments.

Experiment	Bacterial species	$\delta^{18}O_{H_2O}$ in media (‰ vs. VSMOW)	x_{NOB} measured	$^{18}\varepsilon_{k,H_2O,2}$ measured	$^{18}\varepsilon_{k,NO_2}$ measured
1	*Nitrobacter* sp. Nb 355	−5.6	No	No	Yes
2	*Nitrospira marina*	−4.8	No	No	Yes
3	*Nitrococcus mobilis*	−6.2, +41.5	Yes	Yes	Yes
4	*Nitrococcus mobilis*	−5.5, +88.4	Yes	Yes	Yes
5	*Nitrobacter* sp. Nb 355	−5.2, +88.6	Yes	Yes	Yes
6	*Nitrococcus mobilis*	−5.5, +33.4, +73.4, +148.9	Yes	Yes	No
	Nitrobacter sp. Nb 355	−5.5, +33.4, +73.4, +148.9	Yes	Yes	No
	Nitrobacter sp. Nb 297	−5.5, +33.4, +73.4, +148.9	Yes	Yes	No
7	*Nitrococcus mobilis*	−5.1, +32.5, +72.6, +149.7	Yes	Yes	No
	Nitrobacter sp. Nb 355	−5.1, +32.5, +72.6, +149.7	Yes	Yes	No
	Nitrobacter sp. Nb 297	−5.1, +32.5, +72.6, +149.7	Yes	Yes	No

(Watson and Waterbury 1971). *Nitrobacter* sp. Nb 297 and *Nitrospira marina* were both originally isolated from the Gulf of Maine. Lastly, *Nitrobacter* sp. Nb 355 was isolated from Black Sea surface water. All bacteria were grown in a defined medium containing 75% artificial seawater and 25% distilled water amended with 400 μmol L^{-1} $MgSO_4$, 30 μmol L^{-1} $CaCl_2$, 5 μmol L^{-1} $KHPO_4$, 2.3 μmol L^{-1} Fe(III)-EDTA ("Geigy iron"), 0.1 μmol L^{-1} Na_2MoO_4, 0.25 μmol L^{-1} $MnCl_2$, 0.002 μmol L^{-1} $CoCl_2$, and 0.08 μmol L^{-1} $ZnSO_4$ (Watson and Waterbury 1971). Filter-sterilized $NaNO_2$ working stock (5 mol L^{-1}) was added after autoclaving to achieve 10 mmol L^{-1} NO_2^- in *Nitrococcus* and *Nitrobacter* cultures and 2 mmol L^{-1} in *Nitrospira* cultures. Media were adjusted to pH 8.2 with sterile K_2CO_3 after NO_2^- addition. All cultures were maintained in a 23°C dark incubator in 1-liter flasks.

Nitrite oxidation experiments—To measure the three different isotope effects during nitrite oxidation (Fig. 2), batch culture incubations were conducted with pure cultures of nitrite-oxidizing bacteria. Results from seven different experiments are reported here. The experiments differed slightly on the basis of the bacterium used, the media $\delta^{18}O_{H_2O}$ values, and the sampling frequency. These details are summarized in Table 1.

Media for incubation experiments were prepared as described above, with the following modifications. First, ^{18}O-labeled water (with a $\delta^{18}O_{H_2O}$ value of approximately +5000‰ vs. VSMOW) was added in amounts of 3–33 mL L^{-1} of medium to achieve $\delta^{18}O_{H_2O}$ values for the media of −5‰ to +150‰ vs. VSMOW. The labeled water was added before autoclaving to ensure adequate mixing of the labeled water throughout the media. After autoclaving, $NaNO_2$ was added to 50 μmol L^{-1}, and the media were neutralized to pH 8.2 with sterile K_2CO_3.

The maintenance cultures (300–500 mL) were harvested either by centrifugation (4000 rpm for 30 min) or filtration (0.22-μm pore size filter), depending on the cell density in the culture. The harvested bacteria were then washed and resuspended with 0.22-μm filtered artificial seawater. The experiments were initiated with inoculation of the bacteria into the prepared media. In experiments in which $^{18}\varepsilon_{k,NO_2}$ was measured, duplicate flasks were inoculated for each initial $\delta^{18}O_{H_2O}$ value. One flask received twice the amount of inoculum as the other flask to gain higher resolution for the isotope effect estimate over the full range of nitrite consumption. In all other experiments, replicate incubations received the same amount of inoculum. In all experiments, sterile controls were analyzed in parallel to check for abiotic oxidation of nitrite to nitrate.

After inoculation, the flasks were subsampled (10–15 mL) immediately and then periodically throughout conversion of nitrite to nitrate and again after all nitrite had been consumed. Each subsample was 0.22-μm filtered immediately after collection. Nitrite concentrations were measured immediately after sampling and then used to calculate the sample volume needed to obtain 5–20 nmol of nitrite for isotopic analysis. Azide reactions for nitrite isotope analyses (*see* below for details) were conducted within 1 h of sampling to avoid abiotic exchange of oxygen atoms between nitrite and water during storage of samples (Casciotti et al. 2007). The rest of each subsample was stored frozen in 15-mL centrifuge tubes until analyses for nitrate concentration and isotopic composition.

Concentration analyses—Nitrite concentrations were analyzed according to the Greiss–Ilosvay colorimetric reaction (Strickland and Parsons 1972). Samples were reacted in duplicate and measured at a wavelength of 543 nm on Amersham Biosciences Ultrospec 2100 spectrophotometer with a Gilson 220XL autosampler. Nitrate plus nitrite concentrations were analyzed in duplicate following the chemiluminescence detection method after hot vanadium (III) reduction to nitric oxide (Braman and Hendrix 1989). Samples (1 mL) were injected into a flask containing vanadium chloride held at 95°C, and the resulting nitric oxide was measured in a Nitrogen Oxides Detector (model 8840, Monitor Labs) against nitrate concentration standards prepared gravimetrically.

Isotopic analyses—Nitrite $\delta^{15}N$ and $\delta^{18}O$ values were measured with the azide method developed by McIlvin and Altabet (2005). Briefly, sample nitrite was reduced to nitrous oxide in a sealed 20-mL vial with 2 mol L^{-1} sodium azide in 20% acetic acid. The nitrous oxide analyte was

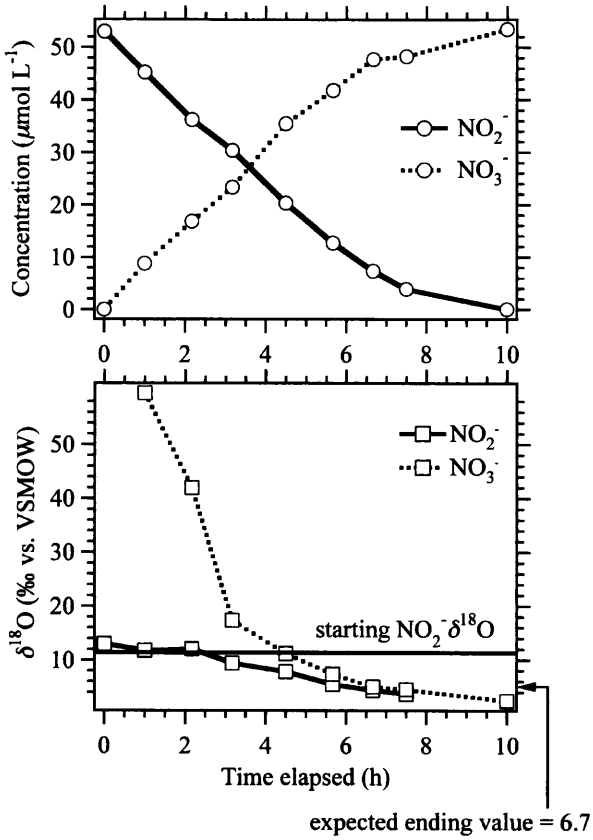

Fig. 3. (a) Nitrite and nitrate concentrations and (b) $\delta^{18}O$ values of nitrite and nitrate during a typical time course incubation with *Nitrococcus mobilis* (Expt. 3). The $\delta^{18}O_{NO_2}$ started at a value of +13‰ and decreased over time because of the (inverse) isotope effect for nitrite oxidation ($^{18}\varepsilon_{k,NO_2}$). The $\delta^{18}O_{NO_3}$ of produced nitrate is initially high and then decreases over time because of both closed-system mass balance constraints and the incorporation of H_2O with a low $\delta^{18}O$ value. Eventually, $\delta^{18}O_{NO_3}$ reaches a value that reflects the complete oxidation of NO_2^- to NO_3^- and the incorporation of H_2O with a kinetic isotope effect ($^{18}\varepsilon_{k,H_2O,2}$).

then purged from the sample vial, trapped cryogenically with liquid nitrogen, and measured for nitrogen and oxygen isotopic composition on a Finnigan Delta^{PLUS} XP isotope ratio mass spectrometer. The volume of sample analyzed was calculated from the concentration of nitrite to obtain 5–20 nmol of N. Nitrite isotopic standards N23, N7373, and N10219—$NaNO_2$ salts with known $\delta^{18}O_{NO_2}$ values of +4.5‰, +11.4‰, and +88.5‰, respectively (Casciotti et al. 2007)—were analyzed in parallel, with amounts tuned to match the samples (5–20 nmol N). The maximum sample volume that could be used in the isotopic analysis was 10 mL, meaning at least 0.5 μmol L^{-1} nitrite needed to be present to obtain an accurate isotopic measurement with our system. Precision on replicate $\delta^{18}O_{NO_2}$ analyses is 0.5‰ (McIlvin and Altabet 2005).

Nitrate (plus nitrite) $\delta^{15}N$ and $\delta^{18}O$ analyses were made by the denitrifier method (Sigman et al. 2001; Casciotti et al. 2002). The sample volumes were calculated with the combined nitrite and nitrate concentrations to obtain 5–20 nmol of nitrite plus nitrate-N in each vial. Both nitrite and nitrate standards were analyzed with each denitrifier run to allow mass and isotope subtraction of nitrite from the combined (nitrate plus nitrite) isotope measurements (Casciotti and McIlvin 2007). The nitrate standards used were USGS32, USGS34, and USGS35, with known $\delta^{18}O_{NO_3}$ values of +25.7‰, −27.9‰, and +57.5‰, respectively (Böhlke et al. 2003). The same nitrite standards employed in the azide method were reanalyzed by the denitrifier method to calibrate the nitrite isotopic contribution to samples containing both nitrate and nitrite (Casciotti and McIlvin 2007). Samples containing both nitrite and nitrate were measured using both azide and denitrifier methods, and the nitrate isotopes were calculated using a mass balance subtraction described in Casciotti and McIlvin (2007). Precision on replicate $\delta^{18}O_{NO_3}$ analyses is approximately 0.6‰ (Casciotti and McIlvin 2007).

The $\delta^{18}O$ of water was measured according to the method described in McIlvin and Casciotti (2006), which uses rapid abiotic oxygen isotope exchange between nitrite and water at low pH (Bunton et al. 1959), followed by the azide method for nitrite $\delta^{18}O$ analysis. Water samples received 5 μL of 6 mol L^{-1} hydrochloric acid (HCl) per 0.4-mL sample to bring the pH below 4. Samples containing no nitrite were amended with 5–20 nmol nitrite before acidification, whereas samples containing nitrite did not require this addition. The addition of the acid facilitates abiotic equilibration of oxygen atoms between nitrite and water, so that the equilibrated $\delta^{18}O$ value of the nitrite reflects that of the water plus an equilibration isotope effect of approximately +14‰ at room temperature (Casciotti et al. 2007). After equilibration, the azide method for nitrite isotopes was conducted following the above procedure. Sample analyses were calibrated against water standards H_2O-1, H_2O-2, and H_2O-3, with independently calibrated $\delta^{18}O$ values of −5.82‰, +18.04‰, +41.35‰, respectively, vs. VSMOW (McIlvin and Casciotti 2006). The water standards were run in triplicate, with each set of water samples receiving the same nitrite, HCl, and azide treatments. Precision of replicate $\delta^{18}O_{H_2O}$ analyses is 0.5‰ (McIlvin and Casciotti 2006).

Results

Oxidation of nitrite to nitrate was complete in all experiments. Experiments with *Nitrococcus* and *Nitrobacter*, which grew to higher densities (~ 10^7 cells L^{-1}) completely consumed the nitrite in 10–48 h. The *Nitrospira* cultures, which grew to a lower cell density, took 2 weeks to consume all of the nitrite. Figure 3 shows the nitrate and nitrite concentrations and $\delta^{18}O$ values for a typical time course incubation of *N. mobilis* in medium with a $\delta^{18}O_{H_2O}$ value of −6‰. In this experiment, $\delta^{18}O_{NO_2}$ decreased over time as it was oxidized to nitrate. $\delta^{18}O_{NO_3}$ was initially elevated relative to nitrite but obtained a value of −0.8‰ once all of the NO_2^- had been oxidized to NO_3^-. These

results reflect the combination of isotope effects for nitrite oxidation ($^{18}\varepsilon_{k,NO_2}$) and water incorporation ($^{18}\varepsilon_{k,H_2O,2}$), as will be discussed in detail below. However, we emphasize here that the final $\delta^{18}O$ value of the nitrate (−0.8‰) was lower than expected (+6.7‰) on the basis of Eq. 2, which neglects any isotope effects.

$$\delta^{18}O_{NO_3\ final} = \frac{2}{3}\left(\delta^{18}O_{NO_2\ initial}\right) + \frac{1}{3}\left(\delta^{18}O_{H_2O}\right) \quad (2)$$

The deviation of the $\delta^{18}O_{NO_3\ final}$ from Eq. 2 could be the result of isotope effects associated with either water incorporation ($^{18}\varepsilon_{k,H_2O,2}$) or the exchange of oxygen between nitrite and water (x_{NOB}). The isotope effect for nitrite selection ($^{18}\varepsilon_{k,NO_2}$) can be neglected in this case because nitrite was eventually consumed fully. We can amend Eq. 2 to include these factors:

$$\delta^{18}O_{NO_3\ final} = \frac{2}{3}\left[(1-x_{NOB})\delta^{18}O_{NO_2\ initial} + x_{NOB}\left(\delta^{18}O_{H_2O} + {}^{18}\varepsilon_{eq}\right)\right] + \frac{1}{3}\left(\delta^{18}O_{H_2O} - {}^{18}\varepsilon_{k,H_2O,2}\right) \quad (3)$$

As defined previously, x_{NOB} is the fraction of nitrite oxygen atoms that have exchanged with water before conversion to nitrate. A nonzero value for x_{NOB} causes the $\delta^{18}O$ of the reacting nitrite to change over time, which introduces an additional dependence on the $\delta^{18}O$ of water in Eq. 3. During equilibration, there is also an equilibrium isotope effect ($^{18}\varepsilon_{eq}$), which causes the water that "sticks" to nitrite to have a higher $\delta^{18}O$ value than the bulk water.

We can determine values for x_{NOB} and $^{18}\varepsilon_{k,H_2O,2}$ by analyzing data from parallel incubations conducted at a variety of $\delta^{18}O_{H_2O}$ values. This becomes apparent after rearranging Eq. 3 with $\delta^{18}O_{H_2O}$ as the independent variable:

$$\delta^{18}O_{NO_3\ final} = \left[\frac{2}{3}(x_{NOB}) + \frac{1}{3}\right]\delta^{18}O_{H_2O} + \left\{\frac{2}{3}\left[(1-x_{NOB})\delta^{18}O_{NO_2\ initial} + {}^{18}\varepsilon_{eq}(x_{NOB})\right] - \frac{1}{3}{}^{18}\varepsilon_{k,H_2O,2}\right\} \quad (4)$$

If x_{NOB} and $^{18}\varepsilon_{k,H_2O,2}$ are constant for a given experiment (do not change with different $\delta^{18}O_{H_2O}$ values), then the slope (m) and intercept (b) of this linear equation are constants. Therefore, if $\delta^{18}O_{NO_2\ initial}$, $^{18}\varepsilon_{eq}$, and $\delta^{18}O_{NO_3\ final}$ are known, then x_{NOB} can be calculated from the slope and $^{18}\varepsilon_{k,H_2O,2}$ from the intercept of Eq. 4.

Nitrite and water exchange (x_{NOB})—$\delta^{18}O_{NO_3\ final}$ values corresponding to the media $\delta^{18}O_{H_2O}$ values of five experiments are plotted in Fig. 4. The slopes from the linear regressions for each experiment and bacterial species were similar to 0.333 and did not show species-dependent variations (Table 2). The slopes of the linear regressions from Fig. 4 can then be used to calculate x_{NOB} values from the coefficient of $\delta^{18}O_{H_2O}$ term from Eq. 4:

$$m = \frac{2}{3}(x_{NOB}) + \frac{1}{3} \quad (5)$$

These x_{NOB} values have been calculated (Table 2) by solving Eq. 5 individually for each bacterial species and experiment. The uncertainty in x_{NOB} for each experiment was calculated from the uncertainty of the linear fit. All values of x_{NOB} were less than 3%, indicating that there was little exchange between nitrite and water during nitrite oxidation. The average and standard deviation of x_{NOB} in all experiments using *N. mobilis*, *Nitrobacter* sp. Nb 355, and *Nitrobacter* sp. Nb 297 were 1.5% ± 0.8%, 0.2% ± 0.9%, and 0.3% ± 0.5%, respectively. The differences between species were not statistically significant ($p > 0.05$).

Water incorporation isotope effect ($^{18}\varepsilon_{k,H_2O,2}$)—Whereas the slopes of the linear regression of $\delta^{18}O_{H_2O}$ vs. $\delta^{18}O_{NO_3\ final}$ were all very similar between bacteria and experiments, the intercepts showed more variability (Fig. 4; Table 2). The equation that describes the intercept is:

$$b = \frac{2}{3}\left[(1-x_{NOB})\delta^{18}O_{NO_2\ initial} + {}^{18}\varepsilon_{eq}(x_{NOB})\right] - \frac{1}{3}{}^{18}\varepsilon_{k,H_2O,2} \quad (6)$$

The kinetic isotope effect for water incorporation ($^{18}\varepsilon_{k,H_2O,2}$) can be calculated by rearranging Eq. 6 and substituting in measured values of b, x_{NOB}, and $\delta^{18}O_{NO_2\ initial}$ and an estimate of $^{18}\varepsilon_{eq}$.

$${}^{18}\varepsilon_{k,H_2O,2} = -3b + 2\left[\left(\frac{3}{2} - \frac{3}{2}m\right)\delta^{18}O_{NO_2\ initial} + {}^{18}\varepsilon_{eq}\left(\frac{3}{2}m - \frac{1}{2}\right)\right] \quad (7)$$

A value of +14‰ for $^{18}\varepsilon_{eq}$, as measured by Casciotti et al. (2007) for abiotic nitrite and water oxygen isotope exchange, was used here to calculate $^{18}\varepsilon_{k,H_2O,2}$. We justify this assumption by noting that although enzymes might accelerate the approach to equilibrium, they are not expected to alter the equilibrium point or the isotope effect between two species at equilibrium. Moreover, given the low amount of exchange estimated for nitrite oxidation (Table 2) our estimates of $^{18}\varepsilon_{k,H_2O,2}$ are not very sensitive to this assumption, which affects estimates of $^{18}\varepsilon_{k,H_2O,2}$ by only 0.05‰ for every 1‰ change in $^{18}\varepsilon_{eq}$. The averages and standard deviations of $^{18}\varepsilon_{k,H_2O,2}$ across experiments were +17.8‰ ± 4.7‰, +12.3‰ ± 3.0‰, and +15.6‰ ± 0.03‰ for *N. mobilis*, *Nitrobacter* sp. Nb 355, and *Nitrobacter* sp. Nb 297, respectively (Table 2). The greater variability in the *N. mobilis* and *Nitrobacter* sp. Nb 355 can be attributed to results from Expts. 3 and 5, in which the intercepts were anomalously low and high, respectively. If these outliers are discarded, the isotope effects for water incorporation would be 15.4‰ ± 0.3‰ and 14.0‰ ± 0.9‰ for *N. mobilis* and *Nitrobacter* sp. Nb 355, respectively, which are much closer to the isotope effect for *Nitrobacter* sp. Nb 297.

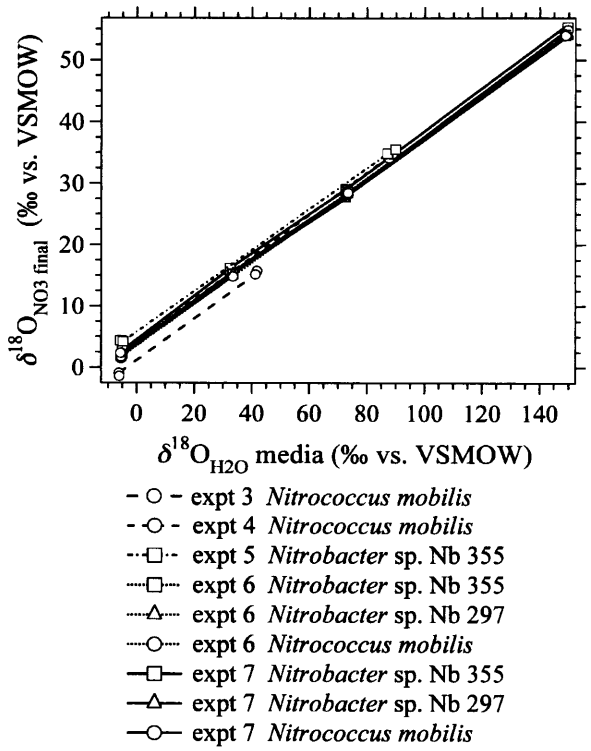

Fig. 4. $\delta^{18}O_{NO_3}$ produced in different $\delta^{18}O_{H_2O}$ media after all NO_2^- has been oxidized to NO_3^- in Expts. 3, 4, 5, 6, and 7. Slopes and intercepts of the linear regressions were used to calculate x_{NOB} and $^{18}\varepsilon_{k,H_2O,2}$, as shown in Table 2.

However, in Expts. 6 and 7, in which the intercepts and derived $^{18}\varepsilon_{k,H_2O,2}$ values were more consistent within and between species, *Nitrobacter* sp. Nb 355 did display a statistically lower $^{18}\varepsilon_{k,H_2O,2}$ than the other two species within a 90% confidence interval ($p = 0.08$). In each case, the measured $^{18}\varepsilon_{k,H_2O,2}$ is positive or "normal," meaning that the $\delta^{18}O$ value of water molecules incorporated into nitrate is lower than the $\delta^{18}O$ value of the bulk water, indicating that nitrite-oxidizing bacteria are preferentially incorporating $H_2{}^{16}O$ into nitrate.

Nitrite kinetic isotope effect ($^{18}\varepsilon_{k,NO_2}$)—Figure 5 shows the $\delta^{18}O$ of nitrite plotted vs. $-\ln(f)$, where f is the fraction of nitrite remaining ($f = [NO_2^-]/[NO_2^-]_{initial}$), for the five experiments in which $\delta^{18}O_{H_2O}$ was approximately −6‰. In closed-system Rayleigh fractionation with a constant kinetic isotope effect, a linear relationship is expected between $-\ln(f)$ and $\delta^{18}O_{NO_2}$, with the slope of the regression equaling $^{18}\varepsilon_{k,NO_2}$ (Mariotti et al. 1981; Scott et al. 2004). However, the data from our experiments were found to fit a quadratic function more closely, implying that the isotope effect decreased linearly over the course of the experiment (Fig. 5).

Oxygen atom exchange could cause curvature in the Rayleigh plots for $\delta^{18}O_{NO_2}$, depending on the relative $\delta^{18}O$ values of NO_2^- and H_2O. In fact, we believe that exchange did cause curvature in experiments conducted with higher $\delta^{18}O_{H_2O}$ media, where isotopic fractionation (decreasing $\delta^{18}O_{NO_2}$) and exchange (increasing $\delta^{18}O_{NO_2}$) produced counteracting effects. However, in experiments conducted in the media with the lowest $\delta^{18}O_{H_2O}$ value (−6‰; Fig. 5), exchange with an equilibrium isotope effect of +14‰ would push $\delta^{18}O_{NO_2}$ toward +8‰. At the lowest $\delta^{18}O$ values reached (+1‰; Fig. 5), 3% exchange would cause a change of only 0.4‰ in $\delta^{18}O_{NO_3}$. Therefore, in the experiments presented in Fig. 5, we can exclude exchange as a factor in producing the observed curvature.

As the experiments progressed, the concentrations of nitrite would also have been decreasing, suggesting that the magnitude of the expressed isotope effect might be dependent on nitrite concentration. We have tested this by conducting additional experiments with *N. mobilis* at four different initial concentrations of nitrite, ranging from 5 to 500 μmol L^{-1}. The expressed kinetic isotope effects for nitrite oxidation ($^{15}\varepsilon_{k,NO_2}$ and $^{18}\varepsilon_{k,NO_2}$ for ^{15}N and ^{18}O, respectively) were smaller at lower initial nitrite concentrations (not shown). This is consistent with concentration dependence underlying the quadratic fit, yielding the decreasing slopes near the end of the experiments presented in Fig. 5. Similar patterns have been observed in other systems and have been interpreted to reflect the effects of co-occurring processes, such as transport and reaction of substrate (Farquhar et al. 1982; Needoba et al. 2004). In these cases, it was shown that the enzyme-level kinetic isotope effect is expressed more strongly at high concen-

Table 2. Results for water incorporation ($^{18}\varepsilon_{k,H_2O,2}$) and exchange ($x_{NOB}$).

Bacteria	Expt.	Slope (m)	Intercept (b)	x_{NOB} (fraction)	$^{18}\varepsilon_{k,H_2O,2}$ (‰)
Nitrococcus mobilis	3	0.351±0.006	0.8±0.2	0.026±0.006	24.9±0.9
	4	0.343±0.001	4.2±0.1	0.015±0.001	15.0±1.6
	6	0.339±0.001	3.5±0.0	0.008±0.001	15.6±0.5
	7	0.341±0.002	3.7±0.1	0.011±0.002	15.6±1.6
	Average			**0.015±0.008**	**17.8±4.7**
Nitrobacter sp. Nb 355	5	0.328±0.002	6.1±0.2	−0.008±0.002	9.0±1.0
	6	0.337±0.000	3.9±0.0	0.006±0.000	14.6±0.5
	7	0.339±0.002	4.5±0.1	0.009±0.002	13.3±1.6
	Average			**0.002±0.009**	**12.3±3.0**
Nitrobacter sp. Nb 297	6	0.338±0.001	3.6±0.1	0.007±0.001	15.6±0.5
	7	0.333±0.002	3.7±0.2	0.000±0.002	15.7±1.6
	Average			**0.003±0.005**	**15.6±0.03**

trations of substrate, gradually approaching the (smaller) isotope effect for transport at low substrate concentrations. Our results are consistent with a similar concentration-dependent expression of the isotope effect for nitrite oxidation.

To compare the most relevant enzyme-level kinetic isotope effects between experiments, $^{18}\varepsilon_{k,NO_2}$ was calculated at time 0 by using the linear coefficient of the quadratic fit in experiments that started with 50 μmol L^{-1} nitrite (Table 3). *N. mobilis* and *Nitrobacter* sp. Nb 355 had $^{18}\varepsilon_{k,NO_2}$ values averaging $-8.2‰ \pm 2.5‰$ and $-6.5‰ \pm 1.8‰$, respectively, which are not significantly different ($p > 0.05$). *N. marina*, however, had a significantly lower $^{18}\varepsilon_{k,NO_2}$ value of $-1.3‰ \pm 0.4‰$ compared with the other two species ($p < 0.05$).

The observed $^{18}\varepsilon_{k,NO_2}$ values were negative or "inverse" for all experiments, indicating that the nitrite became depleted in the heavy isotope (^{18}O) as the pool was consumed. This might be surprising at first, given that most enzymatic reactions cause heavy-isotope enrichment in the substrate pool. However, it has previously been shown that an inverse isotope effect is to be expected for N-isotope fractionation in this simple bond-forming reaction (Casciotti 2009). Here we observe inverse kinetic fractionation for both N and O isotopes, with the ^{18}O isotope effects being smaller, or less inverse, than the ^{15}N isotope effects (Table 3).

Discussion

Reaction mechanism and oxygen isotope exchange (x_{NOB})—During nitrite oxidation, the enzyme nitrite oxidoreductase first binds to an oxygen atom from water, forming an enzyme–oxygen complex. This complex then binds nitrite to form an enzyme-bound intermediate that can either decompose back to nitrite or proceed to form nitrate (Friedman et al. 1986; Fig. 2). If the intermediate loses one of the original nitrite oxygen atoms during back-reaction, some of the oxygen atoms in the original nitrite will have been replaced by water. Such an exchange would be expected to alter the $\delta^{18}O$ of nitrite over time and lead to an increased dependence of nitrite and nitrate $\delta^{18}O$ on variations in water $\delta^{18}O$, which was not observed in our experiments. Our observations are consistent with earlier studies, which also showed little, if any, exchange between nitrite and water during nitrite oxidation (DiSpirito and Hooper 1986; Friedman et al. 1986). This implies that either back-reaction within the nitrite oxidoreductase enzyme is minimal or that it routinely extracts the oxygen atom added from H_2O.

During back-reaction from the transition state, the removal of the new oxygen atom would require breaking only one N–O bond, whereas removal of one of the original nitrite oxygen atoms would require breaking two N–O bonds and reforming one. Less energy would be required to break the one bond (between the water oxygen and nitrite nitrogen) than between two bonds (between the water oxygen and the enzyme and between the nitrite nitrogen and oxygen), lending some support for preferential removal of the oxygen atom added from H_2O. Also, because of resonance within the double-bond structure of the original nitrite molecule, these bonds are most likely stronger than the newly formed bond and thus harder to break. Therefore, the defined mechanism for the addition of oxygen during nitrite oxidation supports our observations of little isotopic exchange catalyzed between nitrite and water during nitrite oxidation, and it is unlikely that this will change under different growth conditions or with other species.

Inverse kinetic isotope effect ($^{18}\varepsilon_{k,NO_2}$)—An inverse isotope effect is rare in biology but could be expected for this bond-forming reaction because of stabilization of the transition state by the heavier isotopes (Casciotti 2009). An inverse isotope effect for nitrite oxidation in *N. mobilis* has been observed previously for ^{15}N ($^{15}\varepsilon_{k,NO_2} \approx -13‰$; Casciotti 2009). In the current study, we observed inverse kinetic isotope effects for both oxygen isotope fractionation ($^{18}\varepsilon_{k,NO_2}$) and nitrogen isotope fractionation ($^{15}\varepsilon_{k,NO_2}$) during nitrite oxidation (Table 3). The observed $^{18}\varepsilon_{k,NO_2}$ values were smaller in magnitude than the $^{15}\varepsilon_{k,NO_2}$ values in all cases, perhaps because the nitrite oxygen atoms are not directly involved with formation of the new bond, whereas the nitrogen atom is. Heavy isotope substitution for oxygen might be expected to lower the vibrational frequencies of the nitrite molecule overall but are expected to have a smaller, secondary effect on the oxidation rates of nitrite to nitrate.

The magnitude of isotopic fractionation was similar in *N. mobilis* and *Nitrobacter* species but significantly smaller in *N. marina*. These differences could be related to the location of nitrite oxidation (cytoplasm vs. periplasm), as discussed below for $^{18}\varepsilon_{k,H_2O,2}$, or differences in the enzyme active sites of the nitrite-oxidizing systems of these organisms. Substrate concentration dependence, which was observed to differing extents in our experiments (less in *Nitrospira* than in *Nitrobacter* or *Nitrococcus*), could also be exacerbated by the location of the nitrite-oxidizing system and the dependence on cellular transport of nitrite before oxidation. It has been shown in other systems that the concentration of substrate (nitrite, in this case) can have an effect on the expressed isotope effect because of transport limitation (Farquhar et al. 1982; Granger et al. 2004; Needoba et al. 2004). If lower nitrite concentrations cause diffusive limitation, there would be less expression of the enzyme isotope effect, and the transport isotope effect (which is commonly small and positive) would be expressed instead. Further experimentation to manipulate these experimental variables might reveal systematic changes in the $\delta^{18}O$ isotope effects for nitrite oxidation.

Interpretations of $\Delta(15,18)$—In the introduction of the nitrate isotope anomaly, $\Delta(15,18)$, Sigman et al. (2005) reasoned that this anomaly could be caused by two processes occurring in suboxic water columns: remineralization of newly fixed nitrogen and nitrite reoxidation. In modeling the contributions of these processes, the best available information about the oxygen isotope systematics of nitrification were used to assign a $\delta^{18}O$ of 0‰ for NO_3^- produced via nitrification and nitrite reoxidation. This was

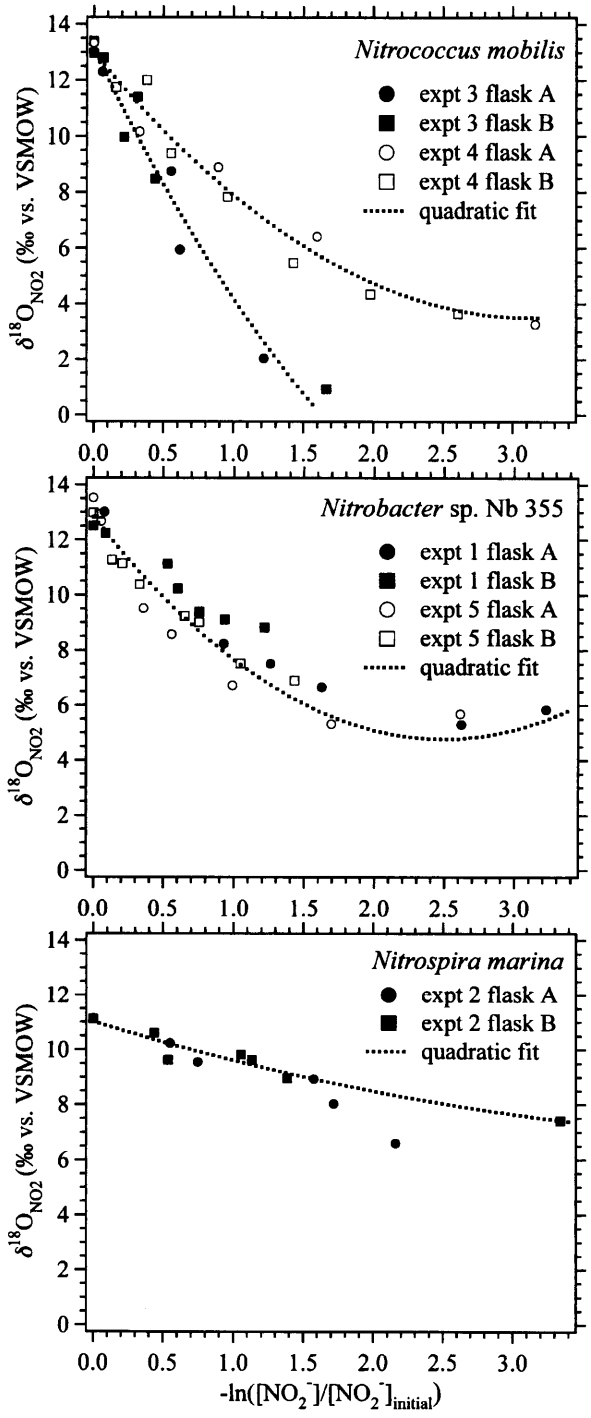

Fig. 5. Rayleigh plots for nitrite oxidation for three different species of bacteria in five different experiments. In panel A, quadratic fits are shown independently for experiments 3 and 4. In panel B, data are combined from experiments 1 and 5 to produce the fit. In panel C, the quadratic fit is shown for experiment 2. Derived values for $^{18}\varepsilon_{k,NO_2}$ are given in Table 3.

based on the assumptions that the produced nitrate reflects complete exchange of oxygen isotopes between nitrite and water (with no equilibrium isotope effect) followed by the addition of water with no isotope effect. Casciotti and McIlvin (2007) used much the same model for determining the amounts of nitrite reoxidation, remineralized newly fixed nitrogen, or both, except with the incorporation of an equilibrium isotope effect for equilibration between nitrite and water of +14‰.

Since then, our experiments have provided further insight into the mechanisms of variation in $\delta^{18}O_{NO_3}$ and the corresponding Δ(15,18) values. Our current results suggest that $\delta^{18}O_{NO_3}$ of microbially produced nitrate could be much lower than 0‰ (*see* below). Using these lower $\delta^{18}O_{NO_3}$ values, it would be more difficult to produce a the observed negative Δ(15,18) signals from either remineralization of newly fixed nitrogen or nitrite reoxidation. That is, a greater flux of nitrate from remineralization or reoxidation would be needed to generate the observed Δ(15,18) signals. Furthermore, interpretation of Δ(15,18) in the euphotic zone of Monterey Bay suggested that negative $\delta^{18}O$ values for microbially produced nitrate could even lead to positive Δ(15,18) anomalies in the euphotic zone, where nitrification supplies a large fraction of the available NO_3- (Wankel et al. 2007).

On the other hand, the inverse kinetic isotope effect for nitrite oxidation could also be expressed in and around suboxic zones where nitrite accumulates up to 10 μmol L^{-1}. In these regions, the observed $\delta^{18}O$ of nitrate is higher than the more constant deep ocean value, not only because of the fractionation imposed by the reduction of nitrate, but perhaps also from the reoxidation of nitrite to nitrate (Sigman et al. 2005; Casciotti and McIlvin 2007). An inverse isotope effect during nitrite oxidation would cause the $\delta^{18}O$ of nitrate to be higher than expected for a normal isotope effect, which has been previously assumed when interpreting Δ(15,18) values (Sigman et al. 2005; Casciotti and McIlvin 2007). In this case, an inverse kinetic isotope effect would make nitrite reoxidation more efficient at generating nitrate isotope anomalies, and perhaps less reoxidation would be required to explain a given Δ(15,18) anomaly.

Separating the effects of nitrite reoxidation and nitrogen fixation on Δ(15,18) in suboxic water columns remains a challenge, and additional lines of evidence are needed to determine the relative contribution of each process. We have proposed that the $\delta^{15}N$ difference between NO_2^- and NO_3^- ($\Delta\delta^{15}N = \delta^{15}N_{NO_3} - \delta^{15}N_{NO_2}$; Casciotti 2009) could provide an independent estimate of nitrite reoxidation. Nitrite oxygen isotope measurements might provide additional insight on this problem.

Implications for a global fixed nitrogen budget—The balance of oceanic fixed nitrogen inputs and outputs is currently poorly constrained. The isotopes of nitrogen and oxygen in deep-water nitrate can help constrain the sources and sinks of fixed nitrogen, although the best estimates of these fluxes are only possible with additional knowledge of isotope effects associated with each process. The $\delta^{18}O$ value of nitrate produced during nitrification is one important piece of information required to create a $\delta^{18}O$ budget for

Table 3. Measured $^{18}\varepsilon_{k,NO_2}$ and $^{15}\varepsilon_{k,NO_2}$ for three different species of nitrite-oxidizing bacteria.

Bacteria	Experiment	Flask	$^{18}\varepsilon_{k,NO_2}$ (‰)	Average $^{18}\varepsilon_{k,NO_2}$ (‰)	$^{15}\varepsilon_{k,NO_2}$ (‰)	Average $^{15}\varepsilon_{k,NO_2}$ (‰)
Nitrococcus mobilis	3	A	−10.2	−8.2±2.5	−20.8	−20.2±2.8
		B	−10.4		−22.0	
	4	A	−5.2		−16.0	
		B	−7.0		−21.8	
Nitrobacter sp. Nb 355	1	A	−5.8	−6.5±1.8	−18.1	−20.6±3.2
		B	−4.4		−17.5	
	5	A	−8.7		−23.1	
		B	−7.0		−23.6	
Nitrospira marina	2	A	−1.0	−1.3±0.4	−7.8	−9.1±1.8
		B	−1.5		−10.3	

oceanic nitrate and to interpret gradients in oceanic $\delta^{18}O_{NO_3}$ values.

From the results presented here, the value for $\delta^{18}O_{NO_3}$ produced by microbial nitrification in the ocean can now be estimated from Eq. 8, which is derived from Eq. 3 assuming $x_{NOB} = 0$.

$$\delta^{18}O_{NO_3\ produced} = \frac{2}{3}\delta^{18}O_{NO_2\ source} + \frac{1}{3}\left(\delta^{18}O_{H_2O} - {}^{18}\varepsilon_{k,H_2O,2}\right) \quad (8)$$

With the use of previously measured values for the $\delta^{18}O$ of nitrite produced by ammonia-oxidizing bacteria (−3.3‰ to +5.3‰; Casciotti et al. 2010), a $\delta^{18}O_{H_2O}$ value equal to 0‰ for seawater, and the $^{18}\varepsilon_{k,H_2O,2}$ measured here of +12.8‰ to +18.2‰, the expected range of nitrate $\delta^{18}O$ values produced during nitrification in seawater is −8.3‰ to −0.7‰ (Fig. 6). These $\delta^{18}O_{NO_3}$ values are much lower than those calculated neglecting oxygen isotope effects (+7.8‰ to +12‰) and are also lower than the $\delta^{18}O$ values of deep ocean nitrate (+1.5‰ to +2.5‰) that are required to balance the oceanic nitrate $\delta^{18}O$ budget against fractionating nitrogen loss fluxes.

Despite advances made in this study, a large range of values are still possible for the $\delta^{18}O$ of newly produced nitrate (Fig. 6). Whether this represents the true range of possible $\delta^{18}O_{NO_3}$ values or whether field populations have less inherent variability is unknown at this time. The two greatest sources of uncertainty are in the $\delta^{18}O$ of nitrite produced by ammonia oxidation (Casciotti et al. 2010) and the isotope effect for water incorporation by nitrite-oxidizing bacteria (this study).

This study has shown that oxygen isotope effects are expected to play an important role in setting the $\delta^{18}O$ of microbially produced nitrate in the sea, and would be

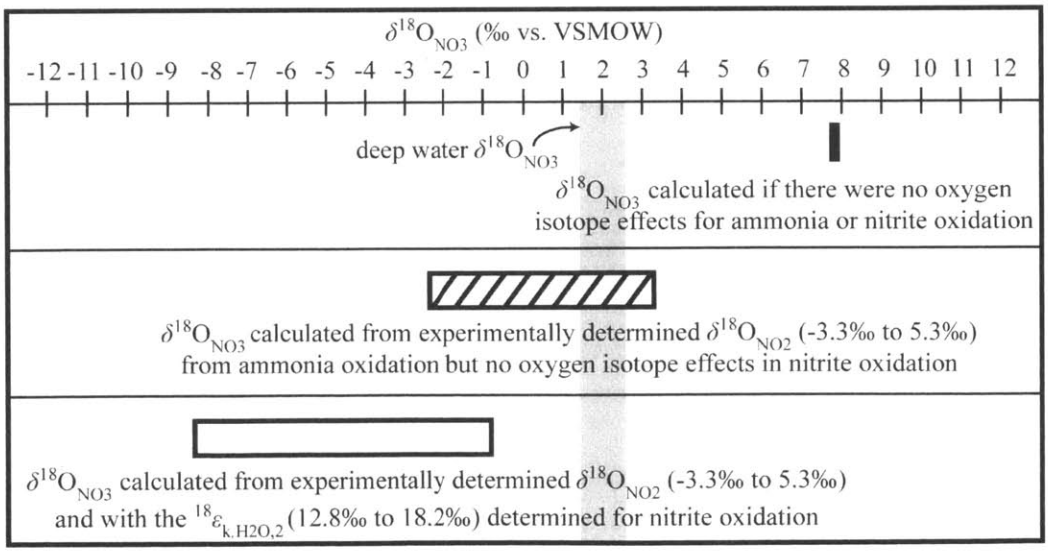

Fig. 6. Recalculation of the $\delta^{18}O$ of nitrate produced from nitrification with a $\delta^{18}O_{O_2}$ value of +23.5‰ and a $\delta^{18}O_{H_2O}$ of 0‰, and observed $\delta^{18}O_{NO_2}$ values from ammonia-oxidizing bacteria (Casciotti et al. 2010). Incorporating observed oxygen isotope effects for nitrite oxidation causes produced $\delta^{18}O_{NO_3}$ to be lower than that of deep ocean nitrate, which is needed to balance a fixed nitrogen budget using $\delta^{18}O$.

expected as well in other environments. We observed both inter- and intraspecies variability in $^{18}\varepsilon_{k,H_2O,2}$. The intraspecies variability can only be attributed to differences in the growth state of the culture at the time of each experiment because all other variables were kept constant between experiments. Although the source(s) of interspecies variability in $^{18}\varepsilon_{k,H_2O,2}$ are currently unknown, possible factors that could contribute to this variability include both real enzyme level differences among nitrite-oxidizing systems and apparent differences due to different cytoplasmic $\delta^{18}O_{H_2O}$ values. It is not known with certainty which of these factors might be most important; however, additional experiments with *Nitrospira*, which oxidizes nitrite in the periplasm, rather than in the cytoplasm, could provide insight into the nature of oxygen isotope fractionation during water incorporation.

The ultimate goal of our work is to understand and predict how these isotope effects are expressed by natural assemblages of bacteria and archaea in the ocean. Because there are not yet data on the oxygen isotope systematics of ammonia-oxidizing archaea, which may represent important contributors to the marine nitrogen cycle (Francis et al. 2007), working with these organisms in pure or mixed culture should be a priority. However, because other processes could simultaneously affect the nitrite and nitrate pools in mixed communities, care must be taken in interpreting such data. These concurrent processes might also have isotope effects associated with them, making it difficult to track the role that each process plays in the observed $\delta^{18}O$ variations of nitrate and nitrite pools if multiple parameters are unknown. However, progress is possible on this front with the use of different kinds of manipulative experiments, using ^{18}O-labeled H_2O in much the same way that we have here. These experiments could involve incubating field samples in the dark with or without added ammonia and determining the incorporation of H_2O into the nitrite and nitrate pools. Concurrent analysis of the microbial communities present will help us understand the microbes involved in the observed transformations.

Acknowledgments

We thank Frederica Valois and John Waterbury for generously providing the nitrite-oxidizing bacteria used in this study and Matthew McIlvin for his help processing isotope samples. We also thank the anonymous reviewers for their insightful comments and Erin Banning, Dan Rogers, Alyson Santoro, and Caitlin Frame for critiques of the manuscript. This research was supported by the National Science Foundation grant in Chemical Oceanography 05-26277 to K.L.C.

References

Andersson, K. K., and A. B. Hooper. 1983. O_2 and H_2O are each the source of one O in NO_2^- produced from NH_3 by *Nitrosomonas*: ^{15}N-NMR evidence. FEBS Letters **164:** 236–240.

Bender, M. L. 1990. The $\delta^{18}O$ of dissolved O_2 in sea water: A unique tracer of circulation and respiration in the deep-sea. J. Geophys. Res. **95:** 22,243–22,252, doi:10.1029/JC095iC12p22243

Böhlke, J. K., S. J. Mroczkowski, and T. B. Coplen. 2003. Oxygen isotopes in nitrate: New reference materials for O-18: O-17: O-16 measurements and observations on the nitrate–water equilibration. Rapid Commun. Mass Spectrom. **17:** 1835–1846.

Braman, R. S., and S. A. Hendrix. 1989. Nanogram nitrite and nitrate determination in environmental and biological materials by vanadium (III) reduction with chemiluminescence detection. Anal. Chem. **61:** 2715–2718, doi:10.1021/ac00199a007

Brandes, J. A., and A. H. Devol. 2002. A global marine-fixed nitrogen isotopic budget: Implications for Holocene nitrogen cycling. Glob. Biochem. Cycles **16:** 1–14.

Bunton, C. A., D. R. Llewellyn, and G. Stedman. 1959. Oxygen exchange between nitrous acid and water. J. Chem. Soc. **1959:** 568–573, doi:10.1039/jr9590000568

Casciotti, K. L. 2009. Inverse kinetic isotope fractionation during bacterial nitrite oxidation. Geochim. Cosmochim. Acta **73:** 2061–2076, doi:10.1016/j.gca.2008.12.022

———, J. K. Böhlke, M. R. McIlvin, S. J. Mroczkwski, and J. E. Hannon. 2007. Oxygen isotopes in nitrite: Analysis, calibration and equilibration. Anal. Chem. **79:** 2427–2436, doi:10.1021/ac061598h

———, and M. R. McIlvin. 2007. Isotopic analyses of nitrate and nitrite from reference mixtures and application to eastern Tropical North Pacific waters. Mar. Chem. **107:** 184–201, doi:10.1016/j.marchem.2007.06.021

———, ———, and C. Buchwald. 2010. Oxygen isotopic fractionation and exchange during bacterial ammonia oxidation. Limnol. Oceanogr **55:** 753–762.

———, D. M. Sigman, G. H. Hastings, J. K. Böhlke, and A. Hilkert. 2002. Measurement of the oxygen isotopic composition of nitrate in seawater and freshwater using the denitrifier method. Anal. Chem. **74:** 4905–4912, doi:10.1021/ac020113w

———, T. W. Trull, D. M. Glover, and D. Davies. 2008. Constraints on nitrogen cycling in the Subtropical North Pacific Station ALOHA from isotopic measurements of nitrate and particulate nitrogen. Deep-Sea Res. II **55:** 1661–1672.

Codispoti, L. A., J. A. Brandes, J. P. Christensen, A. H. Devol, S. W. A. Naqvi, H. W. Paerl, and T. Yoshinari. 2001. The oceanic fixed nitrogen and nitrous oxide budgets: Moving targets as we enter the anthropocene? Sci. Mar. **65:** 85–105, doi:10.3989/scimar.2001.65s285

Deutsch, C., D. M. Sigman, R. C. Thunell, A. N. Meckler, and G. H. Haug. 2004. Isotopic constraints on glacial/interglacial changes in the oceanic nitrogen budget. Glob. Biogeochem. Cycles **18:** GB4012, doi:10.1029/2003GB002189

DiSpirito, A. A., and A. B. Hooper. 1986. Oxygen-exchange between nitrate molecules during nitrite oxidation by *Nitrobacter*. J. Biol. Chem. **261:** 10,534–10,537.

Eppley, R. W., and B. J. Peterson. 1979. Particulate organic matter flux and planktonic new production in the deep ocean. Nature **282:** 677–680, doi:10.1038/282677a0

Epstein, S., and T. Mayeda. 1953. Variation in ^{18}O content of waters from natural sources. Geochim. Cosmochim. Acta **4:** 213–224, doi:10.1016/0016-7037(53)90051-9

Farquhar, G. D., M. H. O'Leary, and J. A. Berry. 1982. On the relationship between carbon isotope discrimination and the inter-cellular carbon-dioxide concentration in leaves. Aust. J. Plant. Physiol. **9:** 121–137, doi:10.1071/PP9820121

Francis, C. A., J. M. Beman, and M. M. M. Kuypers. 2007. New processes and players in the nitrogen cycle: the microbial ecology of anaerobic and archaeal ammonia oxidation. ISME Journal **1:** 19–27.

FRIEDMAN, S. H., W. MASSEFSKI, AND T. C. HOLLOCHER. 1986. Catalysis of intermolecular oxygen atom transfer by nitrite dehydrogenase of *Nitrobacter agilis*. J. Biol. Chem. **261:** 10,538–10,543.

GRANGER, J., D. M. SIGMAN, M. F. LEHMAN, AND P. D. TORTELL. 2008. Nitrogen and oxygen isotope fractionation during dissimilatory nitrate reduction by denitrifying bacteria. Limnol. Oceanogr. **53:** 2533–2545.

———, ———, J. A. NEEDOBA, AND P. J. HARRISON. 2004. Coupled nitrogen and oxygen isotope fractionation of nitrate during assimilation by cultures of marine phytoplankton, Limnol. Oceanogr. **49:** 1763–1773.

GRUBER, N. 2004. The dynamics of the marine nitrogen cycle and atmospheric CO_2, p. 97–148. *In* T. Oguz and M. Follows [eds.], Carbon climate interaction. Kluwer.

———, AND J. L. SARMIENTO. 1997. Global patterns of marine nitrogen fixation and denitrification. Glob. Biogeochem. Cycles **11:** 235–266, doi:10.1029/97GB00077

KUMAR, S., D. J. D. NICHOLAS, AND E. H. WILLIAMS. 1983. Definitive N-15 NMR evidence that water serves as a source of O during nitrite oxidation by *Nitrobacter-agilis*. FEBS Lett. **152:** 71–74, doi:10.1016/0014-5793(83)80484-0

LEHMANN, M. F., D. M. SIGMAN, AND W. M. BERELSON. 2004. Coupling the $^{15}N/^{14}N$ and $^{18}O/^{16}O$ of nitrate as a constraint on benthic nitrogen cycling. Mar. Chem. **88:** 1–20.

MARIOTTI, A., J. C. GERMON, P. HUBERT, P. KAISER, R. LETOLLE, A. TARDIEUX, AND P. TARDIEUX. 1981. Experimental determination of nitrite kinetic isotope fractionation: Some principles; illustration for the denitrification and nitrification processes. Plant Soil **62:** 413–430, doi:10.1007/BF02374138

MCILVIN, M. R., AND M. A. ALTABET. 2005. Chemical conversion of nitrate and nitrite to nitrous oxide and nitrogen and oxygen isotopic analysis in freshwater and seawater. Anal. Chem. **77:** 5589–5595, doi:10.1021/ac050528s

———, AND K. L. CASCIOTTI. 2006. Method for the analysis of $\delta^{18}O$ in water. Anal. Chem. **78:** 2377–2381, doi:10.1021/ac051838d

NEEDOBA, J. A., D. M. SIGMAN, AND P. J. HARRISON. 2004. The mechanism of isotope fractionation during algal nitrate assimilation as illuminated by the $^{15}N/^{14}N$ of intracellular nitrate. J. Phycol. **40:** 517–522, doi:10.1111/j.1529-8817.2004.03172.x

SCOTT, K. M., X. LU, C. M. CAVANAUGH, AND J. S. LIU. 2004. Optimal methods for estimating kinetic isotope effects from different forms of the Rayleigh distillation equation. Geochim. Cosmochim. Acta **68:** 433–442, doi:10.1016/S0016-7037(03)00459-9

SIGMAN, D. M., K. L. CASCIOTTI, M. ANDREANI, C. BARFORD, M. GALANTER, AND J. K. BOHLKE. 2001. A bacterial method for the nitrogen isotopic analysis of nitrate in seawater and freshwater. Anal. Chem. **73:** 4145–4153, doi:10.1021/ac010088e

———, P. J. DIFIORE, M. P. HAIN, C. DEUTSCH, Y. WANG, D. M. KARL, A. N. KNAPP, M. F. LEHMANN, AND S. PANTOJA. 2009. The dual isotopes of deep nitrate as a constraint of the cycle and budget of oceanic fixed nitrogen. Deep-Sea Res. Part I Oceanogr. Res. Pap. **56:** 1419–1439, doi:10.1016/j.dsr.2009.04.007

———, J. GRANGER, P. J. DIFIORE, M. M. LEHMANN, R. HO, G. CANE, AND A. VAN GREEN. 2005. Coupled nitrogen and oxygen isotope measurements of nitrate along the eastern North Pacific margin. Glob. Biogeochem. Cycles **19:** 1–14, doi:10.1029/2005GB002458

STRICKLAND, J. D. H., AND T. R. PARSONS. 1972. A practical handbook of seawater analysis. Bull. Fish. Res. Bd. Can. **167:** 1–310.

WANKEL, S. D., C. KENDALL, J. T. PENNINGTON, F. P. CHAVEZ, AND A. PAYTON. 2007. Nitrification in the euphotic zone as evidenced by nitrate dual isotopic composition: Observations from Monterey Bay, California. Glob. Biogeochem. Cycles **21:** GB2009, doi:10.1029/2006GB002723

WATSON, S. W., AND J. B. WATERBURY. 1971. Characteristics of two marine nitrite oxidizing bacteria, *Nitrospina gracilis* nov. gen. nov. sp. and *Nitrococcus mobilis* nov. gen. nov. sp. Arch. Microbiol. **77:** 203–230.

Associate editor: Robert R. Bidigare

Received: 30 July 2009
Accepted: 03 December 2009
Amended: 11 December 2009

Chapter 3

Oxygen isotope composition of nitrite and nitrate produced by nitrifying cocultures and natural marine assemblages

Carolyn Buchwald, Alyson E. Santoro, Matthew R. McIlvin and Karen L. Casciotti

This chapter was originally published in Limnology and Oceanography and is reprinted here with their permission.

Buchwald, C., Santoro, A. E., McIlvin, M. R. and K. L. Casciotti. 2012. Oxygen isotope composition of nitrite and nitrate produced by nitrifying cocultures and natural marine assemblages. *Limnol. Oceanogr.* **57:** 1361-1375.

Limnol. Oceanogr., 57(5), 2012, 1361–1375

doi:10.4319/lo.2012.57.5.1361

Oxygen isotopic composition of nitrate and nitrite produced by nitrifying cocultures and natural marine assemblages

Carolyn Buchwald,[a,*] Alyson E. Santoro,[b,1] Matthew R. McIlvin,[b] and Karen L. Casciotti [b,2]

[a] Massachusetts Institute of Technology/ Woods Hole Oceanographic Institution Joint Program in Chemical Oceanography, Woods Hole Oceanographic Institution, Woods Hole, Massachusetts

[b] Marine Chemistry and Geochemistry Department, Woods Hole Oceanographic Institution, Woods Hole, Massachusetts

Abstract

The $\delta^{18}O$ value of nitrate produced during nitrification ($\delta^{18}O_{NO_3,nit}$) was measured in experiments designed to mimic oceanic conditions, involving cocultures of ammonia-oxidizing bacteria or ammonia-oxidizing archaea and nitrite-oxidizing bacteria, as well as natural marine assemblages. The estimates of $\delta^{18}O_{NO_3,nit}$ ranged from −1.5‰ ± 0.1‰ to +1.3‰ ± 1.4‰ at $\delta^{18}O$ values of water (H_2O) and dissolved oxygen (O_2) of 0‰ and 24.2‰ vs. Vienna Standard Mean Ocean Water, respectively. Additions of ^{18}O-enriched H_2O allowed us to evaluate the effects of oxygen (O) isotope fractionation and exchange on $\delta^{18}O_{NO_3,nit}$. Kinetic isotope effects for the incorporation of O atoms were the most important factors for setting overall $\delta^{18}O_{NO_3,nit}$ values relative to the substrates (O_2 and H_2O). These isotope effects ranged from +10‰ to +22‰ for ammonia oxidation (O_2 plus H_2O incorporation) and from +1‰ to +27‰ for incorporation of H_2O during nitrite oxidation. $\delta^{18}O_{NO_3,nit}$ values were also affected by the amount and duration of nitrite accumulation, which permitted abiotic O atom exchange between nitrite and H_2O. Coculture incubations where ammonia oxidation and nitrite oxidation were tightly coupled showed low levels of nitrite accumulation and exchange (3% ± 4%). These experiments had $\delta^{18}O_{NO_3,nit}$ values of −1.5‰ to +0.7‰. Field experiments had greater accumulation of nitrite and a higher amount of exchange (22% to 100%), yielding an average $\delta^{18}O_{NO_3,nit}$ value of +1.9‰ ± 3.0‰. Low levels of biologically catalyzed exchange in coculture experiments may be representative of nitrification in much of the ocean where nitrite accumulation is low. Abiotic oxygen isotope exchange may be important where nitrite does accumulate, such as oceanic primary and secondary nitrite maxima.

A supply of bioavailable nitrogen (N) in the form of nitrate (NO_3^-) is important for primary production and carbon export to the deep ocean (Eppley and Peterson 1979), and understanding the oceanic nitrate budget is essential to understanding past, present, and future ocean productivity (Codispoti et al. 2001). Stoichiometry-based geochemical estimates of the oceanic nitrate budget often return a nearly balanced budget, albeit with large uncertainties (Gruber and Sarmiento 1997; Gruber and Galloway 2008). Construction of an oceanic nitrate budget based on $\delta^{15}N$ ($\delta^{15}N$ (‰) = ($^{15}N/^{14}N_{sample} \div {}^{15}N/^{14}N_{standard} - 1) \times 1000$) leads to a budget with sinks (burial, denitrification, and anammox) far outweighing the sources (N fixation, continental runoff, and atmospheric deposition; Brandes and Devol 2002; Deutsch et al. 2004). Because sedimentary records are inconsistent with such an imbalance (Deutsch et al. 2004; Altabet 2007), this prediction demonstrates gaps in our understanding of the oceanic nitrogen budget and its isotopic systematics.

Since the development of the denitrifier method for isotopic analysis of nitrate (Sigman et al. 2001; Casciotti et al. 2002), many studies have focused on the use of coupled N and oxygen (O) isotopes in nitrate to help constrain oceanic N cycling and the nitrate budget. The value of the coupled isotope approach is that the $\delta^{18}O$ ($\delta^{18}O$ (‰) = ($^{18}O/^{16}O_{sample} \div {}^{18}O/^{16}O_{standard} - 1) \times 1000$) value of nitrate ($\delta^{18}O_{NO_3}$) is set by a different set of processes than its $\delta^{15}N$ value ($\delta^{15}N_{NO_3}$) (Sigman et al. 2005). Water column denitrification, sedimentary denitrification, and nitrate assimilation are processes that fractionate N and O isotopes equally (Granger et al. 2004; Granger et al. 2008), but nitrate regeneration can decouple the N and O isotopes in nitrate (Sigman et al. 2009). During nitrate uptake and regeneration, N atoms are recycled between fixed N pools, while O atoms are removed, then replaced by the nitrification process. Therefore, while the N isotope budget is sensitive only to input (nitrogen fixation) and output (denitrification) processes, the O isotopes in nitrate are sensitive to internal cycling (assimilation, regeneration, nitrification) as well. To determine the relative amounts of water column denitrification and sedimentary denitrification using the $\delta^{18}O$ values of deep ocean nitrate, it is necessary to account for the nitrate $\delta^{18}O$ variations caused by internal cycling, and a key parameter here is the $\delta^{18}O$ value of nitrate produced by nitrification ($\delta^{18}O_{NO_3,nit}$).

The microbial process of nitrification is carried out in two main steps: ammonia oxidation to nitrite, followed by nitrite oxidation to nitrate (Fig. 1). $\delta^{18}O_{NO_3,nit}$ is determined by the $\delta^{18}O$ values of O atom sources (O_2 and H_2O; Andersson and Hooper 1983; Kumar et al. 1983), the amount of O atom exchange between nitrite and H_2O (x), and the isotope effects involved with O atom incorporation

* Corresponding author: cbuchwald@whoi.edu

Present addresses:

[1] Horn Point Laboratory, University of Maryland Center for Environmental Science, Cambridge, Maryland

[2] Department of Environmental Earth System Science, Stanford University, Stanford, California

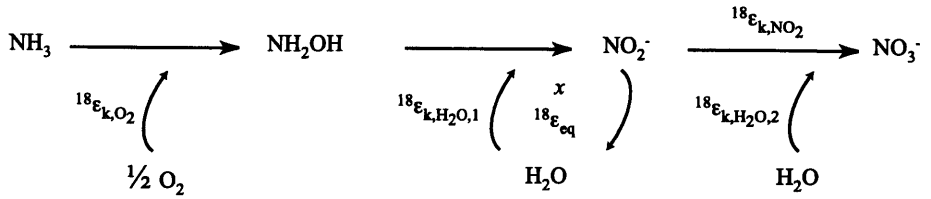

Fig. 1. Nitrification pathway showing oxygen atom sources with isotope effects for incorporation and exchange.

($^{18}\varepsilon_{k,O_2}$, $^{18}\varepsilon_{k,H_2O,1}$, $^{18}\varepsilon_{k,H_2O,2}$) and exchange ($^{18}\varepsilon_{eq}$; Casciotti et al. 2010; Buchwald and Casciotti 2010). In the deep ocean, $\delta^{18}O_{H_2O}$ values vary little (−0.5‰ to +0.5‰ vs. Vienna Standard Mean Ocean Water [VSMOW]; Epstein and Mayeda 1953), while $\delta^{18}O_{O_2}$ values range from +24.2‰ to near +36‰ vs. VSMOW (Bender 1990). The $\delta^{18}O$ value of deep ocean nitrate, which sets an upper limit on $\delta^{18}O_{NO_3,nit}$, is less than +2.5‰ vs. VSMOW on average and varies little (± 1.0‰) relative to variations in $\delta^{18}O_{O_2}$ in the ocean interior (Casciotti et al. 2002; Sigman et al. 2009). These features of oceanic $\delta^{18}O_{NO_3}$ (low $\delta^{18}O$ value and little variation in intermediate and deep water) would seem to argue against retention of O from O_2 introduced during ammonia oxidation.

Early studies of ammonia oxidation suggest that a large amount of oxygen isotope exchange may occur between nitrite and H_2O, consistent with a loss of the primary O_2 signal (Dua et al. 1979; Andersson et al. 1982). Therefore, efforts to use $\delta^{18}O_{NO_3}$ values as constraints on oceanic nitrogen cycling have generally assumed that $\delta^{18}O_{NO_3,nit}$ is equal to that of seawater (near 0‰ vs. VSMOW) due to full equilibration of nitrite with H_2O during ammonia oxidation (Casciotti and McIlvin 2007; DiFiore et al. 2009; Sigman et al. 2009). However, equilibration between nitrite and H_2O has recently been shown to involve a temperature-dependent equilibrium isotope effect between nitrite and H_2O of +11‰ to +15‰ (Casciotti et al. 2007; C. Buchwald and K. L. Casciotti unpubl.). Full expression of the equilibrium isotope effect during nitrification, or abiotic exchange thereafter, should lead to production of nitrite with $\delta^{18}O$ values of +11‰ to +15‰ vs. VSMOW. While incorporation of H_2O during nitrite oxidation can lower the $\delta^{18}O$ value of the final nitrate produced, in order to achieve $\delta^{18}O_{NO_3}$ source values near 0‰, H_2O incorporation would need to occur with an isotope effect ($^{18}\varepsilon_{k,H_2O,2}$) of approximately 28‰, which is larger than has been observed to date (12.8‰ to 18.2‰; Buchwald and Casciotti 2010).

Some recent experiments accounting for abiotic exchange have shown that ammonia oxidation is likely to retain a significant fraction of the O atoms incorporated from O_2 (Casciotti et al. 2010). These experiments also demonstrated that isotopic fractionation associated with O atom incorporation during ammonia oxidation (Casciotti et al. 2010) and nitrite oxidation (Buchwald and Casciotti 2010) provides an additional mechanism for achieving low $\delta^{18}O_{NO_3,nit}$ values with incomplete O atom exchange. Putting together results from laboratory monoculture experiments, Buchwald and Casciotti (2010) predicted $\delta^{18}O_{NO_3,nit}$ = −8.3‰ to −0.7‰ in seawater with $\delta^{18}O_{H_2O}$ = 0‰ and $\delta^{18}O_{O_2}$ = +24.2‰. The large range in predicted $\delta^{18}O_{NO_3,nit}$ occurred as a result of variations in the amount of exchange and kinetic isotope fractionation expressed during ammonia oxidation and nitrite oxidation among the different bacterial species studied. While these values span the range required to explain a deep ocean $\delta^{18}O_{NO_3}$ value of +2.5‰, they lack sufficient predictive power for use in interpretation or modeling of oceanic nitrate isotope distributions. Determination of the oxygen isotopic exchange and fractionation during nitrification under natural environmental conditions is therefore critical to predicting the source of $\delta^{18}O$ in nitrate and its variation with seawater $\delta^{18}O_{H_2O}$ and $\delta^{18}O_{O_2}$.

The goal of this study was to determine the $\delta^{18}O$ value of nitrate that is produced during nitrification under more natural conditions than the previous experiments, using mixed communities where ammonia oxidation and nitrite oxidation are tightly coupled. Laboratory cocultures of ammonia-oxidizing bacteria (AOB) or archaea (AOA) with nitrite-oxidizing bacteria (NOB) and natural microbial assemblages from temperate and tropical ocean sites were used to examine the importance of nitrite accumulation (magnitude and duration) and isotopic exchange on the resulting $\delta^{18}O_{NO_3}$ values. This information is important for evaluating the factors controlling the $\delta^{18}O$ value of newly produced nitrate and interpreting $\delta^{18}O_{NO_3}$ in the ocean.

Methods

Culture maintenance—Three cultures were used in paired laboratory coculture experiments: *Nitrosomonas* sp. C-113a, a marine AOB isolated from the Red Sea (Ward and Carlucci 1985); CN25, an AOA enrichment from the California Current (Santoro and Casciotti 2011); and *Nitrococcus mobilis*, a marine NOB isolated from the Galapagos Islands (Watson and Waterbury 1971). Maintenance batch cultures of C-113a were grown in Watson medium (Watson 1965) with 10 mmol L^{-1} NH_4^+. The ammonia-oxidizing archaeal enrichment was grown in oligotrophic North Pacific medium consisting of 0.2-μm–filtered North Pacific surface seawater amended with 10–100 μmol L^{-1} NH_4Cl, 1 mL L^{-1} chelated trace elements solution (Balch et al. 1979), and 2 mg L^{-1} KH_2PO_4 (Santoro and Casciotti 2011). The nitrite-oxidizing species, *N. mobilis*, was grown in batch culture in medium with 75% artificial seawater and 25% distilled water amended with 400 μmol L^{-1} $MgSO_4$, 30 μmol L^{-1} $CaCl_2$, 5 μmol L^{-1} K_2HPO_4, 2.3 μmol L^{-1} Fe(III)-ethylenediaminetetraacetic acid ("Geigy iron"), 0.1 μmol L^{-1} Na_2MoO_4, 0.25 μmol L^{-1} $MnCl_2$, 0.002 μmol L^{-1} $CoCl_2$, 0.08 μmol L^{-1} $ZnSO_4$, and 10 mmol L^{-1} NO_2^- (Watson and Waterbury 1971).

Coculture experimental conditions—Two types of coculture experiments were conducted in the laboratory: (1) cocultures of C-113a and *N. mobilis* and (2) cocultures of an ammonia-oxidizing archaeal enrichment (CN25) and *N. mobilis* (Table 1; Fig. 2). Incubations of C-113a and *N. mobilis* were conducted in Watson medium made with artificial seawater and an initial ammonium concentration of 50 μmol L^{-1}. To ensure consistent behavior with previous experiments, monoculture incubations of each bacterium were run in parallel. Finally, abiotic equilibration of nitrite O atoms with H_2O was tracked through incubation of abiotic controls (uninoculated sterile media) with 50 μmol L^{-1} nitrite added.

For each coculture experiment (CCE), media with four different $\delta^{18}O_{H_2O}$ values (between −5‰ and +216‰) were prepared in replicate 200-mL volumes with additions of 0, 2.5, 5, and 10 mL of ^{18}O-enriched ($\delta^{18}O_{H_2O}$ = +5000‰) water. Cells for each CCE were harvested from maintenance cultures by filtration (200 mL for AOB and 10 mL for NOB, to achieve similar cell densities). Filtered cells were washed and resuspended in 8 mL of filtered artificial seawater, then added to the incubation bottles (1 mL per bottle). In CCE 4, three parallel treatments were carried out with AOB and three different volumes of NOB inoculum (1 mL, 100 μL, or 10 μL concentrated cell suspension), which yielded approximately 1.7×10^4, 1.7×10^3, 1.7×10^2 cells mL^{-1}, respectively. Each inoculum level was incubated with four different $\delta^{18}O_{H_2O}$ media, as described above. In CCEs 1, 2, and 4, subsamples of 15 mL were collected throughout the incubations to monitor changes in the concentrations of ammonia, nitrite, and nitrate over time (3–16 d). In CCE 3 only initial and final (22 d) time points were collected.

The incubations involving AOA enrichments were initiated by splitting a 1-liter batch culture among eight different bottles, rather than filtering and resuspending the cells, which has a deleterious effect on AOA growth. Four of the eight bottles were inoculated with NOB, and four were incubated without NOB. For the incubations including NOB, 10 mL of *N. mobilis* cells were filtered, washed, and resuspended in 4 mL of filtered seawater, then injected into the four coculture bottles (1 mL per bottle). Both sets of four bottles were comprised of four media $\delta^{18}O_{H_2O}$ values, achieved by additions of ^{18}O-enriched water ($\delta^{18}O_{H_2O}$ = +5000‰) as described above. Because the AOA cultures were maintained in their spent medium, each experiment began with preexisting nitrite and ammonium. At the beginning of the coculture experiments, ammonium was amended to a total of 100 μmol L^{-1} in each bottle. Samples were collected initially and periodically over the course of 23–59 d to monitor changes in the concentrations and isotopic composition of nitrite and nitrate over time. Bottles of sterile AOA medium with varying $\delta^{18}O_{H_2O}$ additions were spiked with 100 μmol L^{-1} ammonium and 100 μmol L^{-1} nitrite and sampled in parallel to assess abiotic exchange rates in this medium.

Natural community experiments—Three field experiments (FEs) were conducted using surface water collected from Vineyard Sound in Woods Hole, Massachusetts in September 2009, October 2009, and March 2010. Nine field experiments were conducted on a cruise to the Costa Rica Upwelling Dome (CRD) in July 2010 (MV1008), only three of which were successful and will be discussed here. Finally, two field experiments were conducted in the Eastern Tropical South Pacific (ETSP) in March–April 2011 (MV1104).

Vineyard Sound surface water was bucket sampled into 4-liter amber bottles, which were rinsed with sample water prior to filling and brought back to the laboratory to initiate experiments. In each of the first two Vineyard Sound experiments (FEs 7 and 8), three large (1 liter) bottles of natural seawater were incubated with 50 μmol L^{-1} ammonium but no ^{18}O-enriched water, and 12 smaller (160 mL) serum bottles were incubated with different amounts of ^{18}O-enriched water in addition to the added ammonium. Nitrification was never detected in the 160-mL bottles, and they will not be discussed further. In FE 9, 500 mL of water was incubated in four different Erlenmeyer flasks that each received 50 μmol L^{-1} ammonium and a different amount (0, 2.5, 5, or 10 mL) of ^{18}O-enriched water ($\delta^{18}O_{H_2O}$ = +5000‰). In FE 9, 500 mL of sea water was also 0.22-μm filtered and then incubated with nitrite in a sterile flask with 10 mL of ^{18}O-enriched water to monitor abiotic exchange. All experiments were initiated by the addition of ammonium and then monitored and subsampled during conversion to nitrite and nitrate over a period of 50 to 84 d.

Successful incubations from the CRD were set up using water from the surface (2 m) and from the primary nitrite maximum (20 m) at one station (10°8′N, 93°0′W, Sta. 3) and the primary nitrite maximum (30 m) at another station (8°59′N, 90°30′W, Sta. 2). At each station and depth, whole water was collected from 100-liter Niskin bottles and split among eight 500-mL acid-cleaned clear polycarbonate bottles (to have duplicate incubations at each $\delta^{18}O_{H_2O}$ value). Four bottles were also set up as abiotic controls by 0.2-μm filtering water from the same depths into acid-cleaned polycarbonate bottles. Each experiment received the ^{18}O-enriched H_2O spikes and a starting ammonium concentration of 50 μmol L^{-1} and was subsampled over a period of 67, 113, or 98 d.

Nearly identical incubations were set up using water from the surface (2 m) and from just below the primary nitrite maximum (111 m) in the ETSP (10°0′S, 89°59′W). The main difference was that at each depth, two sets of eight acid-cleaned polycarbonate bottles were set up with lower starting ammonium concentrations (one set at 1 μmol L^{-1} and the second set at 5 μmol L^{-1}). Bottles were subsampled periodically to check nitrite concentrations but were only sampled for $\delta^{18}O_{NO_3}$ measurements initially and after full conversion of ammonium to nitrate (180 d).

Concentration analysis—Ammonium concentrations were measured using the indophenol blue assay (Solorzano 1969). Nitrite concentrations were measured using the Greiss–Ilosvay colorimetric method (Strickland and Parsons 1972). Ammonium and nitrite samples were measured at wavelengths of 640 and 543 nm, respectively, on an

Table 1. Summary of experiments.

Expt	Organisms or field location and depth	Duration of incubation (d)	Days of nitrite accumulation	Maximum accumulated nitrite (μmol L^{-1})	Δ[Nitrate] ÷ Δ[Ammonium]	$\delta^{18}O_{H_2O}$ (‰ vs. VSMOW)*	$\delta^{18}O_{NO_3,nit}$ (‰ vs. VSMOW)†
1	C-113a, *N. mobilis*	3	2	4.0	0.91	−5.4	−5.2
				4.0	0.90	−5.4	−5.3
				4.0	0.89	17.7	10.8
				4.0	0.90	17.7	10.8
				4.0	0.90	40.5	26.6
				4.0	0.88	40.7	26.9
				4.0	0.90	85.6	58.1
				4.0	0.92	85.7	58
2	C-113a, *N. mobilis*	5.4	3.5	1.1	0.98	−5.8	−5.7
				1.1	1.05	−5.8	−5.2
				1.1	0.98	85.4	56.7
				1.1	1.01	85.4	56.9
3	C-113a, *N. mobilis*	nd	nd	nd	0.98	−5.2	−4.3
				nd	1.04	−5.2	−4.4
				nd	0.99	48.8	30.8
				nd	0.96	48.8	30.9
				nd	0.97	106.1	68.2
				nd	0.99	106.1	68.0
				nd	1.01	216.0	137.3
				nd	1.07	216.0	140.1
4a	C-113a, *N. mobilis*	3.25	3	1.4	1.04	−5.3	−5.3
				1.4	1.18	16.9	10.9
				1.3	1.15	39.6	25.4
				1.2	1.09	82.1	54.8
4b	C-113a, *N. mobilis*	7.25	7	25.5	1.18	−6.9	−4.0
				25.2	0.96	17.3	12.2
				24.9	0.99	39.5	28.1
				24.2	1.18	81.2	58.6
4c	C-113a, *N. mobilis*	16.25	16	45.1	1.16	−5.2	−3.7
				45.5	0.99	17.1	12.9
				45.8	1.01	39.4	30.3
				45.1	0.97	81.1	61.3
5	AOA enrichment, *N. mobilis*	23	15	1.7	0.79	0.2	−1.4
				1.9	1.04	19.6	11.7
				1.1	1.06	37.2	23.8
				0.9	0.95	75.5	50.4
6	AOA enrichment, *N. mobilis*	59	nd	1.7	1.09	−0.4	0.4
				1.9	1.00	20.1	14.1
				1.1	1.15	41.3	20.0
				0.9	1.14	80.5	54.1
7	Vineyard Sound 1, surface	59	13–39	46.7	1.24	−1.5	0.5
				49.2	1.09	−1.5	1.3
8	Vineyard Sound 2, surface	50	10–39	48.4	0.99	−1.8	−0.3
				47.2	1.09	−1.8	−0.7
				47.9	1.05	−1.8	−0.1
9	Vineyard Sound 3, surface	84	nd	52.0	1.05	−2.2	2.7
				52.1	1.07	22.1	22.8
				51.9	1.07	44.4	45.4
				51.4	1.04	90.7	83.0
10	Costa Rica Dome, Sta. 2 (30 m)	79	26–58	41.6	0.93	−0.1	0.6
				35.0	0.92	−0.0	0.1
				31.4	0.91	22.2	24.5
				26.6	0.94	21.5	20.2
				32.7	0.86	43.5	46.4
				36.1	0.87	88.8	88.3
				38.7	0.88	85.1	90.6
11	Costa Rica Dome, Sta. 3 (2 m)	93	na	46.5	0.14	−0.3	na
				44.3	0.14	0.0	na
				44.7	0.11	22.3	na

Table 1. Continued.

Expt	Organisms or field location and depth	Duration of incubation (d)	Days of nitrite accumulation	Maximum accumulated nitrite (μmol L^{-1})	Δ[Nitrate] ÷ Δ[Ammonium]	$\delta^{18}O_{H_2O}$ (‰ vs. VSMOW)*	$\delta^{18}O_{NO_3,nit}$ (‰ vs. VSMOW)†
				44.7	0.11	21.8	na
				44.7	0.14	42.9	na
				46.4	0.20	87.6	na
				31.2	0.05	86.5	na
12	Costa Rica Dome, Sta. 3 (20 m)	113	na	46.3	0.13	−0.1	na
				46.8	0.11	22.6	na
				46.5	0.13	21.3	na
				42.0	0.04	42.3	na
13	Eastern Tropical South Pacific, Sta. 9 (111 m)	nd	nd	nd	1.61	0.2	3.5
				nd	1.53	0.5	5.2
				nd	1.46	22.1	18.8
				nd	1.50	22.5	20.7
				nd	1.87	46.3	37.7
				nd	1.44	45.4	44.2
				nd	1.47	89.1	76.9
				nd	1.57	82.6	69.6

nd, not determined because there was too little nitrite or sampled too infrequently; na, not applicable because nitrate was not produced.
* Uncertainties in $\delta^{18}O_{H_2O}$ were less than 0.5‰.
† Uncertainties in $\delta^{18}O_{NO_3}$ were less than 0.5‰.

Amersham Biosciences Ultrospec 2100 spectrophotometer using a Gilson 220XL autosampler. Nitrate plus nitrite was measured using hot vanadium reduction to nitric oxide (Cox 1980; Garside 1982) and detection on a Monitor Labs Nitrogen Oxides Detector (model No. 8840). Bracketing standards were used for each method, with concentrations ranging from 0 to 100 μmol L^{-1}. Measurement precision was 0.2 μmol L^{-1} for all methods.

Isotopic analysis—Nitrite $\delta^{15}N$ and $\delta^{18}O$ measurements were made using the azide method (McIlvin and Altabet 2005). Samples were analyzed in duplicate against three standards with known isotopic values: N-23, N-7373, and N-10219 (Casciotti et al. 2007), which were analyzed in triplicate with each run and are reported in per mil (‰) notation vs. atmospheric N_2 (air) for $\delta^{15}N$ and vs. VSMOW for $\delta^{18}O$ measurements. Sample volumes were injected to obtain 5–20 nmoles of N_2O with matching standard amounts. The standard deviation for $\delta^{15}N_{NO_2}$ and $\delta^{18}O_{NO_2}$ analyses was better than 0.2‰ and 0.3‰, respectively, within and between runs.

Water $\delta^{18}O$ values were measured by equilibration of oxygen atoms with nitrite, followed by a modified azide method (McIlvin and Casciotti 2006). Samples were analyzed in duplicate and reported on the VSMOW reference scale by calibration against replicate $\delta^{18}O_{H_2O}$ and $\delta^{18}O_{NO_2}$ reference materials analyzed in parallel (McIlvin and Casciotti 2006). The standard deviation for $\delta^{18}O_{H_2O}$ analyses is 0.3‰, within and between runs.

Nitrate $\delta^{15}N$ and $\delta^{18}O$ values were measured using the denitrifier method (Sigman et al. 2001; Casciotti et al. 2002; McIlvin and Casciotti 2011). Samples were analyzed in

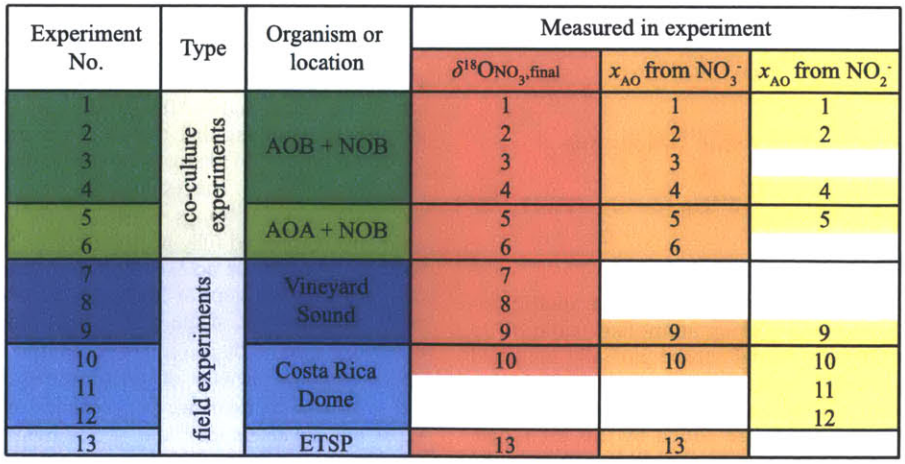

Fig. 2. A schematic of the experiments indicating the parameters that were measured in each experiment.

duplicate against three reference materials with known isotopic values: USGS32, USGS34, and USGS35 (Böhlke et al. 2003) and are reported vs. air for $\delta^{15}N$ and VSMOW for $\delta^{18}O$. Each reference material was analyzed six times per set of 60 samples. The standard deviation for $\delta^{15}N_{NO_3}$ and $\delta^{18}O_{NO_3}$ analyses was better than 0.2‰ and 0.3‰, respectively, within and between runs. Samples containing both nitrite and nitrate were treated with sulfamic acid to remove nitrite prior to nitrate isotopic analysis (Granger and Sigman 2009).

Calculating exchange and kinetic isotope effects—$\delta^{18}O_{NO_2}$ and $\delta^{18}O_{NO_3}$ produced during nitrification ($\delta^{18}O_{NO_2,nit}$ and $\delta^{18}O_{NO_3,nit}$, respectively) depend on many factors, including the $\delta^{18}O$ values of substrates ($\delta^{18}O_{O_2}$ and $\delta^{18}O_{H_2O}$), isotopic fractionation associated with incorporation of these substrates during ammonia oxidation ($^{18}\varepsilon_{k,O_2}$, $^{18}\varepsilon_{k,H_2O,1}$) and nitrite oxidation ($^{18}\varepsilon_{k,H_2O,2}$), and oxygen isotope exchange between nitrite and H_2O ($^{18}\varepsilon_{eq}$; Fig. 1; Casciotti et al. 2010, 2011; Snider et al. 2010). The fraction of nitrite oxygen atoms exchanged with H_2O during nitrite oxidation (x_{NO}) is generally negligible (Kumar et al. 1983; DiSpirito and Hooper 1986; Buchwald and Casciotti 2010), while the exchange during ammonia oxidation (x_{AO}) is highly variable and dependent on organism and growth conditions (Dua et al. 1979; Andersson et al. 1982; Casciotti et al. 2010). The oxygen isotope effect for nitrite oxidation ($^{18}\varepsilon_{k,NO_2}$) will also affect $\delta^{18}O_{NO_2}$ and $\delta^{18}O_{NO_3}$ if nitrite oxidation is incomplete (Buchwald and Casciotti 2010) but is excluded here in the formulation for $\delta^{18}O_{NO_3,final}$.

Equation 1 describes the $\delta^{18}O_{NO_2}$ produced through ammonia oxidation (Casciotti et al. 2010), and Eq. 2 describes the $\delta^{18}O_{NO_3}$ produced when nitrite oxidation goes to completion ($\delta^{18}O_{NO_3,final}$; Buchwald and Casciotti 2010). The symbols are as defined above.

$$\delta^{18}O_{NO_2} = \left[\frac{1}{2}\left(\delta^{18}O_{O_2} - {}^{18}\varepsilon_{O_2}\right) + \frac{1}{2}\left(\delta^{18}O_{H_2O} - {}^{18}\varepsilon_{k,H_2O,1}\right)\right](1 - x_{AO}) + \left(\delta^{18}O_{H_2O} + {}^{18}\varepsilon_{eq}\right)(x_{AO}) \quad (1)$$

$$\delta^{18}O_{NO_3,\,final} = \frac{2}{3}\left[(1 - x_{NO})\delta^{18}O_{NO_2} + x_{NO}\left(\delta^{18}O_{H_2O} + {}^{18}\varepsilon_{eq}\right)\right] + \frac{1}{3}\left(\delta^{18}O_{H_2O} - {}^{18}\varepsilon_{k,H_2O,2}\right) \quad (2)$$

The first term in Eq. 1 represents the enzymatic incorporation of O_2 and H_2O during ammonia oxidation to nitrite. This incorporation signal can be partially modified if exchange (x_{AO}) occurs between nitrite and H_2O during ammonia oxidation. The second term represents the $\delta^{18}O$ contribution of O atoms that are added by this exchange. The first term in Eq. 2 represents the $\delta^{18}O$ value of the substrate nitrite used by nitrite oxidizers, which may be modified by exchange of oxygen atoms between nitrite and H_2O during nitrite oxidation (x_{NO}). x_{NO} is included here for completeness, although it has been found to have a negligible effect on $\delta^{18}O_{NO_3,nit}$ (DiSpirito and Hooper 1986; Friedman et al. 1986; Buchwald and Casciotti 2010). The second term describes the $\delta^{18}O$ value of H_2O incorporated during nitrite oxidation to nitrate.

If Eq. 1 is arranged to group $\delta^{18}O_{H_2O}$ terms (Eq. 3), the equation can be used to interpret the slope and intercept of the linear regression between $\delta^{18}O_{NO_2}$ and $\delta^{18}O_{H_2O}$.

$$\delta^{18}O_{NO_2} = \left[\frac{1}{2} + \frac{1}{2}x_{AO}\right]\delta^{18}O_{H_2O} + \frac{1}{2}\left[\left(\delta^{18}O_{O_2} - {}^{18}\varepsilon_{k,O_2} - {}^{18}\varepsilon_{k,H_2O,1}\right)(1 - x_{AO})\right] + {}^{18}\varepsilon_{eq}x_{AO} \quad (3)$$

The first term represents the slope of the linear regression and is dependent on the fraction of O incorporated enzymatically from H_2O (1/2) and x_{AO}. If there is no exchange ($x_{AO} = 0$) a slope of 0.5 would be expected, and if there is full exchange ($x_{AO} = 1$) the slope would be 1 (Fig. 3a). The last two terms of Eq. 3 represent the intercept, which refers to the $\delta^{18}O$ value of nitrite produced at a $\delta^{18}O_{H_2O}$ value of 0‰. The intercept can be used to calculate the sum of the incorporation isotope effects for ammonia oxidation ($^{18}\varepsilon_{k,O_2} + {}^{18}\varepsilon_{k,H_2O,1}$) by using the exchange (x_{AO}) calculated from the slope and assuming $\delta^{18}O_{O_2}$ = +24.2‰ (appropriate for seawater equilibrated with tropospheric O_2, Kroopnick and Craig 1972) and $^{18}\varepsilon_{eq}$ = +12.5‰ ± 0.5‰ (applicable for experiments at room temperature; C. Buchwald and K. L. Casciotti unpubl.).

$$\delta^{18}O_{NO_3,\,final} = \left[\frac{2}{3} + \frac{1}{3}x_{AO}\right]\delta^{18}O_{H_2O} + \frac{1}{3}\left[\left(\delta^{18}O_{O_2} - {}^{18}\varepsilon_{k,O_2} - {}^{18}\varepsilon_{k,H_2O,1}\right)(1 - x_{AO}) - {}^{18}\varepsilon_{k,H_2O,2}\right] + \frac{2}{3}{}^{18}\varepsilon_{eq}x_{AO} \quad (4)$$

Equation 4 describes the full isotope systematics of nitrification, combining Eqs. 2 and 3. After substituting Eq. 3 into Eq. 2, we simplify by assuming that there is no exchange during nitrite oxidation ($x_{NO} = 0$) (discussed above) and then regroup terms containing $\delta^{18}O_{H_2O}$. The resulting Eq. 4 can be used to interpret the $\delta^{18}O_{NO_3}$ vs. $\delta^{18}O_{H_2O}$ regression for experiments where ammonia is oxidized fully to nitrate (Fig. 3b). A slope of two thirds would indicate no exchange during ammonia oxidation ($x_{AO} = 0$), while a slope of 1 would indicate full exchange ($x_{AO} = 1$). The intercept of the nitrate regression is dependent on $\delta^{18}O_{O_2}$, $^{18}\varepsilon_{k,O_2}$, $^{18}\varepsilon_{k,H_2O,1}$, $^{18}\varepsilon_{k,H_2O,2}$, $^{18}\varepsilon_{eq}$, and x_{AO}. Using values from the intercept of the nitrite regression for $^{18}\varepsilon_{k,O_2} + {}^{18}\varepsilon_{k,H_2O,1}$ and the exchange (x_{AO}) calculated from the slope in Eq. 4, one can determine $^{18}\varepsilon_{k,H_2O,2}$ assuming $\delta^{18}O_{O_2}$ = +24.2‰ and $^{18}\varepsilon_{eq}$ = +12.5‰, as described above. Uncertainty in $^{18}\varepsilon_{eq}$ (± 0.5‰) is propagated through to incorporation isotope effects.

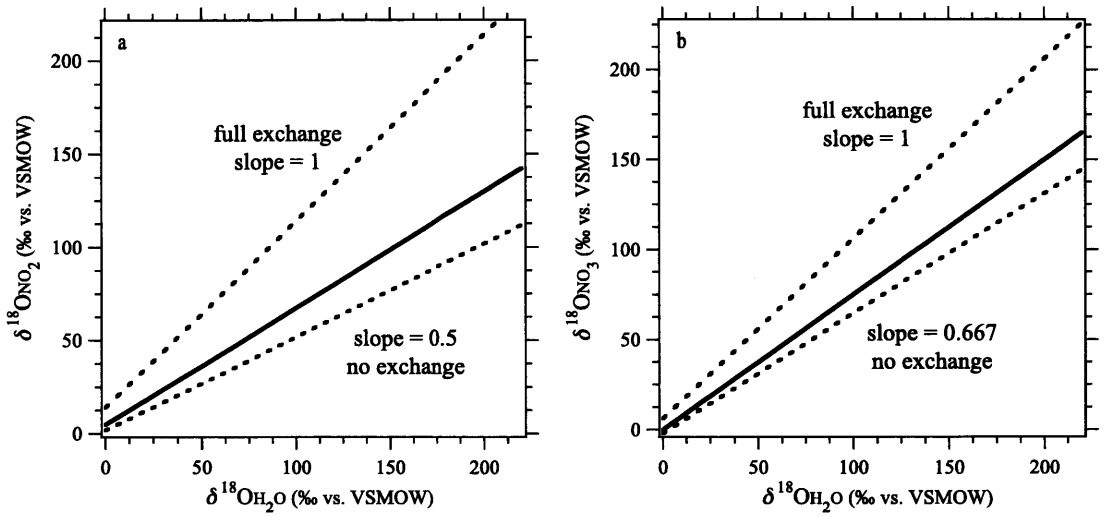

Fig. 3. A conceptual model of expected results from coculture experiments with varying $\delta^{18}O_{H_2O}$ media. (a) $\delta^{18}O_{H_2O}$ vs. $\delta^{18}O_{NO_2}$ (b) $\delta^{18}O_{H_2O}$ vs. $\delta^{18}O_{NO_{3,final}}$. In both plots the 0% and 100% exchange scenarios are indicated in dotted lines, and an exchange of 25% is shown with the solid line. The water incorporation isotope effects used in the model are ${}^{18}\varepsilon_{k,O_2} + {}^{18}\varepsilon_{k,H_2O,1}$ = 20‰ and ${}^{18}\varepsilon_{k,H_2O,2}$ = 10‰.

Kinetic isotope fractionation of nitrite during oxidation (${}^{18}\varepsilon_{k,NO_2}$; Fig. 1) may complicate interpretation of the intercept of accumulated nitrite and of nitrate isotopes in intermediate samples, when oxidation is incomplete. Inverse fractionation of oxygen atoms in nitrite during nitrite oxidation (Buchwald and Casciotti 2010) will cause nitrite $\delta^{18}O_{NO_2}$ values to be lower and $\delta^{18}O_{NO_3}$ values to be higher than if no nitrite oxidation had occurred, or if nitrite oxidation were complete. Therefore, in order to interpret intermediate samples, it is important to know whether and how much nitrite oxidation has occurred at the time that the sample is collected. In order to simplify the interpretation, we sampled for $\delta^{18}O_{NO_2}$ early in an experiment (prior to commencement of nitrite oxidation), for interpretation of the incorporation isotope effects associated with ammonia oxidation, and for $\delta^{18}O_{NO_3}$ values late in the experiment (after all the ammonium had been converted to nitrate $\delta^{18}O_{NO_{3,final}}$), for interpretation of the incorporation isotope effect during nitrite oxidation. We should note here that the inverse kinetic isotope effect only affects the intercept at intermediate time points and does not affect the *slope* of $\delta^{18}O_{NO_2}$ or $\delta^{18}O_{NO_{3,final}}$ vs. $\delta^{18}O_{H_2O}$ regressions, so long as all bottles are sampled at the same time (the same progress of ammonia and nitrite oxidation).

Results

Nitrite accumulation in coculture incubations—Total incubation times for the laboratory coculture experiments (CCEs 1–6) ranged from 3 to 59 d, with little accumulation of nitrite (Table 1; Fig. 4a–c). In the first three experiments (CCEs 1, 2, 3), with C-113a and *N. mobilis*, the ammonium was completely converted to nitrate within 6 d. Only a small amount (less than 2 μmol L^{-1}) of nitrite accumulated in these experiments, for a maximum of 4 d. In CCE 4, where we manipulated the AOB:NOB abundance ratio, ammonium was oxidized fully to nitrate in 3, 7, or 16 d, depending on the *N. mobilis* cell density. In this experiment, ammonia and nitrite oxidation became decoupled at lower densities of nitrite-oxidizing bacteria, and increasing amounts of nitrite accumulated (1, 25, and 45 μmol L^{-1}) at lower AOB:NOB ratios (Table 1; Fig. 4b). In CCEs 5 and 6, with AOA and *N. mobilis*, it took 18–59 d for the ammonium to be consumed because of the slower growth rate of the ammonia-oxidizing archaea (Santoro and Casciotti 2011). These incubations had an initial nitrite concentration of 7 μmol L^{-1} as a result of carry-over from the AOA inoculum, which was oxidized to nitrate before the first time point (Fig. 4c). Afterward, NOB maintained low levels (less than 1 μmol L^{-1}) of nitrite in the medium, indicating that ammonia and nitrite oxidation were tightly coupled (Fig. 4c). At the end of the experiment, final $\delta^{18}O_{NO_3}$ values were corrected for nitrate produced through the oxidation of the initial nitrite in order to focus on nitrate produced from ammonium in the variable ^{18}O-enriched media. This was done by calculating the $\delta^{18}O_{NO_3}$ that would have been produced from the preexisting nitrite (with a known $\delta^{18}O_{NO_2}$ value) using Eq. 2. Then the $\delta^{18}O_{NO_3}$ produced was subtracted by mass balance from the $\delta^{18}O_{NO_{3,final}}$ for each bottle.

Nitrite accumulation in field incubations—It took longer for field populations to fully oxidize the added ammonium, with incubations lasting for 50 to 179 d before complete oxidation was observed (Table 1; Fig. 4d–f). In FEs 7 and 8 from Vineyard Sound, nitrite accumulated to 50 μmol L^{-1} before being fully oxidized to nitrate after 50–59 d (Fig. 4d). The accumulated nitrite was present for at least 13 d and may have persisted for as long as 40 d, although the sampling frequency was not high enough to determine the exact duration. For the third Vineyard Sound experiment (FE 9)

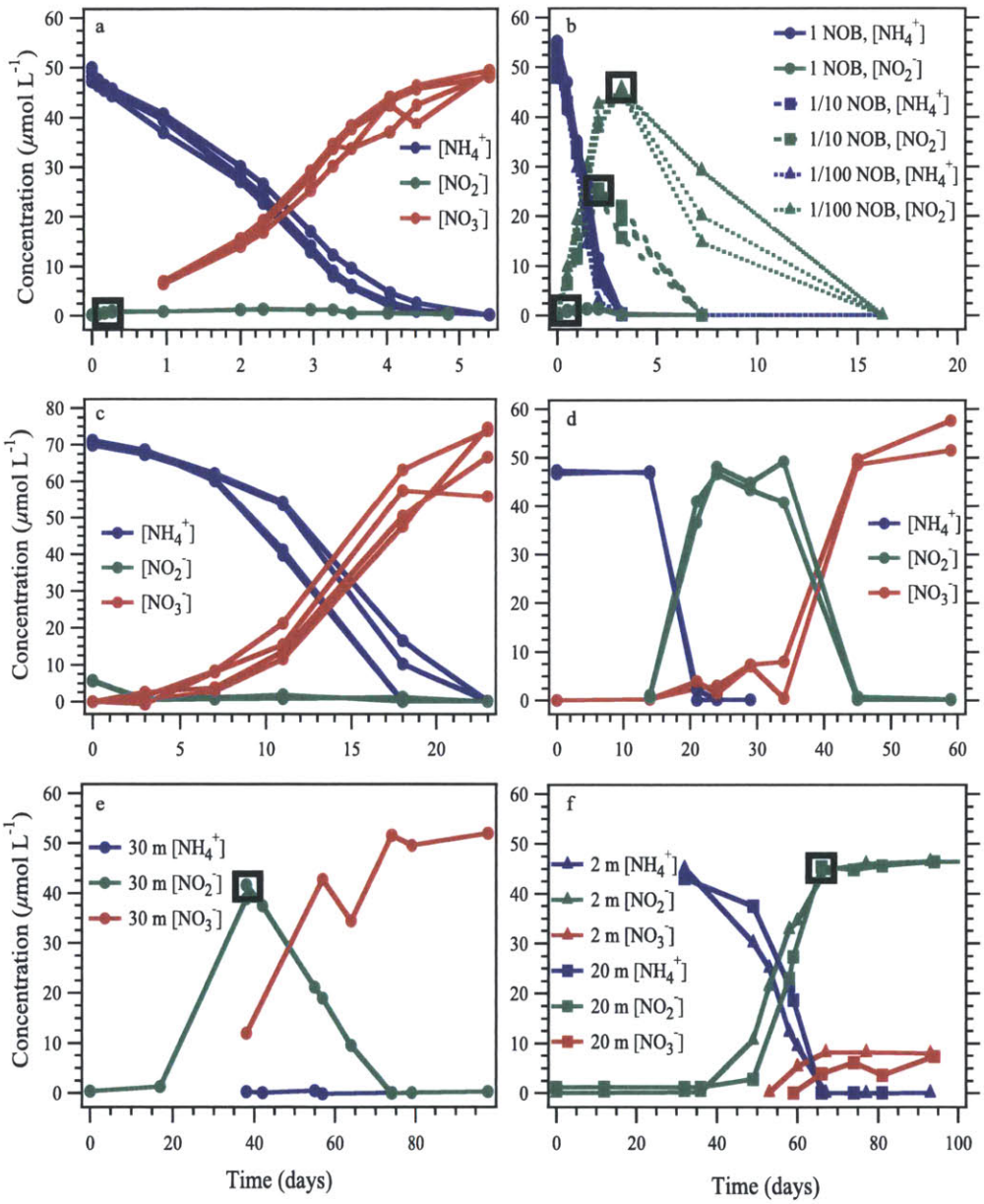

Fig. 4. Time course of ammonium, nitrite, and nitrate concentrations for coculture and field experiments: (a) CCE 2, C-113a, and *N. mobilis*, (b) CCE 4, C-113a, and varied *N. mobilis*, (c) CCE 5, AOA CN25, and *N. mobilis*, (d) FE 7, Vineyard Sound 1, (e) FE 10, CRD, Sta. 2, and (f) FEs 11 and 12, CRD, Sta. 3. Black squares represent which nitrite samples were used for calculations in Tables 2 and 3 and Fig. 5a. Nitrate concentration data for CCE 4 (removed for clarity) confirm N mass balance in the experiment.

oxidation of ammonium to nitrate was completed within 84 d (Table 1), and nitrite accumulated to a maximum concentration of ~52 μmol L^{-1} for as long as 53 d. In each of the Vineyard Sound experiments, the indicated durations may overestimate the true duration because sampling frequency was low near the end of the experiments.

In the Costa Rica Dome, incubations were successful (nitrification was detected) at two stations (2 and 3). At Sta. 2, nitrification occurred in water collected from the primary nitrite maximum (FE 10), while the incubations at Sta. 3 were successful from both the surface (FE 11) and the primary nitrite maximum (FE 12). In FE 10, complete oxidation of ammonium to nitrate occurred in seven of the eight bottles, including at least one from each of the four $\delta^{18}O_{H_2O}$ values, and was completed in 79 d (Table 1). There was a variable lag in initiation of nitrification among the

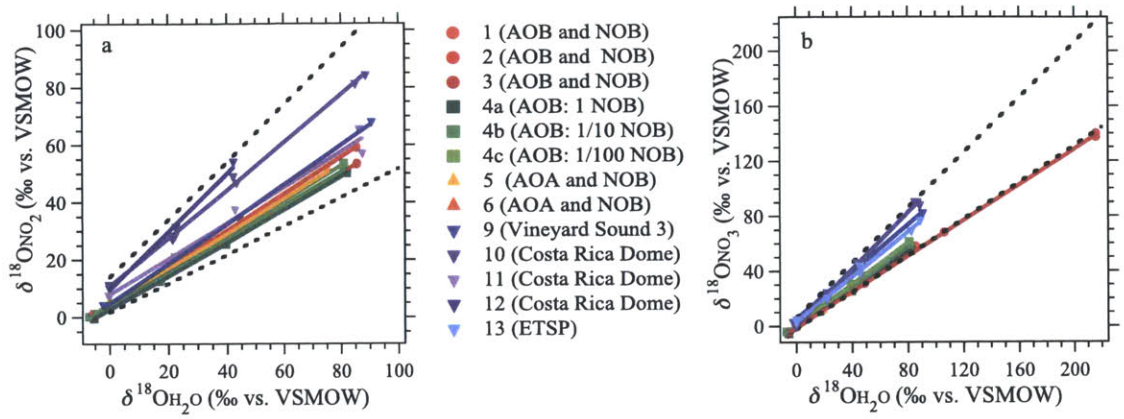

Fig. 5. (a) $\delta^{18}O_{H_2O}$ vs. intermediate $\delta^{18}O_{NO_2}$ in eight experiments and (b) $\delta^{18}O_{H_2O}$ vs. final produced $\delta^{18}O_{NO_3}$ for nine different experiments. In both plots the 0% and 100% exchange scenarios are indicated in dotted lines.

incubation bottles, and therefore the samples collected represent differing stages of nitrification. We also measured different amounts of accumulating nitrite (26 to 41 μmol L^{-1}) and durations of nitrite accumulation (26–58 d), depending on when each subsample was collected. Figure 4e shows the time course for one of seven bottles that had complete nitrification. In the other two experiments (FEs 11 and 12; Table 1) ammonia oxidation to nitrite was detected in five or six bottles out of eight, respectively, including at least one from each of the four $\delta^{18}O_{H_2O}$ values. However, after ammonium was oxidized completely to nitrite no nitrate was produced in the subsequent 3 months (Fig. 4f), so only information on ammonia oxidation can be taken from these two experiments.

In the ETSP the smaller amounts of ammonium (1 μmol L^{-1} or 5 μmol L^{-1}) added to incubations from below the primary nitrite maximum were completely oxidized to nitrate within 31–179 d (Table 1). Bottles were sampled infrequently for nitrite determination, so we do not know the exact amount and duration of accumulation; however, the maximum amount of nitrite accumulation would be 1 μmol L^{-1} or 5 μmol L^{-1}, respectively, based on the ammonium additions. After 17 d of incubation there was a small amount of nitrite $\sim$ 0.2 μmol L^{-1} in some bottles from both 1 μmol L^{-1} and 5 μmol L^{-1} ammonium experiments below the primary nitrite maximum, indicating that it was likely that nitrification was occurring. These bottles had no nitrite left after 31 d. In the two surface incubations ammonium had not been completely oxidized to nitrate after 179 d, and they will not be discussed further.

Oxygen isotopic exchange during ammonia oxidation—Type II regressions were conducted in Matlab (Mathworks) to calculate the slopes and intercepts of $\delta^{18}O_{NO_2}$ vs. $\delta^{18}O_{H_2O}$ data (Fig. 5a) and $\delta^{18}O_{NO_{3,final}}$ vs. $\delta^{18}O_{H_2O}$ data (Fig. 5b) from 8 of 13 and 9 of 13 experiments, respectively (Fig. 2), to account for measurement error in both x ($\delta^{18}O_{H_2O}$) and y ($\delta^{18}O_{NO_2}$ or $\delta^{18}O_{NO_{3,final}}$). The calculations were conducted using a *least squares cubic* fit (York 1966; York et al. 2004).

The fraction of O atoms in nitrite exchanged with H_2O during ammonia oxidation fraction (x_{AO}) was calculated from the slope of $\delta^{18}O_{NO_2}$ vs. $\delta^{18}O_{H_2O}$ (Eq. 3; Table 2). An alternative estimate of x_{AO} was obtained from the slope of $\delta^{18}O_{NO_{3,final}}$ vs. $\delta^{18}O_{H_2O}$ assuming $x_{NO} = 0$ (Eq. 4; Tables 2 and 3). The isotope effect for O atom incorporation during nitrite oxidation ($^{18}\varepsilon_{k,H_2O,2}$) was calculated from the intercept of $\delta^{18}O_{NO_{3,final}}$ vs. $\delta^{18}O_{H_2O}$ and the intermediate $\delta^{18}O_{NO_2}$ data (Eq. 4; Table 3), assuming $x_{NO} = 0$. Comparisons between the data, for example isotope effects from coculture vs. field experiments, were analyzed by using a *t*-test for two samples with equal variance. In these tests, p values greater than 0.05 indicate there is no significant difference between the mean of the two populations. In the cases for which we compared calculated exchange from $\delta^{18}O_{NO_2}$ and $\delta^{18}O_{NO_3}$ data in the same experiment, a paired *t*-test was conducted to determine whether there is a significant difference between each method for calculating exchange.

In CCEs 1, 2, 4a, and 5,where nitrite was maintained at low levels, the amount of exchange measured was relatively low. Estimates of x_{AO} from $\delta^{18}O_{NO_2}$ data ranged from 0.15 to 0.28 (Table 2), which closely matched previous estimates for C-113a grown under similar conditions (Casciotti et al. 2010). Estimates of x_{AO} from $\delta^{18}O_{NO_3}$ data were lower (p = 0.03), ranging from -0.05 to 0.09. It is generally expected that x_{AO} values from $\delta^{18}O_{NO_3}$ would be lower than those estimated from $\delta^{18}O_{NO_2}$ data because nitrate is an accumulated product recording the isotopic composition of nitrite that has seen increasing amounts of exchange over time, whereas $\delta^{18}O_{NO_2}$ is an instantaneous measurement of the total amount of exchange that has occurred at that time. The longer nitrite is accumulating before the $\delta^{18}O_{NO_2}$ is measured, the greater the expected difference between x_{AO} estimates. In the coculture experiments, $\delta^{18}O_{NO_2}$ was measured quite early in the experiment, and it was maintained at low levels for a short duration (3–5 d; Fig. 4a,c), which minimized abiotic exchange. Despite this, x_{AO} values from $\delta^{18}O_{NO_3}$ were still lower than from $\delta^{18}O_{NO_2}$ data, suggesting a contribution from abiotic exchange.

Table 2. The fraction of O atoms in nitrite exchanged during ammonia oxidation (x_{AO})

Experiment	$\delta^{18}O_{NO_3}$ vs. $\delta^{18}O_{H_2O}$ slope	$\delta^{18}O_{NO_2}$ vs. $\delta^{18}O_{H_2O}$ slope	x_{AO} calculated from $\delta^{18}O_{NO_3}$	x_{AO} calculated from $\delta^{18}O_{NO_2}$
1	0.70±0.00	0.58±0.00	0.09±0.05	0.16±0.05
2	0.68±0.00	0.64±0.00	0.05±0.05	0.28±0.05
3	0.65±0.00	nd	−0.05±0.05	nd
4a	0.68±0.02	0.58±0.00	0.04±0.05	0.15±0.05
4b	0.72±0.00	0.60±0.00	0.17±0.05	0.19±0.05
4c	0.75±0.01	0.61±0.00	0.26±0.05	0.21±0.05
5	0.69±0.00	0.58±0.02	0.07±0.05	0.16±0.05
6	0.66±0.00	nd	−0.01± 0.05	nd
9	0.86±0.02	0.68±0.01	0.59±0.07	0.35±0.05
10	1.05±0.05	0.86±0.02	1.15±0.15	0.71±0.05
11	na	0.61±0.03	na	0.22±0.05
12	na	1.03±0.09	na	1.05±0.18
13	0.83±0.03	nd	0.48±0.09	nd

nd, not determined because there was too little nitrite; na, not applicable because nitrate was not produced.

Decreasing the NOB:AOB ratio in CCE 4 led to increased nitrite accumulation and exchange, as seen in both $\delta^{18}O_{NO_2}$ and $\delta^{18}O_{NO_3}$ data (Tables 1 and 2). This trend continued in the field experiments where nitrite accumulated and persisted for even longer periods of time (30–60 d). In FEs 9–13 the exchange was generally high, varying between 0.22 and 1.0, as determined from both $\delta^{18}O_{NO_2}$ and $\delta^{18}O_{NO_3}$ data (Table 2). In FEs 9 and 10, x_{AO} values calculated from $\delta^{18}O_{NO_3}$ data were higher than estimated from $\delta^{18}O_{NO_2}$ data (FE 9, 0.59 vs. 0.36; and FE 10, 1.15 vs. 0.71, respectively). This illustrates an exception to the conceptual argument given above, which occurs when nitrite undergoes further abiotic exchange between the time when $\delta^{18}O_{NO_2}$ is sampled and when $\delta^{18}O_{NO_3}$ is sampled, leading to a greater representation of exchange in the $\delta^{18}O_{NO_3}$ values. In keeping with this, consecutive measurements of $\delta^{18}O_{NO_2}$ from field experiments showed increasing amounts of exchange after the initial $\delta^{18}O_{NO_2}$ measurements were made, in contrast with coculture experiments (CCEs 1, 2, 4a, 5, 6), which showed little change in $\delta^{18}O_{NO_2}$ over time (not shown). In field experiments, we were not able to collect $\delta^{18}O_{NO_2}$ measurements early enough in the experiment to avoid inclusion of abiotic exchange, and we were not able to correct for it, so abiotic exchange is included in both $\delta^{18}O_{NO_2}$ data and $\delta^{18}O_{NO_3}$ data, although to a greater extent in the latter.

Oxygen incorporation isotope effects during nitrification—The *y*-intercepts of the $\delta^{18}O_{NO_2}$ (or $\delta^{18}O_{NO_3}$) vs. $\delta^{18}O_{H_2O}$ regressions (Eqs. 3, 4; Fig. 5; Table 3) represent the $\delta^{18}O$ values of nitrite (or nitrate) produced in water with a $\delta^{18}O_{H_2O}$ value of 0‰. The intercept will be dependent on the isotopic composition of oxygen atom sources (H_2O and O_2), the isotope effects for O atom incorporation during nitrification, and the amount of O atom exchange between nitrite and H_2O. Therefore, if one determines the amount of exchange (from the slope) and measures or assumes $\delta^{18}O$ values for H_2O and dissolved oxygen, the isotope effects for O atom incorporation can be determined from $\delta^{18}O_{NO_2}$ and $\delta^{18}O_{NO_3}$ data (Eqs. 3, 4; Fig. 5; Tables 2 and 3).

The intercepts for $\delta^{18}O_{NO_2}$ in all experiments ranged from +2.8‰ to +9.5‰, increasing with increasing amounts

Table 3. The isotope effects for incorporation of oxygen and water during nitrification.

Experiment	$\delta^{18}O_{NO_3,\,final}$ vs. $\delta^{18}O_{H_2O}$ intercept (‰)	$\delta^{18}O_{NO_2}$ vs. $\delta^{18}O_{H_2O}$ intercept (‰)	Calculated $^{18}\varepsilon_{k,O_2}+{}^{18}\varepsilon_{k,H_2O,1}$ (‰)	Calculated $^{18}\varepsilon_{k,H_2O,2}$ (‰)
1	−1.5±0.0	+3.5±0.1	20.8±0.1	9.7±0.2
2	−1.6±0.1	+4.6±0.1	21.0±0.2	8.6±0.4
3	−0.9±0.2	nd	nd	nd
4a	−1.0±0.5	+2.8±0.2	22.1±0.3	5.8±1.9
4b	−0.4±0.1	+3.0±0.1	22.7±0.2	6.6±0.5
4c	+0.3±0.3	+4.2±0.2	20.3±0.3	8.5±1.0
5	−1.7±0.1	+5.3±0.4	16.4±0.6	12.4±0.6
6	+0.7±0.1	nd	nd	nd
9	+5.2±1.4	+5.9±0.2	19.7±0.6	0.8±4.5
10	−0.7±1.6	+9.5±0.6	20.3±2.9	27.2±5.7
11	na	+7.8±0.7	11.4±1.1	na
12	na	+9.5±2.5	na	na
13	+1.3±1.4	nd	nd	nd

nd, not determined because there was too little nitrite; na, not applicable because nitrate was not produced or because there was full exchange.

Table 4. $\delta^{18}O_{NO_3}$ produced in field experiments.

Field experiment	$\delta^{18}O_{H_2O}$ (‰ vs. VSMOW)	Final $\delta^{18}O_{NO_3}$ (‰ vs. VSMOW)
7	−1.5±0.5	+0.5±0.4
		+1.3±0.3
8	−1.8±0.2	−0.3±0.2
		−0.7±0.2
		−0.1±0.2
9	−2.2±0.2	+2.7±0.4
10	−0.1±0.3	+0.6±0.2
	0.0±0.5	+0.1±0.2
13	+0.2±0.2	+3.5±0.5
	+0.5±0.2	+5.2±0.6

of exchange. Laboratory coculture experiments (average +3.9‰ ± 0.8‰) were significantly lower than field experiments (average +8.2‰ ± 1.7‰) (p = 0.0005). Based on these intercepts, and assuming constant $\delta^{18}O_{O_2}$ values of +24.2‰ in all experiments, the combined incorporation isotope effects for ammonia oxidation ($^{18}\varepsilon_{k,O_2} + {}^{18}\varepsilon_{k,H_2O,1}$) ranged from +11.4‰ to +22.7‰ (Table 3). The isotope effect for O atom incorporation was very consistent among the AOB experiments (+21.4‰ ± 1.0‰) and slightly lower in AOA experiments (+16.4‰ ± 0.6‰; Table 3). Unfortunately, we cannot perform a statistical test between AOB and AOA experiments because there was only one AOA experiment in which $^{18}\varepsilon_{k,O_2} + {}^{18}\varepsilon_{k,H_2O,1}$ was measured. This combined isotope effect was measured in three field experiments (FEs 9, 10, 11) and showed a range of +11.4‰ ± 0.1‰ to +20.3‰ ± 3.1‰. The low value was determined to be an outlier by Chauvenet's criterion, which is defined by the value being greater than two standard deviations from the mean (Taylor 1997). After excluding this value there is no significant difference in the $^{18}\varepsilon_{k,O_2} + {}^{18}\varepsilon_{k,H_2O,1}$ measured in coculture vs. field experiments (p = 0.18), and the overall average is +20.4‰ ± 2.3‰. This indicates that the main cause for the higher $\delta^{18}O_{NO_2}$ intercepts in field experiments compared with coculture experiments is more exchange (a larger x_{AO}), not lower $^{18}\varepsilon_{k,O_2} + {}^{18}\varepsilon_{k,H_2O,1}$ values. In FE 12 there was full exchange, thus erasing any record of $^{18}\varepsilon_{k,O_2} + {}^{18}\varepsilon_{k,H_2O,1}$. In FE 13 nitrite concentrations were too low for $\delta^{18}O_{NO_2}$ analyses.

The intercepts for $\delta^{18}O_{NO_3}$ in the nine complete experiments ranged from −1.5‰ to 5.2‰ (Table 3). Excluding one Vineyard Sound experiment (FE 9), which was determined to be an outlier (greater than two standard deviations from the mean), lowers the upper estimate to +1.3‰. With the slope and intercept from the $\delta^{18}O_{NO_3}$ regression and the isotope effects for H_2O and O_2 incorporation from the $\delta^{18}O_{NO_2}$ data (Fig. 5a; Table 3), the isotope effect for H_2O incorporation during nitrite oxidation ($^{18}\varepsilon_{k,H_2O,2}$) could be calculated using Eq. 3. These values ranged from +0.8 to +27.2‰ (Table 3). Laboratory experiments, all conducted with *N. mobilis*, gave $^{18}\varepsilon_{k,H_2O,2}$ values ranging from +5.8‰ to +12.4‰, with an average of +8.6‰ ± 2.3‰, which is lower than what was reported previously from monoculture incubations (+17.8‰ ± 4.7‰; Buchwald and Casciotti 2010). The current experiments were not shaken, though, and some of the variability observed here may be due to variable amounts of dissolved oxygen consumption, leading to variations in $\delta^{18}O_{O_2}$, which would be erroneously attributed to variations in $^{18}\varepsilon_{k,H_2O,2}$. Field experiments fell at the two extremes, with FE 9 having a $^{18}\varepsilon_{k,H_2O,2}$ value of +0.8‰ and FE 10 having a $^{18}\varepsilon_{k,H_2O,2}$ value of +27.2‰ (Table 3). Even for a biological process, this range in $^{18}\varepsilon_{k,H_2O,2}$ is wider than expected and could represent the activity of different nitrite oxidizer communities in Vineyard Sound, Massachusetts, compared with the Costa Rica Dome.

Among the five field experiments, two (FEs 7 and 8) did not have varied $\delta^{18}O_{H_2O}$, so x_{AO} and incorporation isotope effects could not be determined. Nevertheless, the final $\delta^{18}O_{NO_3}$ values of nitrate produced in these experiments (corrected for the preexisting nitrate) provide an independent estimate of the $\delta^{18}O_{NO_3}$ value produced via nitrification by natural marine assemblages at natural seawater pH and $\delta^{18}O_{H_2O}$ values. The $\delta^{18}O_{NO_3}$ values produced in these experiments were between −0.7‰ and +1.3‰, with $\delta^{18}O_{H_2O}$ values of −1.5‰ and −1.8‰, respectively (Table 4). These values are similar to the $\delta^{18}O_{NO_3}$ intercepts observed in experiments with variable $\delta^{18}O_{H_2O}$ media. Because the $\delta^{18}O_{H_2O}$ values in most of these experiments were lower than bulk seawater $\delta^{18}O_{H_2O}$, the $\delta^{18}O_{NO_3}$ values from these experiments should generally be lower than the intercepts in Table 3 ($\delta^{18}O_{NO_3}$ at $\delta^{18}O_{H_2O}$ = 0‰; produced $\delta^{18}O_{NO_3}$ should increase by 0.67–1‰ per 1‰ increase in $\delta^{18}O_{H_2O}$, depending on the amount of exchange that occurred). In the last experiment (FE 13) the $\delta^{18}O_{H_2O}$ values were higher (0.2‰ and 0.5‰) than bulk seawater, and therefore the $\delta^{18}O_{NO_3}$ values are higher than the intercept given in Table 3.

Discussion

Nitrite accumulation and oxygen isotope exchange in the ocean—Our current estimates from coculture experiments, including those with AOA, indicate that biological equilibration between nitrite and H_2O during ammonia oxidation is most likely less than 25% and that the biological equilibration between nitrite and H_2O during nitrite oxidation is negligible. Field experiments generally showed higher levels of exchange (22–100%), which we attribute to abiotic processes that occur when nitrite accumulates in seawater. Although field experiments may not exhibit some biases of culture work, we suspect that the addition of NH_4^+, which was necessary to create a measurable signal in $\delta^{18}O_{NO_3}$, perturbed the system into an unnatural state. Given the long containment in bottles, large accumulations of nitrite, and long lags before commencement of nitrite oxidation, we argue that the high exchange observed in field experiments most likely does not resemble the tightly coupled nitrification system occurring in much of the ocean.

Even in the coculture experiments the low levels of exchange could potentially be explained by abiotic, rather than biological, exchange. The rate of abiotic exchange is dependent on pH and temperature, and based on typical exchange rates at a seawater pH at room temperature (Casciotti et al. 2007; C. Buchwald and K. L. Casciotti

unpubl.) we would expect about 2% abiotic exchange per day in our experiments. With little biological exchange occurring during ammonia oxidation and nitrite oxidation, any exchange during nitrification in the ocean may be determined strictly by duration of nitrite accumulation relative to the rate of abiotic processes. If nitrite is allowed to accumulate, exchange may be extensive, while if nitrite is kept at low levels exchange may be minimal. This observation mirrors results from Snider et al. (2010), where large amounts of nitrite accumulated during nitrification in incubations of terrestrial and agricultural soils and they measured high amounts of exchange (up to 88%).

While most of the ocean contains very little accumulated nitrite, ammonia and nitrite oxidation can become uncoupled in the primary nitrite maximum (PNM; Wada and Hattori 1971), a region of locally elevated nitrite concentrations that frequently occurs at the base of the euphotic zone (Lomas and Lipschultz 2006). Within the PNM, nitrite oxidation rates can be quite low, and nitrite may have long residence times, on the order of weeks to months (Dore and Karl 1996; C. Buchwald and K. L. Casciotti unpubl.). Under these conditions, abiotic exchange between nitrite and H_2O could be extensive, and much of the nitrate produced may have lost its primary $\delta^{18}O_{O_2}$ signal. Below the PNM, nitrite is generally held in low concentrations, with ammonia and nitrite oxidation tightly coupled. Under these circumstances, little abiotic exchange would be expected.

In addition to the PNM, a secondary nitrite maximum (SNM) occurs in areas of the ocean with low oxygen concentrations in intermediate waters, referred to as oxygen deficient zones (ODZs). The three major ODZs are located in the Eastern Tropical South Pacific, Eastern Tropical North Pacific, and the Arabian Sea. While they account for a small area of the ocean, they can have high nitrite concentrations (Codispoti et al. 1986) and a large effect on the oceanic nitrate isotope budget (Brandes and Devol 2002; Deutsch et al. 2004; Sigman et al. 2009). Nitrification can also occur at the edges of an ODZ, where nitrite and oxygen coexist (Anderson et al. 1982; Ward et al. 1989; Casciotti and McIlvin 2007). Here, too, the oxidized nitrite may have been strongly affected by equilibration. Depending on whether the majority of nitrification is associated with features such as the PNM and SNM, or in parts of the water column with tightly coupled ammonia and nitrite oxidation, oxygen isotope exchange may be more or less important in setting $\delta^{18}O_{NO_3}$ values in the ocean.

Consistency with oceanographic data and models—Relatively small vertical and horizontal gradients have been observed in intermediate and deep ocean $\delta^{18}O_{NO_3}$ values (Casciotti et al. 2002; Sigman et al. 2009), and studies interpreting $\delta^{18}O_{NO_3}$ and $\delta^{15}N_{NO_3}$ values using biogeochemical models have generally assumed $\delta^{18}O_{NO_3}$ values of newly produced nitrate to be near that of seawater (0‰ ± 1‰; Sigman et al. 2005; Casciotti and McIlvin 2007; Wankel et al. 2007). This assumption has been justified by the importance of H_2O as an O atom source to nitrate (Andersson and Hooper 1983; Kumar et al. 1983), from high levels of equilibration between nitrite and H_2O reported in early studies of ammonia oxidation (Dua et al. 1979; Andersson et al. 1982), and the low $\delta^{18}O_{NO_3}$ variations in deep water noted above. However, while equilibration of nitrite with H_2O should indeed remove $\delta^{18}O_{NO_3}$ variations associated with variations in $\delta^{18}O_{O_2}$ and lessen deep ocean gradients in $\delta^{18}O_{NO_3}$ (Sigman et al. 2009), the equilibrium isotope effect ($^{18}\varepsilon_{eq}$) for this exchange should raise $\delta^{18}O_{NO_2}$ to +11.4‰ to +15.1‰ above that of ambient $\delta^{18}O_{H_2O}$, depending on temperature (Casciotti et al. 2007; C. Buchwald and K. L. Casciotti unpubl.). In order to generate $\delta^{18}O_{NO_3}$ values in newly produced nitrate that are near 0‰, the increase in $\delta^{18}O_{NO_2}$ due to equilibration between nitrite and H_2O must be offset by the kinetic isotope effect for O incorporation from H_2O during nitrite oxidation ($^{18}\varepsilon_{k,H_2O,2}$). Our results have shown that this can happen. For example, in this study, we find $\delta^{18}O_{NO_3}$ produced at values of −0.7‰ to +1.3‰, even where large amounts of exchange have taken place. In one of these cases, the estimated $^{18}\varepsilon_{k,H_2O,2}$ value was as high as +27.2‰ (Table 3). It is not known what may cause variation in expressed $^{18}\varepsilon_{k,H_2O,2}$ values at different field sites, but it may be related to the presence of specific nitrite-oxidizing bacteria or changes in their growth conditions.

The results of this study suggest that nitrification in much of the ocean may proceed with little biologically catalyzed exchange but that abiotic equilibration may be important when nitrification occurs in the vicinity of a primary or secondary nitrite maximum. Where nitrification occurs with tightly coupled ammonia and nitrite oxidation, O from dissolved O_2 may be retained as 1 in 3 O atoms in nitrate. This conclusion is in apparent discrepancy with models that are able to simulate the low variation in deep and intermediate ocean $\delta^{18}O_{NO_3}$ only with very little retention of O from dissolved oxygen ($x_{AO} \sim 1$) (Sigman et al. 2009).

In order to test the predicted $\delta^{18}O_{NO_3}$ dependence on $\delta^{18}O_{O_2}$, we constructed a simple Rayleigh model where nitrate is produced by nitrification with no biotic or abiotic exchange, so that it contains 1 in 3 O atoms from dissolved O_2 (Fig. 6). Consumption of O_2 causes $\delta^{18}O_{O_2}$ to increase with an isotope effect of 18‰ (Bender 1990), and nitrate accumulates from that produced instantaneously at increasing $\delta^{18}O_{O_2}$ values, according to Eq. 4. According to this calculation, while $\delta^{18}O_{O_2}$ increases nearly 11.8‰, $\delta^{18}O_{NO_3}$ increases only 1.8‰, which is approximately 15% of the increase in $\delta^{18}O_{O_2}$. In addition to this, only nitrate that is locally produced should track increases in ambient $\delta^{18}O_{O_2}$, and the presence of preformed nitrate will decouple the relationship between $\delta^{18}O_{O_2}$ and $\delta^{18}O_{NO_3}$. The relationship between $\delta^{18}O_{O_2}$ and $\delta^{18}O_{NO_3}$ can also change at extremely low dissolved oxygen concentrations (high $\delta^{18}O_{O_2}$ values), where $\delta^{18}O_{NO_3}$ is elevated because of other processes, such as denitrification. It is difficult to disentangle the effects of nitrification with elevated $\delta^{18}O_{O_2}$ levels, abiotic exchange, and denitrification on $\delta^{18}O_{NO_3}$ in the vicinity of oxygen deficient zones, and more sophisticated models would be required to better evaluate the implications of these processes for deep ocean $\delta^{18}O_{NO_3}$. While we cannot exclude exchange, particularly from abiotic processes, as a factor in $\delta^{18}O_{NO_3}$ in the ocean, full exchange

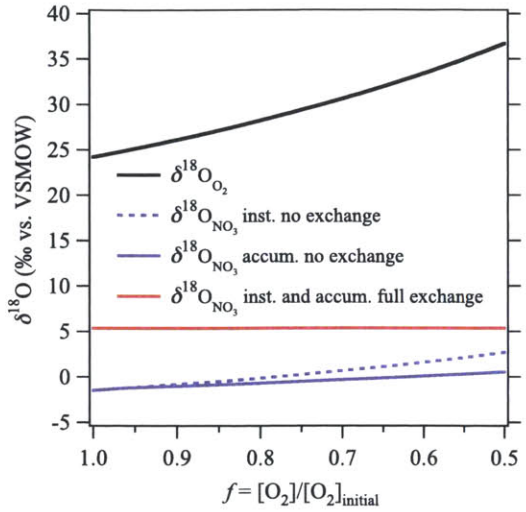

Fig. 6. Rayleigh model for nitrate production in the ocean as $\delta^{18}O_{O_2}$ increases from respiration with an isotope effect of 18‰. Instantaneous nitrate is produced through Eq. 4 with $\delta^{18}O_{H_2O}$ = 0‰, $^{18}\varepsilon_{k,O_2} + {}^{18}\varepsilon_{k,H_2O,1}$ = 19.7‰, $^{18}\varepsilon_{k,H_2O,2}$ = 8.9‰, and $^{18}\varepsilon_{eq}$ = 12.5‰ with x_{AO} = 0 (dashed purple line) and x_{AO} = 1 (red line). Accumulated nitrate is summed from the incremental products and their $\delta^{18}O$ values with x_{AO} = 0 (solid purple line). For x_{AO} = 1 the $\delta^{18}O_{NO_3}$ values are the same for accumulated and instantaneous nitrate.

may not be necessary to explain the small gradients observed in intermediate and deep $\delta^{18}O_{NO_3}$ values.

Expected $\delta^{18}O_{NO_3}$ for nitrification in the ocean— The $\delta^{18}O$ value of newly produced nitrate from nitrification ($\delta^{18}O_{NO_3,nit}$) is an important parameter for biogeochemical models used to interpret oceanic $\delta^{18}O_{NO_3}$ and $\delta^{15}N_{NO_3}$ (Wankel et al. 2007; DiFiore et al. 2009; Sigman et al. 2009). This value is constrained to be less than +2.5‰ (the average $\delta^{18}O$ value of deep ocean nitrate; Casciotti et al. 2002; Knapp et al. 2008; DiFiore et al. 2009) because processes consuming nitrate should cause ^{18}O enrichment in residual nitrate relative to the nitrification source (Granger et al., 2004; Granger et al., 2008). The main goal of this study was to develop a better understanding of the determinants of $\delta^{18}O_{NO_3,nit}$ to use in global ocean nitrate isotope models. Previous experiments with ammonia-oxidizing bacteria and nitrite-oxidizing bacteria grown separately suggested that the $\delta^{18}O_{NO_3}$ values for nitrate produced in well-oxygenated seawater ($\delta^{18}O_{H_2O} \sim$ 0‰, $\delta^{18}O_{O_2} \sim$ +23.5‰) could range from −8.3‰ to −0.7‰, depending on amounts of exchange and fractionation associated with the different species investigated (Buchwald and Casciotti 2010). However, the extent to which variations in $\delta^{18}O_{H_2O}$ and $\delta^{18}O_{O_2}$ would affect $\delta^{18}O_{NO_3,nit}$ in mixed communities was not well constrained. In our current coculture experiments, where very little nitrite accumulated (and consequently a low amount of exchange was observed), $\delta^{18}O_{NO_3}$ values ranged from −1.5‰ to +0.7‰, with an average of −0.9‰ ± 0.8‰. In the field experiments we measured slightly larger $\delta^{18}O_{NO_3}$ intercepts, falling between −0.7‰ and 1.3‰ (neglecting one outlier; Table 4).

One of the main factors driving variations in $\delta^{18}O_{NO_3}$ produced in our experiments appeared to be the duration of nitrite accumulation and the extent to which abiotic exchange altered the $\delta^{18}O_{NO_2}$ value prior to oxidation. When ammonia oxidation outpaced nitrite oxidation and nitrite accumulated, significant amounts of abiotic exchange between nitrite and H_2O could take place, generally leading to higher $\delta^{18}O_{NO_3}$ values. This may be counterintuitive because $\delta^{18}O_{O_2}$ is always higher than $\delta^{18}O_{H_2O}$ in the ocean. However, there is a large kinetic isotope effect for O incorporation, which lowers the overall $\delta^{18}O$ value of the incorporated O atom. Exchange leads to higher $\delta^{18}O_{NO_3}$ values because of the equilibrium isotope effect for exchange between nitrite and H_2O. In one field experiment from the CRD (FE 10), the $\delta^{18}O_{NO_3}$ value was similar (−0.7‰ ± 1.6‰) to coculture data, despite the higher amounts of exchange observed. This is potentially explained by a large isotope effect for H_2O incorporation during nitrite oxidation ($^{18}\varepsilon_{k,H_2O,2}$), which offsets the equilibrium isotope effect. In another case (FE 13) we observed high levels of exchange despite low nitrite accumulations. This highlights the possibility that it is not necessarily the amount of nitrite that accumulates, but rather the duration of nitrite accumulation or rate of biological turnover relative to the rate of abiotic equilibration, that determines the effect of abiotic exchange on $\delta^{18}O_{NO_3}$.

The anomalous Vineyard Sound experiment (FE 9) had a $\delta^{18}O_{NO_3}$ intercept that was determined to be an outlier among all other experiments, although the $\delta^{18}O_{NO_2}$ intercept was not. This combination of $\delta^{18}O_{NO_2}$ and $\delta^{18}O_{NO_3}$ intercepts yielded a low estimate of $^{18}\varepsilon_{k,H_2O,2}$ from Eq. 4. We do not have an explanation for why this experiment is so different from the others, but given the extremely long duration of nitrite accumulation, we do not believe the results to be representative of nitrification in the open ocean. A $\delta^{18}O_{NO_3}$ value of 5.3‰ is also not consistent with deep ocean $\delta^{18}O_{NO_3}$ values of 2.5‰ or less, although we cannot rule out the possibility that nitrification in the euphotic zone produces nitrate with a higher $\delta^{18}O_{NO_3}$ value.

Despite large ranges in measured exchange and incorporation isotope effects, there was remarkably little variation in $\delta^{18}O_{NO_3}$ produced. The current results suggest that $\delta^{18}O_{NO_3}$ of newly produced nitrate in the ocean (when $\delta^{18}O_{H_2O}$ = 0‰ and $\delta^{18}O_{O_2}$ = +24.2‰) most likely lies between −1.5‰ and +1.3‰. This range represents differences in microbial communities and growth conditions under which nitrate is produced, which may lead to different amounts of exchange and/or fractionation during ammonia and nitrite oxidation. The full range in $\delta^{18}O_{NO_3}$ values produced in the ocean may be slightly larger as a result of variations in $\delta^{18}O_{H_2O}$ and $\delta^{18}O_{O_2}$ values in seawater. Variations in $\delta^{18}O_{NO_3,nit}$ due to $\delta^{18}O_{O_2}$ variations are likely to be less than 4‰ (1/3 × variation in $\delta^{18}O_{O_2}$), and those due to $\delta^{18}O_{H_2O}$ are likely to be smaller than that (2/3 × variation in $\delta^{18}O_{H_2O}$). While there may be slight variations in the $\delta^{18}O_{NO_3}$ produced by nitrification

in the ocean, the overall predicted range is narrow, and the better constrained relationship between $\delta^{18}O_{NO_3,nit}$, $\delta^{18}O_{H_2O}$, and $\delta^{18}O_{O_2}$ can be used in future oceanic models.

Acknowledgments

We thank Frederica Valois and John Waterbury for generously providing the ammonia-oxidizing and nitrite-oxidizing bacteria used in this study. We are grateful to Mike Landry (Chief Scientist in Costa Rica), Doug Capone and Will Berelson (co-Chief Scientists in the South Pacific), and the Captain and Crew of the R/V *Melville* for enabling the collection of the samples. We would also like to thank Meredith White for help with the statistical analysis in this study, D. Sigman for helpful discussions, and two anonymous reviewers for their thorough and constructive comments. This research was funded by the National Science Foundation Chemical Oceanography grants 05-26277 and 09-610998 to K.L.C.

References

ALTABET, M. 2007. Constraints on the oceanic N balance/imbalance from sedimentary ^{15}N records. Biogeoscience **4:** 75–86, doi:10.5194/bg-4-75-2007

ANDERSON, J. J., A. OKUBO, A. S. ROBBINS, AND F. A. RICHARDS. 1982. A model for nitrate distributions in oceanic minimum zones. Deep Sea Res. **29:** 1113–1140, doi:10.1016/0198-0149(82)90031-0

ANDERSSON, K. K., S. B. PHILSON, AND A. B. HOOPER. 1982. ^{18}O isotope shift in ^{15}N NMR analysis of biological N-oxidations: H_2O-NO_2^- exchange in the ammonia-oxidizing bacterium *Nitrosomonas*. Proc. Natl. Acad. Sci. USA **79:** 5871–5875, doi:10.1073/pnas.79.19.5871

———, AND A. B. HOOPER. 1983. O_2 and H_2O are each the source of one O in NO_2^- produced from NH_3 by *Nitrosomonas*: ^{15}N-NMR evidence. FEBS Lett. **164:** 236–240, doi:10.1016/0014-5793(83)80292-0

BALCH, W. E., G. E. FOX, L. J. MAGRUM, C. R. WOESE, AND R. S. WOLFE. 1979. Methanogens—re-evaluation of a unique biological group. Microbiol. Rev. **43:** 260–296.

BENDER, M. L. 1990. The $\delta^{18}O$ of dissolved O_2 in seawater—a unique tracer of circulation and respiration in the deep-sea. J. Geophys. Res. Oceans **95:** 22243–22252, doi:10.1029/JC095iC12p22243

BÖHLKE, J. K., S. J. MROCZKOWSKI, AND T. B. COPLEN. 2003. Oxygen isotopes in nitrate: New reference materials for O-18 : O-17 : O-16 measurements and observations on the nitrate-water equilibration. Rapid Commun. Mass Spectrom. **17:** 1835–1846, doi:10.1002/rcm.1123

BRANDES, J. A., AND A. H. DEVOL. 2002. A global marine-fixed nitrogen isotopic budget: Implications for Holocene nitrogen cycling. Glob. Biochem. Cycles **16:** 1–14.

BUCHWALD, C., AND K. L. CASCIOTTI. 2010. Oxygen isotopic fractionation and exchange during bacterial nitrite oxidation. Limnol. Oceanogr. **55:** 1064–1074, doi:10.4319/lo.2010.55.3.1064

CASCIOTTI, K. L., J. K. BÖHLKE, M. R. MCILVIN, S. J. MROCZKWSKI, AND J. E. HANNON. 2007. Oxygen isotopes in nitrite: Analysis, calibration and equilibration. Anal. Chem. **79:** 2427–2436, doi:10.1021/ac061598h

———, C. BUCHWALD, A. E. SANTORO, AND C. FRAME. 2011. Assessment of nitrogen and oxygen isotopic fractionation during nitrification and its expression in the marine environment. Methods Enzymol. **486:** 253–275, doi:10.1016/S0076-6879(11)86011-8

———, AND M. R. MCILVIN. 2007. Isotopic analyses of nitrate and nitrite from reference mixtures and application to eastern tropical North Pacific waters. Mar. Chem. **107:** 184–201, doi:10.1016/j.marchem.2007.06.021

———, ———, AND C. BUCHWALD. 2010. Oxygen isotopic exchange and fractionation during bacterial ammonia oxidation. Limnol. Oceanogr. **55:** 753–762, doi:10.4319/lo.2009.55.2.0753

———, D. M. SIGMAN, G. H. HASTINGS, J. K. BÖHLKE, AND A. HILKERT. 2002. Measurement of the oxygen isotopic composition of nitrate in seawater and freshwater using the denitrifier method. Anal. Chem. **74:** 4905–4912, doi:10.1021/ac020113w

CODISPOTI, L. A., J. A. BRANDES, J. P. CHRISTENSEN, A. H. DEVOL, S. W. A. NAQVI, H. W. PAERL, AND T. YOSHINARI. 2001. The oceanic fixed nitrogen and nitrous oxide budgets: Moving targets as we enter the anthropocene? Sci. Mar. **65:** 85–102, doi:10.3989/scimar.2001.65s285

———, AND OTHERS. 1986. High nitrite levels off Northern Peru: A signal of instability in the marine denitrification rate. Science **233:** 1200–1202, doi:10.1126/science.233.4769.1200

COX, R. D. 1980. Development of analytical methodologies for parts per billion level determination of nitrate, nitrite and *N*-Nitroso group content. Ph.D. thesis. Univ. of Iowa.

DEUTSCH, C., D. M. SIGMAN, R. C. THUNELL, A. N. MECKLER, AND G. H. HAUG. 2004. Isotopic constraints on glacial/interglacial changes in the oceanic nitrogen budget. Glob. Biogeochem. Cycles **18:** GB4012, doi:10.1029/2003GB002189

DIFIORE, P. J., D. M. SIGMAN, AND R. B. DUNBAR. 2009. Upper ocean nitrogen fluxes in the Polar Antarctic Zone: Constraints from the nitrogen and oxygen isotopes of nitrate. Geochem. Geophys. Geosys. **10:** Q11016, doi:10.1029/2009GC002468

DISPIRITO, A. A., AND A. B. HOOPER. 1986. Oxygen-exchange between nitrate molecules during nitrite oxidation by *Nitrobacter*. J. Biol. Chem. **261:** 10534–10537.

DORE, J. E., AND D. M. KARL. 1996. Nitrification in the euphotic zone as a source of nitrite, nitrate and nitrous oxide at Station ALOHA. Limnol. Oceanogr. **41:** 1619–1628, doi:10.4319/lo.1996.41.8.1619

DUA, R. D., B. BHANDARI, AND D. J. D. NICHOLAS. 1979. Stable isotope studies on the oxidation of ammonia to hydroxylamine by *Nitrosomonas europaea*. FEBS Lett. **106:** 401–404, doi:10.1016/0014-5793(79)80541-4

EPPLEY, R. W., AND B. J. PETERSON. 1979. Particulate organic matter flux and planktonic new production in the deep ocean. Nature **282:** 677–680, doi:10.1038/282677a0

EPSTEIN, S., AND T. MAYEDA. 1953. Variation of O^{18} content of waters from natural sources. Geochim. Cosmochim. Acta. **4:** 213–224, doi:10.1016/0016-7037(53)90051-9

FRIEDMAN, S. H., W. MASSEFSKI, AND T. C. HOLLOCHER. 1986. Catalysis of intermolecular oxygen atom transfer by nitrite dehydrogenase of *Nitrobacter agilis*. J. Biol. Chem. **261:** 10538–10543.

GARSIDE, C. 1982. A chemiluminescent technique for the determination of nanomolar concentrations of nitrate and nitrite in seawater. Mar. Chem. **11:** 159–167, doi:10.1016/0304-4203(82)90039-1

GRANGER, J., AND D. M. SIGMAN. 2009. Removal of nitrite with sulfamic acid for nitrate N and O isotope analysis with the denitrifier method. Rapid Commun. Mass Spectrom. **23:** 3753–3762, doi:10.1002/rcm.4307

———, ———, M. F. LEHMANN, AND P. D. TORTELL. 2008. Nitrogen and oxygen isotope fractionation during dissimilatory nitrate reduction by denitrifying bacteria. Limnol. Oceanogr. **53:** 2533–2545, doi:10.4319/lo.2008.53.6.2533

———, ———, J. A. Needoba, and P. J. Harrison. 2004. Coupled nitrogen and oxygen isotope fractionation of nitrate during assimilation by cultures of marine phytoplankton. Limnol. Oceanogr. **49:** 1763–1773, doi:10.4319/lo.2004.49.5.1763

Gruber, N., and J. N. Galloway. 2008. An Earth-system perspective of the global nitrogen cycle. Nature **451:** 293–296, doi:10.1038/nature06592

———, and J. L. Sarmiento. 1997. Global patterns of marine nitrogen fixation and denitrification. Glob. Biogeochem. Cycles **11:** 235–266, doi:10.1029/97GB00077

Knapp, A. N., P. J. DiFiore, C. Deutsch, D. M. Sigman, and F. Lipschultz. 2008. Nitrate isotopic composition between Bermuda and Puerto Rico Implications for N_2 fixation in the Atlantic Ocean. Glob. Biogeochem. Cycles **22:** GB3014, doi:10.1029/2007GB003107

Kroopnick, P. M., and H. C. Craig. 1972. Atmospheric oxygen: Isotopic composition and solubility fractionation. Science **175:** 54–55, doi:10.1126/science.175.4017.54

Kumar, S., D. J. D. Nicholas, and E. H. Williams. 1983. Definitive ^{15}N NMR evidence that water serves as a source of O during nitrite oxidation by. FEBS Lett. **152:** 71–74, doi:10.1016/0014-5793(83)80484-0

Lomas, M. W., and F. Lipschultz. 2006. Forming the primary nitrite maximum: Nitrifiers or phytoplankton. Limnol. Oceanogr. **51:** 2453–2467, doi:10.4319/lo.2006.51.5.2453

McIlvin, M. R., and M. A. Altabet. 2005. Chemical conversion of nitrate and nitrite to nitrous oxide and nitrogen and oxygen isotopic analysis in freshwater and seawater. Anal. Chem. **77:** 5589–5595, doi:10.1021/ac050528s

———, and K. L. Casciotti. 2006. Method for the analysis of $\delta^{18}O$ in water. Anal. Chem. **78:** 2377–2381, doi:10.1021/ac051838d

———, and ———. 2011. Technical updates to the bacterial method for nitrate isotopic analyses. Anal. Chem. **83:** 1850–1856, doi:10.1021/ac1028984

Santoro, A. E., and K. L. Casciotti. 2011. Enrichment and characterization of ammonia-oxidizing archaea from the open ocean: Phylogeny, physiology and stable isotope fractionation. Int. Soc. Microb. Ecol. J. **5:** 1796–1808.

Sigman, D. M., K. L. Casciotti, M. Andreani, C. Barford, M. Galanter, and J. K. Bohlke. 2001. A bacterial method for the nitrogen isotopic analysis of nitrate in seawater and freshwater. Anal. Chem. **73:** 4145–4153, doi:10.1021/ac010088e

———, J. Granger, P. J. DiFiore, M. M. Lehmann, R. Ho, G. Cane, and A. van Green. 2005. Coupled nitrogen and oxygen isotope measurements of nitrate along the eastern North Pacific margin. Glob. Biogeochem. Cycles **19:** 1–14, doi:10.1029/2005GB002458

———, and others. 2009. The dual isotopes of deep nitrate as a constraint of the cycle and budget of oceanic fixed nitrogen. Deep-Sea Res. I **56:** 1419–1439, doi:10.1016/j.dsr.2009.04.007

Snider, D. M., J. Spoelstra, S. L. Schiff, and J. J. Venkiteswaran. 2010. Stable oxygen isotope ratios of nitrate produced from nitrification: ^{18}O-labeled water incubations of agricultural and temperate forest soils. Environ. Sci. Technol. **44:** 5358–5364, doi:10.1021/es1002567

Solorzano, L. 1969. Determination of ammonia in natural waters by the phenolhypochlorite method. Limnol. Oceanogr. **14:** 799–801, doi:10.4319/lo.1969.14.5.0799

Strickland, J. D. H., and T. R. Parsons. 1972. A practical handbook of seawater analysis. Bull. Fish. Res. Board Can. **167:** 1–310.

Taylor, J. R. 1997. An introduction to error analysis, 2nd ed. University Science Books.

Wada, E., and A. Hattori. 1971. Nitrite metabolism in the euphotic layer of the central North Pacific Ocean. Limnol. Oceanogr. **16:** 766–772, doi:10.4319/lo.1971.16.5.0766

Wankel, S. D., C. Kendall, J. T. Pennington, F. P. Chavez, and A. Paytan. 2007. Nitrification in the euphotic zone as evidenced by nitrate dual isotopic composition: Observations from Monterey Bay, California. Glob. Biogeochem. Cycles **21:** GB2009, doi:10.1029/2006GB002723

Ward, B. B., and A. F. Carlucci. 1985. Marine ammonia-oxidizing and nitrite oxidizing bacteria- seriological diversity determined by immunofluorescence in culture and in the environment. Appl. Environ. Microbiol. **50:** 194–201.

———, H. E. Glover, and F. Lipschultz. 1989. Chemoautotrophic activity and nitrification in the oxygen minimum zone off Peru. Deep-Sea Res. **36:** 1031–1051.

Watson, S. W. 1965. Characteristics of a marine nitrifying bacterium, *Nitrosocystis oceanus* sp. n. Limnol. Oceanogr. **10:** R274–R289.

———, and J. B. Waterbury. 1971. Characteristics of two marine nitrite oxidizing bacteria, *Nitrospina gracilis* nov. gen. nov. sp. and *Nitrococcus mobilis* nov. gen. nov. sp. Arch. Microbiol. **77:** 203–230, doi:10.1007/BF00408114

York, D. 1966. Least-squares fitting of straight lines. Can. J. Phys. **44:** 1079–1086, doi:10.1139/p66-090

———, N. M. Evensen, M. L. Martinez, and J. D. B. Delgado. 2004. Unified equations for the slope, intercept, and standard errors of the best straight line. Am. J. Phys. **72:** 367–375, doi:10.1119/1.1632486

Associate editor: H. Maurice Valett

Received: 05 December 2011
Accepted: 08 May 2012
Amended: 19 May 2012

Chapter 4

The $\delta^{18}O$ and $\delta^{15}N$ of nitrite: Novel tracers for the source and age of nitrite in the ocean

Carolyn Buchwald and Karen L. Casciotti

Submitted to Nature Geoscience

The primary nitrite maximum (PNM) is a ubiquitous feature in oceanic nutrient distributions whose origin has been much debated. The controlling processes are linked to the biological carbon pump and production of nitrous oxide, a climatically important greenhouse gas. Here we used oxygen and nitrogen isotope ratio measurements of nitrite to evaluate its sources and average age in the PNM at several sites in the Arabian Sea. Laboratory experiments were first used to determine the rate and equilibrium isotope effects of abiotic oxygen isotope exchange between nitrite and seawater under a variety of conditions (pH, T, S). This framework was used to interpret nitrite isotope data collected from the Arabian Sea. The data suggest that ammonia oxidation was the primary source of nitrite in the Arabian Sea PNM and it ranged from 0-87 days old. Our data suggest a relatively low rate of biological nitrite turnover in the PNM.

Nitrite (NO_2^-) is a central intermediate in the marine nitrogen cycle and is generally held in low concentrations in the ocean. However, nitrite accumulates at the base of the euphotic zone in the primary nitrite maximum (PNM) and in the center of oxygen deficient zones (ODZs) in the secondary nitrite maximum (SNM). The PNM and SNM, which are prominent in the highly productive and low oxygen regions of the ocean such as the Eastern Tropical North Pacific (ETNP), Eastern Tropical South Pacific (ETSP) and Arabian Sea, are both associated with significant production of N_2O [1-3]. The pathways that produce nitrite and N_2O are also an integral part of the recycling and removal of fixed nitrogen in the ocean, which is a major control on the biological pump and subsequent CO_2 removal from the atmosphere. Even though the rates and relative fluxes of the processes that produce and consume nitrite are biogeochemically important, there is still much uncertainty surrounding the reasons for nitrite accumulation in these features.

In the PNM there are two dominant sources of nitrite: ammonia oxidation and nitrate reduction, and two sinks of nitrite: nitrite oxidation and nitrite assimilation (Fig. 1). The relative rates of these processes are often determined by isotope tracer incubation experiments. Such incubations provide valuable insight into the rates of biogeochemical processes, but have potential drawbacks, including: bottle-effects, stimulation of processes by added tracer, and missing heterogeneity of processes in space and time.

Here we present a novel approach, based on static measurements of the nitrogen and oxygen isotope ratios of nitrite to determine its source(s), sink(s) and the rates of transformation.

The nitrogen (N) and oxygen (O) isotopes of nitrite ($\delta^{15}N_{NO2}$ (‰ vs. atmospheric N_2) = ($^{15}N/^{14}N_{NO2} \div {}^{15}N/^{14}N_{N2}$ -1) · 1000; $\delta^{18}O_{NO2}$ (‰ vs. Vienna Standard Mean Ocean Water) = ($^{18}O/^{16}O_{NO2} \div {}^{18}O/^{16}O_{VSMOW}$ -1) · 1000) record the history of processes that have contributed to production and consumption of nitrite. The nitrogen isotopes are affected by fractionation associated with biological processes (production and consumption of nitrite), while the oxygen isotopes will also by affected by abiotic exchange with the oxygen atoms in water, resetting $\delta^{18}O_{NO2}$ values toward equilibrium. Since this abiotic equilibration occurs at a predictable rate (depending on pH, temperature (T) and salinity (S)), we can use this knowledge to determine the competing rates of biological nitrite turnover. While studies using isotope tracers of biological processes are common, the ability to predict a rate from a static isotopic measurement is quite unique.

Sources and sinks of nitrite in the PNM and their isotopic signatures

Interpreting sources and sinks of nitrite from $\delta^{15}N_{NO2}$ and $\delta^{18}O_{NO2}$ values in the PNM requires knowledge of the isotopic signatures and fractionations for each process. The $\delta^{15}N$ of nitrite produced by ammonia oxidation ($\delta^{15}N_{NO2,AO}$) is dependent on the $\delta^{15}N$ of the remineralized organic matter ($\delta^{15}N_{OM}$), the isotope effect for assimilation of ammonium ($^{15}\varepsilon_{k,AA}$), the isotope effect for ammonia oxidation ($^{15}\varepsilon_{k,AO}$), and the relative rates of ammonium assimilation and ammonia oxidation (f_{AA} *and* f_{AO}, respectively; Table 1). The $\delta^{15}N_{OM}$ value (Table 2) can be estimated from the range of values measured in the ocean[4]. The isotope effects for ammonia oxidation (Table 2) were taken from those measured in laboratory cultures of AOB and AOA [5, 6]. The $\delta^{18}O$ of nitrite produced from ammonia oxidation ($\delta^{18}O_{NO2,AO}$) will be dependent on the $\delta^{18}O$ of dissolved oxygen ($\delta^{18}O_{O2}$) and water ($\delta^{18}O_{H2O}$) and the isotope effects for their incorporation ($^{18}\varepsilon_{k,O2}$ and $^{18}\varepsilon_{k,H2O,1}$, respectively) as well as any biotic exchange during ammonia oxidation (x_{AO})[5, 7].

The $\delta^{15}N$ and $\delta^{18}O$ of nitrite produced from nitrate reduction ($\delta^{15}N_{NO2,NR}$ and $\delta^{18}O_{NO2,NR}$, respectively) will be determined by the isotopic values of the nitrate ($\delta^{15}N_{NO3}$ and $\delta^{18}O_{NO3}$) and the isotope effects for assimilatory nitrate reduction ($^{15}\varepsilon_{k,NR}$ and $^{18}\varepsilon_{k,NR}$)[8, 9]. Fractionation at the "branch point" between nitrite and H_2O ($^{18}\varepsilon_{b,NR}$) also controls the $\delta^{18}O$ value of the nitrite produced from the reacted nitrate[10]. For removal of nitrite via oxidation (NO) and assimilation (NA), Rayleigh fractionation will describe the change in the $\delta^{15}N_{NO2}$ and $\delta^{18}O_{NO2}$ based on the fraction removed (f) and the isotope effects for each process for each isotope ($^{15}\varepsilon_{k,NO}$; $^{18}\varepsilon_{k,NO}$; $^{15}\varepsilon_{k,NA}$; $^{18}\varepsilon_{k,NA}$)[11-13]. In addition to isotopic fractionation associated with biological source and sink processes, the $\delta^{18}O_{NO2}$ values will also be affected by abiotic equilibration (Fig. 1). Over time, this process will overwrite the biotic $\delta^{18}O$ signatures, leading to $\delta^{18}O_{NO2}$ values closer to equilibrium the longer nitrite persists. Therefore, while $\delta^{18}O_{NO2}$ values can be used along with $\delta^{15}N_{NO2}$ values to constrain sources and sinks of nitrite, abiotic exchange must be considered.

Determining the average age from the $\delta^{18}O_{NO2}$

Oxygen atoms exchange abiotically between nitrite and water at a set rate that competes with biological turnover for control of $\delta^{18}O_{NO2}$ values. The exchange of oxygen atoms between nitrite and water is a first order reaction, shown in equation 1.

(1) $$\delta^{18}O_{NO2,t} = \left(\delta^{18}O_{NO2,b} - \delta^{18}O_{NO2,eq}\right) \times e^{-kt} + \delta^{18}O_{NO2,eq}$$

$\delta^{18}O_{NO2,t}$ is the measured value of the sample, $\delta^{18}O_{NO2,b}$ is the signature of the biological endmember (in the absence of abiotic equilibration), k is the rate constant for equilibration, which is dependent on the pH and temperature of seawater at a given depth, and $\delta^{18}O_{NO2,eq}$ is the $\delta^{18}O_{NO2}$ value expected at equilibrium for a given temperature and $\delta^{18}O_{H2O}$. Given that biological $\delta^{18}O_{NO2}$ values are generated out of equilibrium (see more below), the measured $\delta^{18}O_{NO2}$ values can be used as a clock recording the relative rates of biological and abiotic turnover of nitrite. If nitrite is turned over quickly relative to abiotic exchange, it will remain out of equilibrium, but if biological turnover is slow relative to abiotic exchange, $\delta^{18}O_{NO2}$ will approach equilibrium on a predictable

timescale. By knowing the rate of abiotic exchange and equilibrium isotope effect under a given set of conditions (T, pH, S), the rate of biological turnover can be modeled from the degree of $\delta^{18}O_{NO2}$ disequilibrium.

This method determines an "age" and not a "turnover time" of nitrite because we are not assuming a steady state of nitrite concentration. We allow production, consumption and equilibration in a stepwise manner, rather than occurring all at the same time. A steady-state model was originally tested but using this method it was impossible to create the very low $\delta^{15}N_{NO2}$ values measured in oceanic samples without allowing consumption of nitrite. The experimental basis of this model and the parameters used to determine the average age of nitrite are discussed in the following sections.

Determining the biological endmember ($\delta^{18}O_{NO2,b}$)

The disequilibrium model relies on knowing the $\delta^{18}O_{NO2}$ value that would be set by biological sources and sinks in the absence of abiotic equilibration, which we refer to as the 'biological endmember' ($\delta^{18}O_{NO2,b}$). This parameter depends on the sources and sinks of nitrite in the PNM, the substrates involved, and isotope effects associated with the reactions. Due to the number and complexity of these parameters, it is the most uncertain parameter in equation 1.

Here we use the $\delta^{15}N_{NO2}$ values to constrain $\delta^{18}O_{NO2,b}$ given knowledge of the isotope effects for N and O isotopes in the relevant processes (Tables 1 and 2). The $\delta^{15}N_{NO2}$ value is not altered abiotically so its measured value will directly reflect the biological sources and sinks, and the extent of removal. We model the $\delta^{15}N_{NO2}$ according to equation (2) by evaluating the relative contributions of ammonia oxidation (r_{AO}) and nitrate reduction (r_{NR}) based on their estimated $\delta^{15}N$ signatures at a particular site (Table 1). We then allow the $\delta^{15}N_{NO2}$ value to change due to Rayleigh fractionation during consumption. The isotope effects for nitrite oxidation ($^{15}\varepsilon_{k,NO}$) and nitrite assimilation ($^{15}\varepsilon_{k,NA}$) (Table 2) are weighted by their relative fluxes (r_{NO} and r_{NA}, respectively) to determine the expressed isotope effect for nitrite consumption. Using the known isotope signatures for each of the four processes (Table 2), the fraction of nitrite remaining (f) can

be determined using equation 2. Since f must be between 0 and 1, this puts constraints on the possible sources and sinks in order to match the measured $\delta^{15}N_{NO2}$ value.

(2) $$\delta^{15}N_{NO2,measured} = \left(r_{AO}\delta^{15}N_{NO2,AO} + r_{NR}\delta^{15}N_{NO2,NR}\right) - \left(r_{NO}{}^{15}\varepsilon_{k,NO} + r_{NA}{}^{15}\varepsilon_{k,NA}\right)\ln(f)$$

After calculating the f values, and applying the same r values for sources and sinks, $\delta^{18}O_{NO2,b}$ can be calculated from the $\delta^{18}O$ values and isotope effects for each process (equation 3).

(3) $$\delta^{18}O_{NO2,b} = \left(r_{AO}\delta^{18}O_{NO2,AO} + r_{NR}\delta^{18}O_{NO2,NR}\right) - \left(r_{NO}{}^{18}\varepsilon_{k,NO} + r_{NA}{}^{18}\varepsilon_{k,NA}\right)\ln(f)$$

Its application is similar to equation 2 except here $\delta^{18}O_{NO2,b}$ is the unknown instead of f. The value predicted for $\delta^{18}O_{NO2,b}$ provides an additional constraint on the source and sink processes since the measured $\delta^{18}O_{NO2}$ value should fall between $\delta^{18}O_{NO2,b}$ and $\delta^{18}O_{NO2,eq}$. Currently there is some uncertainty in many of these measured isotope effects (Table 2) for ^{15}N and ^{18}O, of usually a few per mil, this would cause changes in estimate ln(f) and subsequently the predicted $\delta^{18}O_{NO2,b}$. A ±5 per mil change in each of the isotope effects will change the $\delta^{18}O_{NO2,b}$ by less than 3%.

Rate of abiotic oxygen atom equilibration between nitrite and water (k)

The rate constant for abiotic equilibration of oxygen atoms (k) depends on T, pH and S. We determined values of k at relevant oceanic pH (6.7-8), T (277-280 K), and S (32-41) values in laboratory experiments. These experiments were conducted by incubating two nitrite reference materials (N-10219 and N-7373) with different $\delta^{18}O_{NO2}$ values (N-101219 above the expected $\delta^{18}O_{NO2,eq}$ value and N-7373 below it) in buffered seawater with a known $\delta^{18}O_{H2O}$ at a constant temperature. Each bottle was subsampled over time until the two nitrite reference materials reached the same $\delta^{18}O_{NO2}$ value, indicating that they had reached equilibrium. 20 different combinations of pH, T, and S were analyzed in duplicate. Figure 2 shows the time courses of $\delta^{18}O_{NO2}$ in all sample bottles in each experiment. An exponential fit of the form $y = y_0 + A \bullet \exp(-k \bullet x)$, similar in form to equation 1, was calculated from the data for each sample bottle. The k value represents the first order equilibration rate constant needed to solve equation 1 at a given

pH, T, and S. Our experiments show that k is sensitive to changes in pH and T that are relevant to oceanic conditions, but showed little dependence on S between 32 and 41.

In order to produce general relationships between k, pH, and T, linear regressions were fit between k (y-axis) and pH (x-axis) (for a pH > 7.0) for each temperature (306, 303, 296, 293, 281, and 277 K). The slopes and intercepts of these linear regressions changed with temperature, with faster rates (larger k) at higher temperatures for a given pH (Figure S1 a,b). There was log-normal relationship between the slope and T as well as between the intercept and T (equations 4 and 5). To calculate k for a given T and pH you can combine equations 4 and 5 into one equation (equation 6).

(4) $\text{slope} = -0.0166 - 1.4123 * e^{-\left(\frac{\ln(T/317.71)}{0.0462}\right)^2}$

(5) $\text{intercept} = 0.1467 - 10.193 * e^{-\left(\frac{\ln(T/316.48)}{0.042}\right)^2}$

(6) $k = \left(-0.0166 - 1.4123 * e^{-\left(\frac{\ln(T/317.71)}{0.0462}\right)^2}\right)\text{pH} + 0.1467 - 10.193 * e^{-\left(\frac{\ln(T/316.48)}{0.042}\right)^2}$

Temperature dependence of the equilibrium isotope effect ($^{18}\varepsilon_{eq}$) and $\delta^{18}O_{NO2,eq}$

The abiotic endmember is set by the temperature-dependent equilibrium isotope effect for oxygen exchange between nitrite and water ($^{18}\varepsilon_{eq}$) and the local δ^{18}O value of the seawater ($\delta^{18}O_{H2O}$). Here $^{18}\varepsilon_{eq}$ was determined in two ways. The first set of estimates comes from the final $\delta^{18}O_{NO2}$ value to which both nitrite standards converged in the incubations with varied pH and T (Figure 2; described above). The second set of estimates comes from rapid equilibration of nitrite samples in seawater adjusted to a pH ~ 5 at multiple temperatures. In each experiment, $\delta^{18}O_{H2O}$ was measured and subtracted from the final $\delta^{18}O_{NO2}$ to calculate $^{18}\varepsilon_{eq}$, according to equation 7.

(7) $\delta^{18}O_{NO2,eq} = \delta^{18}O_{H2O} + {}^{18}\varepsilon_{eq}$

There is a linear relationship between $^{18}\varepsilon_{eq}$ and temperature in the range of 277 to 309 K (Figure S2). The equation for this line is shown in equation 8. At room temperature (294 K) the average $^{18}\varepsilon_{eq}$ is 13.5‰.

(8) $^{18}\varepsilon_{eq} = -0.12 \times T + 48.79$

Average age of nitrite in the Arabian Sea PNM

Nitrate and nitrite isotope data were collected from a cruise to the Arabian Sea in September-October 2007. At five different stations at least one nitrite sample from the primary nitrite maximum was analyzed, with a total of 8 samples. The average collection depth was 42 meters. The nitrite concentrations ranged from 0.3 to 2.7 μM, with an average of 1.5 μM. The measured $\delta^{15}N_{NO2}$ values ranged from -3.7‰ to 2.4‰, while the $\delta^{18}O_{NO2}$ values varied from 7.4‰ to 14.7‰ (Fig. 3, red triangles).

To calculate the average age of the nitrite in these samples (equation 1), the equilibration rate constant (k) for each sample was calculated from pH and T data using equation 6. pH was determined from a linear relationship between pH and dissolved oxygen concentration and *in situ* T was measured directly. The pH vs. O_2 relationship was determined by measuring pH at sea using m-cresol purple (described below) and comparing these values to oxygen concentration data from an *in situ* sensor. $\delta^{18}O_{NO2,eq}$ was determined for each sample (equation 7) from $^{18}\varepsilon_{eq}$ based on the T data (equation 8) and $\delta^{18}O_{H2O}$ calculated from S (Sigman et al., 2009). Finally, the biological endmember, $\delta^{18}O_{NO2,b}$, was predicted at every $\delta^{15}N_{NO2}$ value, as described above (equations 2 and 3). Based on the measured $\delta^{15}N_{NO2}$ and $\delta^{18}O_{NO2}$ values, we determined that for most samples the source and sink for this nitrite were ammonia oxidation and nitrite oxidation, respectively. Ammonia oxidation was determined to be the primary source because most of the $\delta^{18}O_{NO2}$ values were lower than the equilibrated value (Figure 3), whereas nitrate reduction would have given $\delta^{18}O_{NO2}$ values higher than $\delta^{18}O_{NO2,eq}$. The range of $\delta^{15}N_{NO2}$ values relative to the prospective sources requires consumption with an inverse kinetic isotope effect, characteristic of nitrite oxidation[13]. Nitrite assimilation has a small positive isotope effect, so consumption by this process could not explain the measured $\delta^{15}N_{NO2}$ values. Nitrite oxidation also leads to decreases in $\delta^{18}O_{NO2}$, although with a smaller inverse isotope effect (Figure 3, solid lines; [11]). The closer individual $\delta^{18}O_{NO2}$ values fall to their respective $\delta^{18}O_{NO2,b}$ values, the younger the nitrite is inferred to be.

The closer they fall to their individual $\delta^{18}O_{NO2,eq}$ values, the older the nitrite is inferred to be. The calculation also takes into consideration the distance between $\delta^{18}O_{NO2,b}$ and $\delta^{18}O_{NO2,eq}$ for each sample so that the same measured $\delta^{18}O_{NO2}$ value for two samples may represent different ages.

The average age of the nitrite in these samples ranged from 0 days to 87 days with an average of 37 days. These ages are reasonable for the concentrations of nitrite and ammonia oxidation rates measured in the Arabian Sea PNM [14]. Newell et al. measured ammonia oxidation rates of 4 to 20 nM d^{-1}, and then using the measured nitrite concentrations in the PNM, it would equate to a turnover time of nitrite of 42 to 62 days, which is in the range of our determined ages. These rates are also similar to ammonia oxidation rates in the PNM of other areas of the ocean, such as the Eastern Tropical South Pacific and California current. In two different studies[15, 16] they measured ammonia oxidation rates and nitrite concentrations, which equate to nitrite turnover times of 20-50 days for both of these locations. However, if the processes are episodic, the long-term average can be very difficult to evaluate with tracer experiments due to sampling limitations of incubation measurements. Using isotope measurements to integrate rates over periods on the order of a month or two is therefore powerful and complementary to more traditional isotope tracer techniques.

There was one sample that had a $\delta^{18}O_{NO2}$ value higher than $\delta^{18}O_{NO2,eq}$, indicating that ammonia oxidation was not the only source of nitrite. We can constrain the $\delta^{18}O_{NO2,b}$ value for this sample based on the nitrite oxidation fractionation factors, the $\delta^{15}N$ and $\delta^{18}O$ source values, and the concentration of nitrite. Assuming nitrite oxidation is the primary sink (given the low $\delta^{15}N_{NO2}$ value), we know the slope of the consumption trend in $\delta^{18}O_{NO2}$ vs. $\delta^{15}N_{NO2}$ space (solid lines, Figure 3). The starting point for the consumption line (blue squares, Figure 3) depends on the source contributions from ammonia oxidation and nitrate reduction. If we allow 40% to be produced from nitrate reduction and 60% from ammonia oxidation, the nitrite would have an age of 39 days. When allowing only 30% from nitrate reduction, $\delta^{18}O_{NO2,b}$ falls below $\delta^{18}O_{NO2,eq}$ after nitrite oxidation has taken place. If nitrate reduction is assumed to comprise 50% of the

nitrite source, the calculated *f* value becomes 0.3, which seems too low given the relatively high nitrite concentration. The nitrite production from nitrate reduction is therefore most likely between 30-50% for this sample, and assuming 40% from nitrate reduction places the nitrite age within the range of other samples.

Nitrite is an important intermediate in the nitrogen cycle, and many studies have tried to determine the reason for nitrite accumulation in the primary nitrite maximum[17], but there has been no consensus. One reason for this may be that the sources and sinks of nitrite in the PNM actually vary among regions of the ocean. Based on the range of $\delta^{15}N_{NO2}$ and $\delta^{18}O_{NO2}$ values of our samples from the Arabian Sea PNM and the known values of the isotope sources and isotope effects (Tables 1 and 2), we conclude that the main processes responsible for nitrite production and consumption at these stations and depths are ammonia oxidation and nitrite oxidation, respectively. Assuming that the sources and sinks of nitrite can differ from location to location, application of this technique at other locations can provide additional insight into the cycling of nitrite in the ocean and the sensitivity of these processes to light, nutrients, and other oceanographic parameters.

The processes involved with nitrite turnover are linked to primary production and N_2O production in the ocean. The amount of nitrification in the euphotic zone, for example, can alter new production estimates in the ocean[18, 19]. When neglecting nitrification these estimates can be grossly overestimated, and will overestimate CO_2 uptake by the ocean. Secondly, N_2O production by nitrification in and around the PNM may also be climatically important, especially since N_2O produced in the PNM would be easily mixed out of the water column into the atmosphere. Interpretations of nitrite isotope measurements in the context of microbial isotope fractionation factors, such as shown here, can provide us a greater understanding on oceanic nitrogen cycling and its role in ocean biogeochemistry.

Methods

Abiotic equilibration experiments

Three experiments with a total of 40 individual incubations were conducted to determine the rate of abiotic nitrite and oxygen atom exchange at different temperatures, salinities, and pH values. At each pH, temperature, and salinity condition two 160 mL glass serum bottles were filled with 140 mL of buffered seawater, made with Vineyard Sound or Bermuda Atlantic Time Series Station (BATS) surface seawater, Tris buffer and 0.2 mol L^{-1} HCl. The different pH values were obtained by adding different ratios of 0.2 mol L^{-1} HCl and Tris Buffer[20]. The incubation pH was verified by using the spectrophotometric method with phenol red dye[21]. Briefly, 1 mL of sample and 10 μL of phenol red, adjusted to a similar pH, was measured at both 433 nm and 558 nm. The ratio of the absorbances was used to determine the pH. Since the pH is sensitive to temperature, all pH measurements were conducted at room temperature and then corrected to the incubation temperature using a pH/temperature relationship previously determined for Tris buffer[22].

To begin an experiment, 7 μmoles of KNO_2 standard N-7373 ($\delta^{18}O_{NO2}$ = 4.5‰ vs. VSMOW) or 7 μmoles of KNO_2 standard N-10219 ($\delta^{18}O_{NO2}$ = 88.5‰ vs. VSMOW) were added to separate bottles for each pH and temperature treatment to obtain a nitrite concentration of 50 μmol L^{-1} in each bottle. For experiment 2, the salinities were also adjusted by adding different amounts of DI water, which were already adjusted to a pH similar to the seawater so that all bottles would have similar pHs. Salinity was measured using a Fisher Scientific (13-946-27) portable refractometer.

After preparation, each pair of bottles was sampled immediately for [NO_2^-], $\delta^{15}N_{NO2}$ and $\delta^{18}O_{NO2}$, then incubated in different temperature-controlled incubators or in the laboratory at room temperature. Bottles were sampled every 2 to 3 days for the first week and then sampled less frequently as they approached equilibrium. 200 μL from each bottle was sub-sampled directly into replicate 20 mL glass vials for nitrite isotope analysis using the azide method[23]with nitrite standards N-10219, N-23, and N-7373.

Arabian Sea nitrite isotope measurements

On a cruise to the Arabian Sea nitrite isotope samples were collected in September-October of 2007. Depths were selected in order to locate the narrow primary nitrite maximum feature at the base of the euphotic zone. At each station, 25 mL water was collected into 50 mL centrifuge tubes, for nitrite concentration analysis using the Greiss-Ilosvay colorimetric method[24]. 500 μL of sulfanilamide in 10% HCL (SAN) and 500 μL of naphthyl-ethylene diamine (NED) was added to each tube and then measured at 540 nm on a spectrophotometer. After the concentration was determined, 5 or 10 nmol of nitrite, depending on the concentration, was added to a 20 mL vial, and prepped for conversion of nitrite to N_2O using the azide reaction[23]. Nitrite standards N-23, N-7373, N-10219 were prepared at sea along with each batch of nitrite samples to achieve the same nanomole amount of N as the samples. The time between sampling and azide addition was minimized to avoid any additional abiotic exchange. However, since the rates of exchange at seawater pH of ~8 are low the time between sampling and conversion will have a negligible affect on the nitrite isotopic value. N_2O vials from samples and standards were then stored at room temperature and measured on a Finnigan Delta^{PLUS} XP isotope-ratio mass spectrometer immediately upon return from sea.

Acknowledgements

We would like to thank Matthew McIlvin and Brian Peters for help collecting data. We would like to thank the chief scientist Bess Ward and the captain and crew of the *R/V Revelle* for the collection of nitrite isotope samples in the Arabian Sea.

References

1. Codispoti, L. A. & Christensen, J. P. Nitrification, Denitrification and Nitrous-Oxide Cycling in the Eastern Tropical South-Pacific Ocean. *Mar. Chem.* **16**, 277-300 (1985).
2. Codispoti, L. A. Interesting Times for Marine N2O. *Science* **327**, 1339-1340 (2010).
3. Freing, A., Wallace, D. W. R. & Bange, H. W. Global oceanic production of nitrous oxide. *Philosophical Transactions of the Royal Society B-Biological Sciences* **367**, 1245-1255 (2012).
4. Wada, E. & Hattori, A. Natural abundance ^{15}N in particulate organic matter in the North Pacific Ocean. *Geochimica et Cosmochimica Acta* **40**, 249-251 (1976).
5. Casciotti, K. L., McIlvin, M. & Buchwald, C. Oxygen isotopic exchange and fractionation during bacterial ammonia oxidation. *Limnol. Oceanogr.* **55**, 753-762 (2010).

6. Santoro, A. E. & Casciotti, K. L. Enrichment and characterization of ammonia-oxidizing archaea from the open ocean: phylogeny, physiology and stable isotope fractionation. *Isme Journal* **5**, 1796-1808 (2011).
7. Buchwald, C., Santoro, A. E., McIlvin, M. R. & Casciotti, K. L. Oxygen isotopic composition of nitrate and nitrite produced by nitrifying cocultures in and natural marine assemblages. *Limnology and Oceanography* **57**, 1361-1375 (2012).
8. Granger, J., Sigman, D. M., Needoba, J. A. & Harrison, P. J. Coupled nitrogen and oxygen isotope fractionation of nitrate during assimilation by cultures of marine phytoplankton. *Limnol. Oceanogr.* **49**, 1763-1773 (2004).
9. Granger, J., Sigman, D. M., Rohde, M. M., Maldonado, M. T. & Tortell, P. D. N and O isotope effects during nitrate assimilation by unicellular prokaryotic and eukaryotic plankton cultures. *Geochim. Cosmochim. Acta* **74**, 1030-1040 (2010).
10. Casciotti, K. L. & McIlvin, M. R. Isotopic analyses of nitrate and nitrite from reference mixtures and application to Eastern Tropical North Pacific waters. *Mar. Chem.* **107**, 184-201 (2007).
11. Buchwald, C. & Casciotti, K. L. Oxygen isotopic fractionation and exchange during bacterial nitrite oxidation. *Limnol. Oceanogr.* **55**, 1064-1074 (2010).
12. Waser, N. A. D., Harrison, P. J., Nielsen, B., Calvert, S. E. & Turpin, D. H. Nitrogen isotope fractionation during the uptake and assimilation of nitrate, nitrite, ammonium, and urea by a marine diatom. *Limnol. Oceanogr.* **43**, 215-224 (1998).
13. Casciotti, K. L. Inverse kinetic isotope fractionation during bacterial nitrite oxidation. *Geochim. Cosmochim. Acta* **73**, 2061-2076 (2009).
14. Newell, S. E., Babbin, A. R., Jayakumar, A. & Ward, B. B. Ammonia oxidation rates and nitrification in the Arabian Sea. *Global Biogeochem. Cycles* **25**, GB4016 (2011).
15. Lipschultz, F. *et al.* Bacterial Transformations of Inorganic Nitrogen in the Oxygen-Deficient Waters of the Eastern Tropical South-Pacific Ocean. *Deep-Sea Research Part A-Oceanographic Research Papers* **37** (1990).
16. Ward, B. B., Olson, R. J. & Perry, M. J. Microbial Nitrification Rates in the Primary Nitrite Maximum Off Southern-California. *Deep-Sea Research Part A-Oceanographic Research Papers* **29** (1982).
17. Lomas, M. W. & Lipschultz, F. Forming the primary nitrite maximum: Nitrifiers or phytoplankton? *Limnol. Oceanogr.* **51**, 2453-2467 (2006).
18. Dugdale, R. C. & Goering, J. J. Uptake of New and Regenerated Forms of Nitrogen in Primary Productivity. *Limnol. Oceanogr.* **12**, 196-206 (1967).
19. Yool, A., Martin, A. P., Fernandez, C. & Clark, D. R. The significance of nitrification for oceanic new production. *Nature* **447**, 999-1002 (2007).
20. Gomori, G. Preparation of Buffers for use in Enzyme Studies. *Meth. Enzymol.* **1**, 138-146 (1955).
21. Robert-Baldo, G. L., Morris, M. J. & Byrne, R. H. Spectrophotometric determination of seawater pH using phenol red. *Anal.Chem.* **57**, 2564-2567 (1985).
22. Durst, R. A. & Staples, B. R. Tris/tris.Hcl - Standard Buffer for use in Physiologic Ph Range. *Clin. Chem.* **18**, 206-& (1972).
23. McIlvin, M. R. & Altabet, M. A. Chemical conversion of nitrate and nitrite to nitrous oxide for nitrogen and oxygen isotopic analysis in freshwater and seawater. *Anal. Chem.* **77**, 5589-5595 (2005).
24. Strickland, J. D. H. & Parsons T. R. A practical handbook of seawater analysis. *Bulletin of Fisheries Research Board of Canada* **167**, 1-310 (1972).

Figures

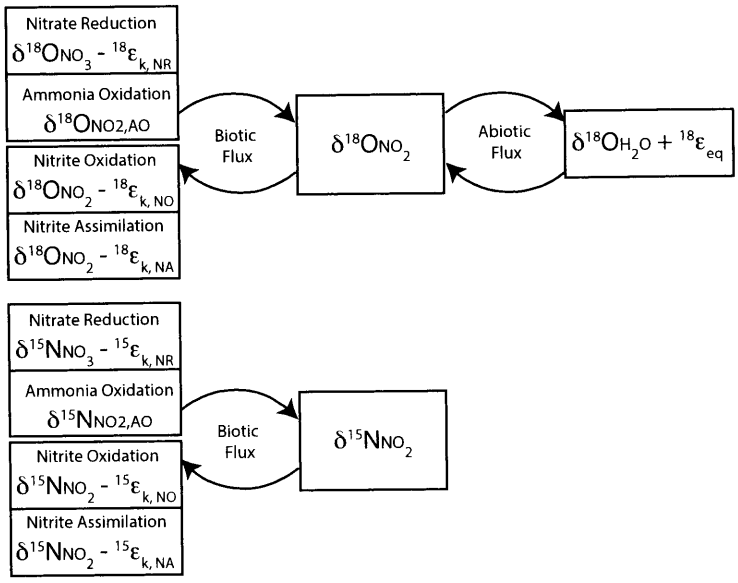

Figure 1. A box model diagram illustrating the processes that control $\delta^{15}N$ and $\delta^{18}O$ of nitrite in the primary nitrite maximum.

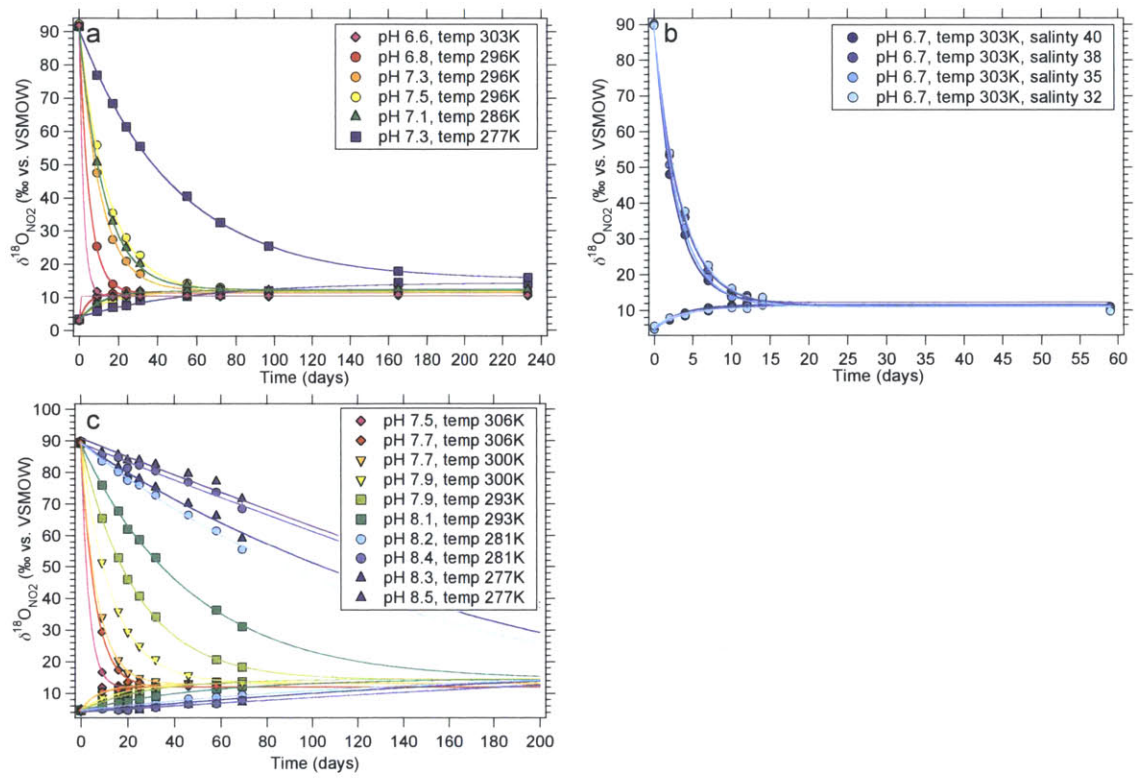

Figure 2. Time courses of $\delta^{18}O_{NO2}$ values during 3 different experiments in which pH, T and salinity were varied. (a) exp 1; includes incubations at 3 different temperatures and 5 different pH values, all with the same salinity, in duplicate (b) exp 2; includes incubations at 4 different salinities with the same temperature and pH, in duplicate. (c) exp 3; includes 10 experiments at 5 different temperatures and 8 different pH values, all with the same salinity, in duplicate. Error bars for $\delta^{18}O_{NO2}$ are smaller than the symbol markers.

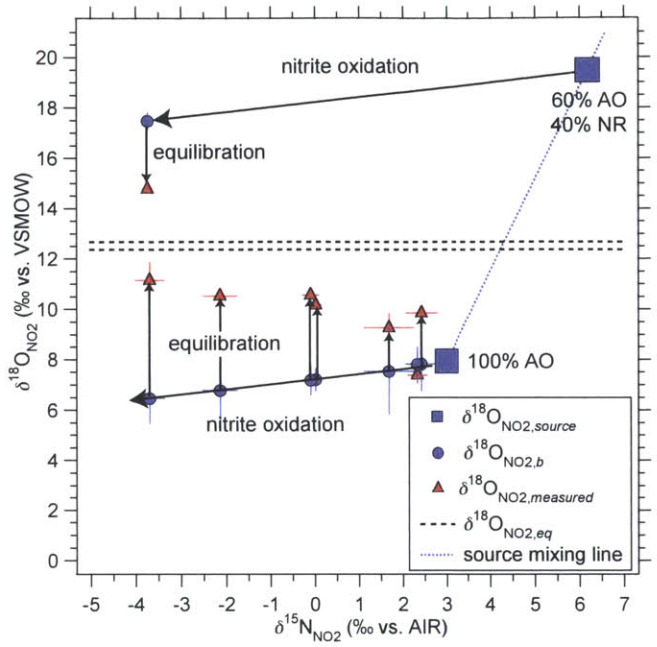

Figure 3. $\delta^{15}N_{NO2}$ and $\delta^{18}O_{NO2}$ values from the Arabian Sea PNM (red triangles). The blue circles represent the biological endmember values ($\delta^{15}N_{NO2}$ and $\delta^{18}O_{NO2,b}$) expected prior to equilibration based on either 100% ammonia oxidation or 60% ammonia oxidation and 40% nitrate reduction source (blue squares) and nitrite oxidation (large arrows) as the sink of nitrite. The vertical arrows represent abiotic equilibration/aging of nitrite. The dashed lines represent the range of $\delta^{18}O_{NO2,eq}$ values for the samples based on their in situ temperatures and salinities. Error bars indicated standard deviation of duplicate measurements of $\delta^{18}O_{NO2}$ and $\delta^{15}N_{NO2}$ for the red triangles and in the blue circles the propagated error from using the $\delta^{15}N_{NO2}$ to predict the $\delta^{18}O_{NO2,b}$.

Table 1. Isotopic source and sink signatures for the primary nitrite maximum

Sources
Ammonia oxidation (AO) $\delta^{15}N_{NO2,AO} = \delta^{15}N_{NH4} - {}^{15}\varepsilon_{k,AO}$ $\delta^{15}N_{NH4} = \delta^{15}N_{OM} + f_{AO} * {}^{15}\varepsilon_{k,AO} + f_{AA} * {}^{15}\varepsilon_{k,AA}$ $\delta^{18}O_{NO2,AO} = \frac{1}{2}[\ \delta^{18}O_{O2} + \delta^{18}O_{H2O} - ({}^{18}\varepsilon_{k,O2} + {}^{18}\varepsilon_{k,H2O,1})](1\text{-}x_{AO}) + (\delta^{18}O_{O2} + {}^{18}\varepsilon_{eq})(x_{AO})$
Assimilatory nitrate reduction (NR) $\delta^{15}N_{NO2,NR} = \delta^{15}N_{NO3} - {}^{15}\varepsilon_{k,NR}$ $\delta^{18}O_{NO2,NR} = \delta^{18}O_{NO3} - {}^{18}\varepsilon_{k,NR} + {}^{18}\varepsilon_{b,NR}$
Sinks
Nitrite oxidation (NO) $\delta^{15}N_{NO2} = \delta^{15}N_{NO2,source} - {}^{15}\varepsilon_{k,NO} * \ln(f_{NO})$ $\delta^{18}O_{NO2} = \delta^{18}O_{NO2,source} - {}^{18}\varepsilon_{k,NO} * \ln(f_{NO})$
Assimilatory nitrite reduction (NA) $\delta^{15}N_{NO2} = \delta^{15}N_{NO2,source} - {}^{15}\varepsilon_{k,NA} * \ln(f_{NA})$ $\delta^{18}O_{NO2} = \delta^{18}O_{NO2,source} - {}^{18}\varepsilon_{k,NA} * \ln(f_{NA})$

Table 2. Isotope term descriptions and values

Term	Description	Value
$^{15}\varepsilon_{k,AO}$	Kinetic N isotope effect for ammonia oxidation	22‰[6]
$^{15}\varepsilon_{k,AA}$	Kinetic N isotope effect for ammonium assimilation	20‰[12]
$^{15}\varepsilon_{k,NR}$	Kinetic N isotope effect for nitrate reduction	5‰[8]
$^{15}\varepsilon_{k,NO}$	Kinetic N isotope effect for nitrite oxidation	-15‰[11, 13]
$^{15}\varepsilon_{k,NA}$	Kinetic N isotope effect for nitrite assimilation	0.9‰[12]
$^{18}\varepsilon_{k,O2}$	Kinetic O isotope effect for O_2 incorporation	combined with $^{18}\varepsilon_{k,H2O,1}$
$^{18}\varepsilon_{k,H2O,1}$	Kinetic O isotope effect for H_2O incorporation	21-22‰ [7]
$^{18}\varepsilon_{k,NR}$	Kinetic O isotope effect for nitrate reduction	5‰[8]
$^{18}\varepsilon_{k,NO}$	Kinetic O isotope effect for nitrite oxidation	-3‰[11]
$^{18}\varepsilon_{k,NA}$	Kinetic O isotope effect for nitrite assimilation	0.9‰[12]
$^{18}\varepsilon_{b,NR}$	Branching O isotope effect for nitrate reduction	25‰ [10]
$^{18}\varepsilon_{eq}$	Equilibrium isotope effect for O atom exchange	10.5-14.5‰; temperature dependent (this study)
$\delta^{15}N_{OM}$	$\delta^{15}N$ value of organic matter	5‰[4]
$\delta^{15}N_{NO3}$	$\delta^{15}N$ value of ambient nitrate	sample dependent
$\delta^{15}N_{NO2,source}$	Flux-weighted average of $\delta^{15}N$ sources	sample dependent
$\delta^{18}O_{O2}$	$\delta^{18}O$ value of ambient dissolved oxygen	24.2‰
$\delta^{18}O_{H2O}$	$\delta^{18}O$ value of water	0‰
$\delta^{18}O_{NO3}$	$\delta^{18}O$ value of ambient nitrate	sample dependent
$\delta^{18}O_{NO2,source}$	Flux-weighted average of $\delta^{18}O$ sources	sample dependent
f_{AO}	Fraction of ammonium regenerated that is oxidized	0-1
f_{AA}	Fraction of ammonium regenerated that is assimilated	0-1
f_{NO}	Fraction of nitrite consumed by nitrite oxidation	sample dependent
f_{NA}	Fraction of nitrite consumed by nitrite assimilation	sample dependent
x_{AO}	Fraction of O atoms exchanged during ammonia oxidation	0-0.25[5, 7]

Supplementary Material

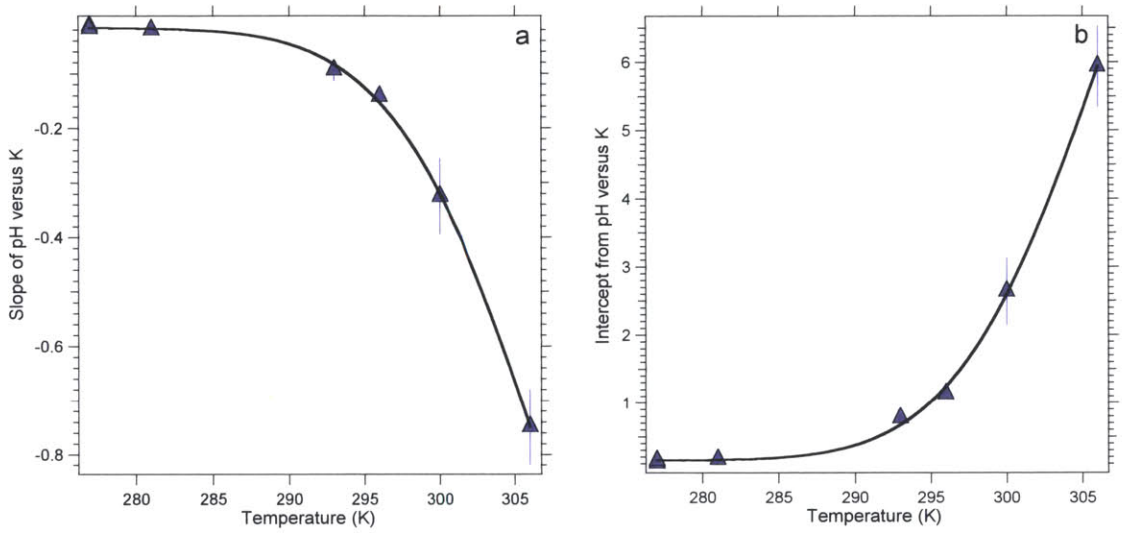

Figure S1. The relationship of temperature vs. the slope (a) and intercept (b) of the linear regression between pH and *k* from experiments 1 and 3. Error bars indicate the error in the linear regression of pH vs. *k*.

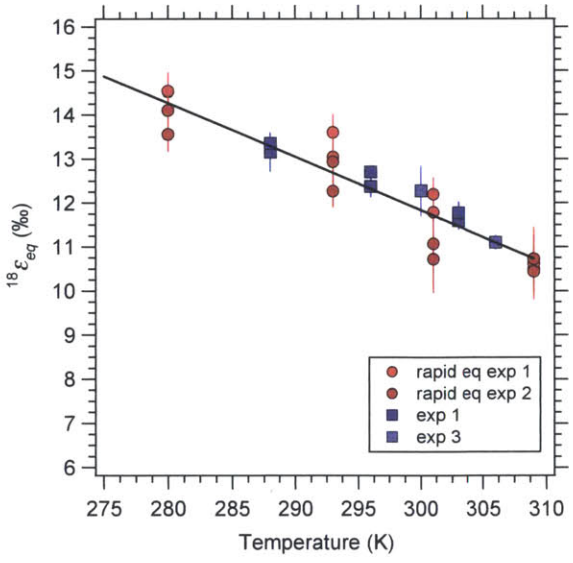

Figure S2. The relationship between equilibrium isotope effect ($^{18}\varepsilon_{eq}$) and temperature. Error bars indicate the propagated error of standard deviation of measurements of $\delta^{18}O_{NO2}$ and $\delta^{18}O_{H2O}$ used to calculate $^{18}\varepsilon_{eq}$.

Chapter 5

Nitrogen Cycling in the Primary and Secondary Nitrite Maximum in the Costa Rica Upwelling Dome

Carolyn Buchwald, Alyson E. Santoro, Rachel H. R. Stanley and Karen L. Casciotti

INTRODUCTION

Fixed nitrogen (N) in the forms of ammonium, nitrite and nitrate is the major limiting nutrient in the ocean, such that the supply of N controls the amount of primary productivity and subsequent carbon export from the surface ocean. The inputs of fixed N to the ocean are coastal run off, atmospheric deposition and nitrogen fixation, and N is removed during anammox and denitrification. The balance of these processes dictates the oceanic N inventory and potential for CO_2 removal from the atmosphere through time. Currently there is disagreement among estimates of the marine fixed N budget; some studies suggest a balanced budget (Gruber and Sarmiento 1997; Gruber and Galloway 2008), where others predict that sinks grossly outweigh sources (Brandes and Devol 2002; Deutsch et al. 2004). The largest areas of the ocean where N removal processes occur are in the Arabian Sea and Eastern Tropical Pacific, which have large expanses of suboxic water column. These areas, known as oxygen deficient zones (ODZs), are linked to increased productivity due to upwelling, and the remineralization of phytoplankton biomass contributes to the low oxygen concentrations in the underlying water column (Wyrtki 1962). These areas comprise only 0.1% of the ocean volume but could account for up to 30% of all fixed N loss in the ocean (Codispoti et al. 2001). These areas are also some of the only places in the water column where nitrite accumulates and N_2O is consumed. The reason for nitrite accumulation has intrigued scientists for over 50 years (Brandhorst 1959). The processes, which produce and consume nitrite are linked to primary productivity as well as fixed N removal from the water column, and therefore the rates and interactions of these processes are important to understand. In this study we use a combination of N and O isotope ratios from water column nitrite and nitrate to determine the rates and distributions of N cycle processes in the Costa Rica Upwelling Dome (CRD), to gain a better understanding of the distribution of nitrification and denitrification in the water column.

The CRD is a unique upwelling feature with a diameter of 150 to 300 km within the Eastern Tropical Pacific at about 9°N and 89°W (Wyrtki 1964). The CRD was first

described from a cruise in November to December of 1959 (Broenkow 1965; Wyrtki 1964) where they found the upwelling zone because of the very thin shallow thermocline located within 10 meters of the surface. The Equatorial Counter Current, Costa Rica Current, and the North Equatorial Current form a cyclone around the upwelling dome (Wyrtki 1964). The surface water in the dome has a slightly lower temperature, and has reduced oxygen and increased nutrients compared to surrounding waters, due to the upwelling of deep waters. Below the surface, the Equatorial Subsurface water resides up until 900 meters, which then transitions to Intermediate Water. A well-developed oxygen minimum, characteristic of the Eastern Tropic Pacific, exists within these two water masses. Accompanied with low oxygen at depth are also increased phosphate and nitrate concentrations from the surface due to remineralization, mostly from the equatorial subsurface water during transport (Broenkow 1965). Since the thermocline is close to the surface, nitrate, nitrite and phosphate have all been detectable at the surface (Thomas 1966). In addition to the unique chemical and physical characteristics of the CRD, it has also been found to have a unique phytoplankton community composition. Recent studies of the CRD have shown that instead of being dominated by larger eukaryotic phytoplankton like most upwelling zones, the CRD has a higher concentration of picoplankton, namely *Synechococcus* (Saito et al. 2005). They hypothesized that this is due to a unique chemical signature of the CRD. In the CRD there is high cobalt and ligand abundance with scarce amounts of zinc and iron and cadmium complexation that allow *Synechococcus* to outgrow diatoms with larger metal requirements.

Vertical profiles of nitrite in the CRD show that there are two distinct maxima, like other productive upwelling regions with intense oxygen minima (Brandhorst 1959; Broenkow 1965). The first nitrite maximum, called the primary nitrite maximum (PNM), exists below the chlorophyll maximum at the base of the euphotic zone. The secondary nitrite maximum (SNM) occurs at the top of the oxygen minimum layer, and exists where there is very low to no oxygen in the water column. Multiple processes may be involved in the production and consumption nitrite in these features. Figure 1 shows the processes involved in nitrite and nitrate transfer in oxic and anoxic waters. In the PNM, two

processes could produce nitrite: ammonia oxidation during remineralization and nitrate reduction during assimilation. Consumption of nitrite occurs by nitrite oxidation or nitrite assimilation. In most cases there is no accumulation of nitrite during nitrification, since the potential for nitrite oxidation is often higher than ammonia oxidation (Dore and Karl 1996); however the PNM at the base of the euphotic zone is a ubiquitous feature in the world's oceans. It has been hypothesized that the decoupling of ammonia oxidation and nitrite oxidation may lead to nitrite accumulation due to light inhibition of nitrite oxidizing bacteria (Guerrero and Jones 1996; Hooper and Terry 1974; Olson 1981). Diatoms will also leak nitrite during assimilation of nitrate when stressed for light and iron because they do not have enough energy to complete nitrite reduction (Collos 1998; Milligan and Harrison 2000). Which mechanism dominates the production and maintenance of the PNM has been debated (Lomas and Lipschultz 2006), with some evidence supporting production via ammonia oxidation (Brandhorst 1959; Olson 1981; Wada and Hattori 1971; Ward et al. 1982) and other evidence supporting nitrate reduction (Collos 1998; Kiefer et al. 1976; Vaccaro and Ryther 1960). For example, it has been noted that higher concentrations of nitrite in the PNM often coincide with higher phytoplankton abundance and productivity, but this is not direct evidence for a particular mechanism of nitrite production. There are most likely real differences in the mechanisms of production from site to site and with depth in the water column (Dore and Karl 1996) that would indicate the factors limiting the organisms living there.

The nitrite formed in the SNM is most likely produced by nitrate reduction during denitrification, which occurs only when there is no oxygen. Loss of this nitrite can then occur through further reduction to nitric oxide or ammonium, or through re-oxidation to nitrite at the fringes of these zones where oxygen is reintroduced. Mounting evidence suggests that nitrite oxidation may play an unexpectedly large role in nitrogen cycling in and around oxygen deficient zones (Anderson et al. 1982; Casciotti 2009; Fuessel et al. 2012; Lam et al. 2011). Early models suggest that up to 39-60% of all nitrate reduced to nitrite in the oxygen deficient layer will be re-oxidized on the edges (Anderson et al. 1982), while direct measurements indicate nitrite oxidizing activity in the oxygen

deficient zone itself (Fuessel et al. 2012; Lipschultz et al. 1990). Understanding how different processes control nitrite production and consumption in the PNM and SNM have important implications for understanding limitations of primary production in the euphotic zone, production of N_2O in the near-surface, and loss of fixed N through denitrification and anammox in the oxygen deficient zone.

In order to disentangle which processes are producing and consuming nitrite (NO_2^-) and nitrate (NO_3^-), the nitrogen (N) and oxygen (O) isotopes of nitrite and nitrate ($\delta^{15}N_{NO2\text{ or }NO3}$ (‰ vs. atmospheric N_2) = ($^{15}N/^{14}N_{NO2\text{ or }NO3} \div {}^{15}N/^{14}N_{N2}$ -1) · 1000; $\delta^{18}O_{NO2\text{ or }NO3}$ (‰ vs. Vienna Standard Mean Ocean Water) = ($^{18}O/^{16}O_{NO2\text{ or }NO3} \div {}^{18}O/^{16}O_{VSMOW}$ -1) · 1000) can be used. Each process imparts a distinct isotope effect leaving a signature on the isotope ratio measured. The isotope systematics of processes involving nitrate have seen continual development since the late 60's (Miyake and Wada, 1967), but nitrite isotopes in seawater have only received attention in the last five years (Casciotti and McIlvin 2007; Casciotti 2009) and therefore provides a new, largely unexplored, tracer for oceanic nitrogen cycle processes.

The nitrogen isotopes in nitrite track biological processes much like other nitrogen isotope systems, with individual processes causing distinct isotopic fractionation patterns in $\delta^{15}N_{NO2}$. However, in addition to biological isotope effects, the oxygen atoms of nitrite equilibrate abiotically with the oxygen atoms in water. Because of this equilibration, $\delta^{18}O_{NO2}$ is altered from its biological source signature at a set rate until it reaches an equilibrated $\delta^{18}O$ value ($\delta^{18}O_{NO2,eq}$), equal to that of the water $\delta^{18}O$ and equilibrium isotope effect ($^{18}\varepsilon_{eq}$) (Casciotti et al. 2007a). The rate of this equilibration is dependent on temperature, pH and salinity (Buchwald and Casciotti, submitted; Chapter 4). If the rate is known, an average age of the nitrite can be estimated based on the difference between the expected equilibrium $\delta^{18}O_{NO2}$ value and what was measured. The largest uncertainty is determining what the original biological signature of nitrite is prior to equilibration (Buchwald and Casciotti, submitted; Chapter 4).

In addition to using the nitrite isotopes, we can incorporate more traditional measurements of nitrate $\delta^{15}N$ and $\delta^{18}O$ into a one-dimensional (1D) reaction diffusion

model to better interpret multiple tracers together. The dual isotopes of nitrate have been shown to be a powerful tracer of nitrite re-oxidation. Sigman et al. (2005) defined $\Delta(15,18) = (\delta^{15}N_{NO3} - \delta^{15}N_{NO3,deep}) - {}^{15}\varepsilon/{}^{18}\varepsilon * (\delta^{18}O_{NO3} - \delta^{18}O_{NO3,deep})$ as the horizontal deviation from a 1:1 line, imposed by nitrate assimilation and denitrification (Granger et al. 2004; Granger et al. 2008). Data of this kind have indicated that there are processes other than denitrification affecting the nitrate, such as nitrite re-oxidation or nitrogen fixation (Casciotti and McIlvin 2007; Sigman et al. 2005). A second coupled tracer, $\Delta\delta^{15}N = \delta^{15}N_{NO3} - \delta^{15}N_{NO2}$, has also been used to determine where nitrite oxidation is occurring (Casciotti 2009). In the current study, we have combined traditional isotope tracers ($\delta^{15}N_{NO3}$ and $\delta^{18}O_{NO3}$) with newer ones ($\delta^{15}N_{NO2}$, $\delta^{18}O_{NO2}$) in a unique way to determine the major nitrogen cycling processes in the CRD. In particular, the combination of these isotopes can be used to determine the major processes that control the pattern of nitrite accumulation in the water column, as well as indicate the average age (or turnover time) of nitrite in these features. Also, by including advection and diffusion of nitrate and nitrite, in and out of the oxygen minimum layer, we are able to test the impact of oxidation on the edges of the SNM on the nitrite and nitrate concentrations and isotopes in the feature. All together these tracers have helped us gain a better understanding of the distribution of nitrification and denitrification in an ODZ.

METHODS

Sample Collection

All samples were collected aboard a cruise to the Costa Rica Upwelling Dome in July 2010 aboard the *R/V Melville* (MV1008). During the 35 day cruise we occupied 5 Lagrangian stations, or cycles, in which a patch of water was followed using a drifting array at 100 meters for 4 days. Figure 2 shows the location of each hydrocast, with a box to indicate the cycle within which each cast was collected. The hydrocast locations within

a cycle were closer or further together depending on the surface currents at each cycle. In each cycle, two or three 24-depth profiles of nutrient and isotope samples were collected.

Ammonium, nitrite and nitrate concentration measurements

Ammonium and nitrite concentrations were measured aboard the ship immediately after collection. Ammonium was measured using the orthophthalahdehyde (OPA) method described in (Holmes et al. 1999). For these measurements, 40 mL water was collected in 60 mL HDPE sample bottles. Bottles were acid washed prior to first use and then pre-conditioned with a small amount of ammonia reagent prior to use to remove any ammonium contamination. Between casts bottles sat with last seawater sample with reagent and then dumped just before rinsing and collection on the next cast. Along with the samples, 10 bottles were used to run five standards in duplicate ranging from 0 to 0.5 μM. Standards were made by collecting water from below 1000 meters into the HDPE bottles and then adding small volumes of 50 μM stock solution that was kept in the refrigerator. New standards were made for each cast. 10 mL of OPA reagent was added to each sample and standard bottle and then allowed to react in the dark for 3 to 10 hours. With each batch of samples, one deep water sample had reagent just before measurement on the fluorometer. This fluorescence value was used as a matrix blank and subtracted from all of the other samples. Fluorescence was measured in each bottle using a handheld fluorometer (Turner Aquafluor 8000). The ammonium detection limit for this method is 10 nM.

Nitrite measurements were made using the Greiss-Isllovay spectrophotometric method (Strickland and Parsons T. R. 1972). Samples (10 mL) were collected in 15 mL centrifuge tubes and 100 μL of sulfanilamide (SAN) and N-(1-naphthyl)ethylenediamine (NED) were added. Then 1mL of each sample was analyzed on a spectrophotometer on board. Bracketing standards (0 to 5 μM) were run in parallel and then used to calculate the concentration in each sample. The nitrite detection limit using this method is 0.2 μM.

Nitrate concentration measurements were done using a WestCo 200 discrete analyzer in the Stanford University Environmental Measurement 1: Gas-Solution Analytical Center. The discrete analyzer is an automated spectrophotometer that first reduces nitrate to nitrite using a cadmium column and then reacts the resulting nitrite with SAN and NED using the Greiss-Isllovay method, like above. Because nitrate conversion to nitrite was incomplete (averaged ~70%), nitrate and nitrite standard curves were run together in order to correct samples that contained both nitrite and nitrate. This was done by first measuring the nitrite concentration, like above, using this value and the nitrite standard curve produced through discrete analyzer, to calculate the absorbance created by nitrite and subtracting this from the total absorbance. The resulting nitrite-corrected absorbance value was then calibrated using the nitrate standard curve to find the nitrate concentration.

Nitrite and nitrate isotope measurements

$\delta^{15}N_{NO2}$ and $\delta^{18}O_{NO2}$ were measured using the azide method (McIlvin and Altabet 2005). All of the samples were prepared in duplicate 20 mL glass vials and converted to N_2O on board the ship, as soon as possible after sampling, to limit the abiotic exchange of oxygen atoms between nitrite and water (Casciotti et al. 2007a). Using the nitrite concentration (measured onboard, as above), the volume of sample needed to make 2.5, 5 or 10 nmol of N_2O was calculated and added to each vial. Nitrite isotope standards N-23, N-7373, N-10219 (Casciotti et al. 2007b), were run in parallel, with triplicate aliquots of each standard for each size of sample. 6M NaOH was added to each vial to stop the reaction 30 minutes after the addition of azide. N_2O samples were analyzed on a Finnigan Delta^{PLUS} XP isotope-ratio mass spectrometer.

At least 60 mL of seawater from each niskin bottle was filtered and frozen for nitrate isotope analysis in the laboratory. Nitrate isotope samples were measured using the denitrifier method (Casciotti et al. 2002; Sigman et al. 2001) with minor modifications (McIlvin and Casciotti 2011). In samples containing both nitrate and

nitrite, nitrite was removed using sulfamic acid (Granger and Sigman 2009). Three standards, USGS32, USGS34, USGS35 (Bohlke et al. 2003), were run 6 times per 60 samples at two different nanomole amounts for size correction.

Nitrification rate measurements

Nitrification rates were measured at three depths at each of cycles 2, 3 and 4. The depths chosen were at the surface, the primary nitrite maximum and just above the secondary nitrite maximum where a small amount of oxygen was present. For the two shallow (oxygenated) depths, six clear polycarbonate bottles were filled with 500 mL of seawater. The water in two of the bottles was filtered using a 0.2 μm filter (Sterivex) prior to filling the bottle. Of the remaining four bottles, two received 0.5 mL of 10 mg/mL allylthiourea (ATU) to inhibit bacterial ammonia oxidation and the other two were incubated as whole water samples. All 6 bottles received 0.5mL of 99.5 atom % ^{15}N-labeled ammonium. 60 mL of water was subsampled from each bottle at 4 time points: 0, 12, 24, and 36 hours, then filtered and frozen. The same procedure was followed for the low oxygen incubations, except clear gas-tight mylar bags were used instead of polycarbonate bottles and a three-way stop cock was used for gas-tight additions (ATU and the ammonium spike) and collection of subsamples in order to minimize any oxygen contamination. Bottles were incubated as close to in situ light and temperature conditions as possible. The surface sample was incubated in a clear blue on-deck incubator with running surface seawater for temperature control. The primary nitrite maximum incubations were conducted in the same incubator but wrapped in black screening to mimic 10% light. The deepest samples were incubated in the dark in an incubator adjusted to 10˚C.

Subsamples from the incubations were filtered through 0.2 μm Sterivex filters upon collection and stored frozen. The $\delta^{15}N_{NO2+NO3}$ was measured using the denitrifier method, described above, except that nitrite was not removed.

DNA extraction and functional gene abundance qPCR

Samples were collected from 4-5 depths in each cycle to measure the quantity of ammonia monooxygenase subunit A (*amoA*) genes from ammonia-oxidizing bacteria (AOB) and archaea (AOA), as well as the 16S ribosomal RNA (rRNA) gene abundance of the nitrite-oxidizing bacteria genus *Nitrospina.* Samples were collected at the surface, PNM, SNM, middle of the ODZ and at the bottom edge of the ODZ. Samples for DNA analysis were collected on 25mm 0.2 μm Supor filters (Pall) using pressure filtration with a peristaltic pump. Samples were immediately added to a 1.5 mL sterile epitube, which was prefilled with 30 μL of 0.1mM beads and frozen in an -80˚C freezer.

For DNA extraction, 700 μL of sucrose EDTA lysis buffer and 100 μL sodium dodecyl sulfate (SDS) were added to the tubes and shaken using a bead beating machine for 1.5 minutes. Following bead beating, tubes were incubated in boiling water for 1 minute and then 50 μL of proteinase K was added and incubated at 55˚C for 2-4 hours. Each tube was then centrifuged to remove debris and the supernatant was transferred to a clean tube. The filter debris was washed once with lysis buffer to remove any remaining DNA and was centrifuged and supernatant was added to new epitube. Lysates were purified using the DNeasy spin columns (Qiagen) following manufacturer's protocol. DNA was eluted in 150 or 200 μL of RNase free water and quantified using a Qubit fluorometer.

Quantitative PCR (qPCR) was carried out in 20 μL reactions, made of 10 μL Mastermix (Bio-Rad ssoAdvanced SYBR), 0.8 μL of each primer, 1 μL of template and 8.4 μL of RNase free water. Samples were analyzed in triplicate along with duplicate sets of standards with 10 to 10^5 templates, on a Bio-Rad CFX96 real-time PCR machine. The betaproteobacterial *amoA* qPCR assay used the 1F/2R primer set (Rotthauwe et al. 1997). The crenarchaeal *amoA* used the Arch-amoAF/Arch-amoAR set with an additional 2 mM $MgCl_2$ (Francis et al. 2005). Lastly, the *Nitrospina*-like 16S rRNA genes were quantified using NitSSU_130F and NitSSU_282F (Mincer et al. 2007).

RESULTS AND DISCUSSION

Nutrient Profiles in the CRD

Figure 3 includes the depth profiles of oxygen, nitrite, and ammonium concentrations, archaeal *amoA* abundance and bacterial *amoA* in all cycles, as well as nitrate concentration and dissolved inorganic nitrogen (DIN) deficits ($N^* = 16*PO_4 - (NO_3+NO_2)+2.9$) for cycles 3-5, and nitrification rates in cycles 2-4. Nitrite showed expected profiles with two distinct maxima at each cycle. The PNM occurred between 20 and 40 meters during every cycle. The highest concentration measured in the PNM was 1.3 μM in cycle 1 (Fig. 3a). Lower concentrations of 0.6 to 0.8 μM were measured in cycles 2, 4 and 5 (Fig. 3 d, j, and m). Sampling using the niskin bottles to capture this narrow feature was difficult, though, such that the lower concentration values could just be from the location sampled within the peak; even a meter difference may have resulted in a higher concentration.

The SNM in the CRD had a maximum concentration of ~1.6 μM at cycle 3 (the farthest offshore), which is lower than reported values for a SNM off the coast of Mexico in the ETNP, or in the Peru upwelling zone and Arabian Sea. Cycle 3 also had the largest vertical extent of nitrite in the water column, where it extended all the way to 1000 meters, and the largest and most intense ODZ (Figure 3g). The lowest concentration and depth range of the SNM was measured at cycles 2 and 4, which were both selected to be in the center of the dome based on satellite ocean color and shipboard fluorescence measurements. These stations also had the smallest ODZ.

Ammonium concentration profiles from the CRD showed distinct maxima of up to 0.6 μM directly above the PNM (Fig. 3b, e, h, k, and n). Since the thermocline was close to the surface, there was also up to 0.35μM ammonium at the surface. The cycle closest to shore (cycle 1) had the lowest ammonium concentration, with only a 100 nM peak just above the PNM. In addition to the near-surface ammonium maximum, there appears to be a small secondary ammonium maximum of 20-40 nM, just above the

detection limit, at the bottom edge of the ODZ in cycles 2, 3 and 5 (Fig 3e, h, and n). This peak is most visible in cycle 5, with at least 3 samples at the bottom edge of the ODZ defining the ammonium peak.

The nitrate profile followed a typical nutrient-like distribution in the upper water column. Nitrate was depleted at the surface and increased with depth to ~45 μM at 800 meters. There were mid-water column DIN deficits calculated for cycles 3-5 (Fig. 3h, k, and n). These deficits occurred between 400-420 meters and were associated with the middle of the ODZ.

Functional gene abundance and nitrification rates in the CRD

Profiles of archaeal *amoA,* bacterial *amoA* and *Nitrospina* 16S rRNA gene abundance are shown for each cycle (Figs. 3 c, f, i, l, and o). We found a very low abundance of AOB throughout the water column in all cycles, averaging 10 copies/mL. At cycle 1 the highest abundance of archaeal *amoA* was measured in the PNM, with a lower abundance in the deeper ODZ samples. *Nitrospina* abundance was highest in the PNM, but was also high in the SNM, consistent with recent studies in the Namibian oxygen minimum zone (Fuessel et al. 2012). In cycles 4 and 5, the measured peak of *Nitrospina* occurred near the SNM at the top of the ODZ. In cycles 1 and 2 the AOA abundance was greater than the *Nitrospina* in the PNM but smaller everywhere else. In cycles 3, 4, and 5 *Nitrospina* abundance was greater than AOA everywhere in the profile. In previous studies where *amoA* and *Nitrospina* gene copies were measured in the same profile, they found that *amoA* were about 4 times higher than *Nitrospina* (Mincer et al. 2007; Santoro et al. 2010). These studies were in Monterey Bay and the California Current, both upwelling systems with high productivity and higher total abundances of archaeal *amoA*. The observation of higher abundances of *Nitrospina* is unique and most likely a product of the ODZ. The *amoA* abundances measured here were lower than previous studies in the Peruvian ODZ (Lam et al. 2009) but similar to measurements in the Arabian Sean (Lam et al. 2011). *Nitrospina* abundance was not measured in these

studies, although *Nitrospina* has since been detected in the Namibian OMZ (Fussel et al., 2012) at abundances about 10 times higher than those found here. The high abundance of *Nitrospina* in the ODZ is intriguing. While the availability of nitrite as a substrate would support this, the supplies of potential oxidants is rather low.

Nitrification rates were measured at 3 locations (cycles 2, 3, and 4) at 3 depths: surface, PNM and just above the SNM (Fig. 3 f, i and l). Overall, the rates were low with a maximum rate of ~3 nM/day. There was no measurable nitrification in the surface (2 m) at any of the cycles. In cycle 2, the highest rate of nitrification occurred at the PNM, and a slightly lower rate was observed at the top of the SNM. In cycles 3 and 4, the highest rate of nitrification occurred at the SNM, with a much lower rate measured at the PNM. Incubations with ATU added all showed lower, but not completely inhibited nitrification activity. Filtering almost always completely inhibited nitrification, except for the two incubations where the rates were highest (cycle 2, 30m and cycle 3, 360m). These rates were overall low compared to the California Current (Santoro et al. 2010) and Peruvian ODZ (Lam et al. 2009), but similar to those measured in the Arabian Sea (Lam et al. 2011).

Multi-isotope profiles ($\delta^{15}N_{NO2}$, $\delta^{18}O_{NO2}$, $\delta^{15}N_{NO3}$, $\delta^{18}O_{NO3}$, $\Delta(15,18)$ and $\Delta\delta^{15}N$)

In all profiles the isotopes of nitrite ($\delta^{15}N_{NO2}$ and $\delta^{18}O_{NO2}$) and nitrate ($\delta^{15}N_{NO3}$ and $\delta^{18}O_{NO3}$) were measured. Using these isotope values, two different tracers can be calculated, $\Delta(15,18)$ and the $\Delta\delta^{15}N$. Fig 4 includes the profiles of all four isotopes of interest in the two oxidized nitrogen species ($\delta^{15}N_{NO2}$, $\delta^{18}O_{NO2}$, $\delta^{15}N_{NO3}$ and $\delta^{18}O_{NO3}$) and their calculated traces ($\Delta(15,18)$, $\Delta\delta^{15}N$) for the casts 72, 76 and 83 from cycle 5. These profiles were chosen because they had highest resolution in sampling in the ODZ. $\delta^{15}N_{NO3}$ and $\delta^{18}O_{NO3}$ shown in the light orange and dark orange symbols, respectively, followed the pattern roughly expected for this location, although some interesting features were observed in the dual isotope anomaly, $\Delta(15,18)$. There was enrichment of both ^{15}N and ^{18}O in surface water and then again deeper in the water column inside the

ODZ. Enrichment in the surface is most likely from assimilation of nitrate by phytoplankton where in the ODZ it is caused by reduction of nitrate by denitrification. Both of these processes have equal isotope effects for ^{15}N and ^{18}O, such that they should not cause deviations from zero in the Δ(15,18) values, shown in black (Figure 4). The Δ(15,18) values had a very unique pattern, however. There were three places in the water column that had large negative Δ(15,18) values: the surface, the upper oxycline and the lower oxycline. These negative deviations are most likely caused by nitrite re-oxidation, especially because they all occur where there is nitrite present. Interestingly, at the SNM the Δ(15,18) returns back to near 0, which is a pattern that has not been previously described.

The $\delta^{15}N_{NO2}$ in the PNM has the most depleted value (-38‰) nearest to the surface and increased with depth to -15‰. The $\delta^{15}N_{NO2}$ within the SNM follows the shape of the nitrite peak. It is most depleted on the bottom edge of the feature (-45‰) and increases to -20‰ at the peak of the SNM and then decreases again at the top of the oxycline. The $\Delta\delta^{15}N$ (Figure 4, blue symbols) had a shape inverse to $\delta^{15}N_{NO2}$. The highest values of $\Delta\delta^{15}N$ coincided with the most negative values of Δ(15,18), which is another indication that nitrite re-oxidation is occurring in these places. The $\Delta\delta^{15}N$ reaches values of over 50‰ in both the PNM and SNM. It is very unlikely that a large isotopic difference between nitrite and nitrate can be achieved with only the reduction pathways (both of which have normal isotope effects). Therefore, there is likely a source of nitrite oxidation, which can easily create these high $\Delta\delta^{15}N$ values since it has a large inverse isotope effect. Lastly, $\delta^{18}O_{NO2}$ in bright pink symbols have a more homogenous profile than all other tracers. In both the PNM and SNM the $\delta^{18}O_{NO2}$ follows a similar shape as the $\delta^{15}N_{NO2}$ but has a much smaller range in value. The average $\delta^{18}O_{NO2}$ value is 13.8‰, which is close to the value expected after equilibration of nitrite and water with a $\delta^{18}O_{H2O}$ of 0‰.

Nitrite sources, sinks and turnover time in the PNM

In the CRD there was a distinct peak in nitrite concentration just below the chlorophyll maximum (between 20 and 40 meters) at all stations. The origin of the PNM has been debated, with multiple competing hypotheses. The first hypothesis is that there is decoupling of ammonia and nitrite oxidation during nitrification. It has been shown in the field and culture that AOB, AOA and NOB are all inhibited by light, but NOB are inhibited more at higher irradiances (Guerrero and Jones 1996; Hooper and Terry 1974; Merbt et al. 2012; Olson 1981). The second possibility is that phytoplankton release nitrite during nitrate assimilation at low light levels. It has been shown in phytoplankton cultures that light limitation can limit nitrite reduction and cause nitrite to leak out of the cell (Collos 1998; Kiefer et al. 1976; Vaccaro and Ryther 1960). This hypothesis seemed plausible for the PNM because it usually occurs at the base of the euphotic zone where light is scarce. It has also been suggested that iron limitation can cause phytoplankton to excrete nitrite. Iron limitation decreases ferredoxin production, which slows nitrite reductase activity compared to nitrate reductase causing a build up of nitrite (Milligan and Harrison 2000). Both light and iron limitation restricts the amount of energy needed to complete intracellular nitrate reduction.

The $\delta^{15}N$ and $\delta^{18}O$ values of nitrite produced in the PNM will record a signature of the sources, sinks and turnover time of the nitrite and therefore may be used to identify the sources and sinks and their relative rates of transformation. $\delta^{15}N_{NO2}$ records biological consumption and production processes, while $\delta^{18}O_{NO2}$ records biological processes as well as the turnover time because it undergoes a constant rate of abiotic equilibration that will cause the $\delta^{18}O_{NO2}$ value to change predictably over time (Buchwald and Casciotti, submitted; Chapter 4). Where biological turnover is slow relative to this abiotic exchange, $\delta^{18}O_{NO2}$ will be close to equilibrium. Where biological turnover is rapid relative to abiotic exchange, $\delta^{18}O_{NO2}$ will be closer to the biological endmember. In some cases, the biological endmember may be close to equilibrium and therefore difficult to determine an age. Fig. 5a shows the $\delta^{15}N$ and $\delta^{18}O$ of all nitrite samples from PNM

measured during the cruise to the CRD. The dotted lines bracket the values expected for the $\delta^{18}O$ of nitrite fully equilibrated with water ($\delta^{18}O_{NO2,eq}$). We can estimate the age of these samples by using the approach outlined in Buchwald and Casciotti (submitted; Chapter 4), which is described briefly here.

First, we estimate the source(s) of nitrite and its extent of consumption from the $\delta^{15}N_{NO2}$ and $\delta^{15}N_{NO3}$ data. In the PNM, the most likely sources of nitrite are ammonia oxidation and nitrate reduction and the sinks are nitrite oxidation and assimilation. In Fig. 5b the data are overlain by pink boxes that show the expected nitrite isotope values for each of the probable sources, prior to consumption. Each of these sources has distinct $\delta^{15}N_{NO2}$ and $\delta^{18}O_{NO2}$ signatures. Ammonia oxidation will give a source signature that is dependent on the $\delta^{15}N$ value of remineralized organic matter. The water and oxygen $\delta^{18}O$ values and the isotope effects (ε) involved with ammonia oxidation (Buchwald et al. 2012; Casciotti et al. 2010). Here we have assumed that the $\delta^{15}N$ the remineralized organic matter is 5‰, and that ammonia oxidation is catalyzed by AOA with an isotope effect of 22‰ (Santoro and Casciotti, 2011). The nitrate reduction sources will be dependent on the local nitrate isotope values and the isotope effects for nitrate reduction. For $\delta^{15}N$, the isotope effect is assumed to be 5‰ (Granger et al. 2004). For $\delta^{18}O$, an isotope effect associated with loss of O during nitrate reduction (the branch point) leads to an additional isotopic offset between the nitrate reactant and the nitrite product (Casciotti et al. 2007b). It is apparent in Figure 5 that both potential sources of nitrite have $\delta^{15}N$ values greater than any of the values measured in the PNM. In order to generate the low $\delta^{15}N_{NO2}$ values measured in our samples there must also be consumption of nitrite by oxidation to nitrate which has an inverse isotope effect for ^{15}N and ^{18}O (Buchwald and Casciotti 2010; Casciotti 2009). Removal of nitrite by assimilation with a small normal isotope effect (Waser et al. 1998) is not supported by the $\delta^{15}N_{NO2}$ data. Given the ratio of N and O isotope effects, the process of nitrite oxidation should lead to nitrite $\delta^{15}N$ and $\delta^{18}O$ values that fall along the black diagonal arrows in Fig. 5b. Using the $\delta^{15}N_{NO2}$ of each measured sample and choosing the source that would create a value above or below $\delta^{18}O_{NO2,eq}$, depending on the sample, the biotic end member ($\delta^{18}O_{NO2,b}$), a

hypothetical pre-equilibrated nitrite $\delta^{18}O$ value that includes biological sources and sinks, is calculated for each sample (indicated by pink dots in Fig. 5b). The distance between the end member $\delta^{18}O_{NO2,b}$ values and the measured $\delta^{18}O_{NO2}$ relates to the average age of the nitrite. Using empirically-derived relationships between equilibration rate, temperature, and pH (Buchwald and Casciotti, submitted; Chapter 4), the average age of nitrite in the PNM at cycles within the CRD was calculated to be 128 ± 97 days. There was no significant difference between cycles (cycle 2: 132 ± 35, cycle 3: 124 ± 110; cycle 4: 121 ± 80; cycle 5: 139 ± 118) nor any relationship to nitrite concentration. The large standard deviations are due to large isotope differences between the depths within the nitrite peak, indicating variations in the extent of nitrite consumption, as well as variations in the average age.

In the CRD, many of the samples had $\delta^{18}O_{NO2}$ values greater than $\delta^{18}O_{NO2,eq}$, indicating that nitrate reduction is a source of nitrite. A previous study in the CRD has shown that the phytoplankton community is limited by Fe and Zn, and the addition of these nutrients have resulted in an increase of large pennate diatoms (Franck et al. 2003), suggesting that diatoms are limited by iron. If they are limited by iron they may also be leaking nitrite as shown in culture studies (Milligan and Harrison 2000). Only a few samples had $\delta^{18}O_{NO2}$ values below equilibrium indicating ammonia oxidation may also be a partial source. It requires a 50% contribution of ammonia oxidation to produce the lower $\delta^{18}O_{NO2}$ values measured. Additional measurements also indicate a contribution of ammonia oxidation to the PNM. Rates of ammonia oxidation and the abundance of *amoA* from both bacteria and archaea were generally low, although *amoA* abundance peaked in the PNM at both cycles 1 and 2, and nitrification rates were highest in the PNM at cycle 2. Unfortunately, rates were not measured at cycle 1. In cycles 3 and 4, the ammonia oxidation rates were low, gene abundance was low (<50 copies/mL), and ammonium concentration at the maximum was higher than in the other 3 cycles, suggesting lower ammonia oxidation activity and/or higher rates of N release from grazing. Finally, if ammonia oxidation was the only source of nitrite, the residence time estimated independently using the measured rates and concentration of nitrite in the PNM would be

thousands of days (compared with 128 days obtained from the $\delta^{18}O_{NO2}$ data), suggesting that this is not the sole source of nitrite.

These results contrast with recent observations in the Arabian Sea PNM (Buchwald and Casciotti, submitted; Chapter 4). In that study the nitrite in the PNM was younger than in the CRD and sourced primarily from ammonia oxidation rather than from nitrate reduction. These results indicate that both processes may share in production and maintenance of PNM features in different locations and depths. This is consistent with detailed studies of the PNM in various locations using ^{15}N tracer techniques (Dore and Karl 1996; Mackey et al. 2011). The chemical conditions of the CRD are unique and may also lead to a different age and consumption of the PNM. In a cruise in 2005 they found that cobalt and metal-binding ligands were high, while zinc and iron were very low, forcing out diatoms and allowing the dominance of cyanobacteria. The shallow thermocline and limiting trace nutrients could be likely causes of leakage of nitrite during nitrate uptake.

Nitrogen cycling in the SNM

In all of the stations in the CRD, there was a small SNM with nitrite concentrations peaking at 1.6 μM. The SNM has been classically assumed to be caused by an imbalance of the reductive pathways, nitrate reduction and nitrite reduction, since this feature occurs only in areas with very low to no oxygen within the ODZ. It was Anderson et al. (1982) first suggested that the nitrite could be re-oxidized due to diffusion and advection on the fringes of the ODZ that allows nitrite to be moved into oxygenated water where it is oxidized to nitrate and transported back into the ODZ. The reaction diffusion model used by Anderson suggests that 39 to 60% of the nitrite is re-oxidized prior to full reduction to N_2 gas. Also recently, there has been direct evidence from incubation studies that nitrite oxidation is occurring within the ODZ (Fuessel et al. 2012). In the CRD we can use multiple tracers and a newly developed 1D model, to predict the relevant processes and their respective rates.

SNM nitrogen cycling: Nitrite isotopic analysis

The $\delta^{15}N_{NO2}$ and $\delta^{18}O_{NO2}$ can be analyzed in the same method as for the PNM, but using a different set of sources and sinks. In the SNM the anoxic processes would be plausible, including dissimilatory nitrate reduction and nitrite reduction. Figure 6a shows the nitrite isotope values for every sample within the SNM. The $\delta^{15}N_{NO2}$ had a large range from -5‰ to -40‰, while the $\delta^{18}O_{NO2}$ had a narrow range of 10-20‰. The most probable source of nitrite here is nitrate reduction, and the values that nitrite would be produced at, based on local nitrate $\delta^{15}N$ and $\delta^{18}O$ values are shown as the pink boxes in Fig. 6b. The DIN deficit and enrichment of the nitrate isotopes (Figs. 3h, k, and n) also suggests that there is nitrate reduction occurring in the ODZ. Again, like the PNM, the majority of samples have extremely low $\delta^{15}N_{NO2}$ values, indicating nitrite oxidation and a dominant sink with an inverse isotope effect. Now, assuming nitrite oxidation as the main consumption term, the pink triangles are the predicted $\delta^{18}O_{NO2,b}$. As shown in Fig. 6b, many of these pink triangles fall at $\delta^{18}O_{NO2}$ values near equilibrium. In this case it is not possible to determine the age using equilibration because the source and equilibrium value are so close. At the high end of consumption, where there is a very depleted $\delta^{15}N_{NO2}$, there is some evidence for equilibration because the $\delta^{18}O_{NO2}$ measured is not as low as it would be predicted based on the inverse oxygen isotope effect of -3‰ during nitrite oxidation.

SNM nitrogen cycling: 1D reaction diffusion model

The compilation of nitrite and nitrate concentration and isotope profiles indicates that nitrate reduction and nitrite oxidation are major players in the nitrogen cycle around the SNM. In order to integrate these measurements into a more quantitative analysis of the relative rates of these processes, a 1D model was constructed that can be used to predict the processes and their rates to match the observed data. The model is a finite difference model with 0.001 year time steps and 1 m depth resolution over 0-1000 m.

Figure 7 shows the processes that were represented in the oxygen deficient portion of the model (400-700 m). Outside of the oxygen deficient zone, nitrate reduction and nitrite reduction were assumed to be negligible. The model includes the physical processes of advection and diffusion assuming constant values of 6 m/y (A) and 3000 m^2/y (D), taken from Anderson et al. 1982. This upwelling rate or advection term is similar to values measured and used in a model of the CRD (Fiedler et al. 1991). The sensitivity of the model to these physical parameters was low; even with a 10-fold change in each of the parameters there was little change in model fit. We have chosen to neglect lateral advection in the model because it is much slower than vertical advection.

The biological processes of nitrite oxidation, nitrite reduction, and nitrate reduction were considered first order processes with rate constants of k_{NO}, k_{NAR}, and k_{NO} in units of d^{-1}. This model has not separated nitrite reduction and oxidation by anammox bacteria from denitrifying organisms and nitrite oxidizers, respectively. We assume that anammox will be included in the nitrite reduction rates and nitrite oxidation rates with similar isotope effects as denitrification and nitrite oxidation.

In addition to the nitrite and nitrate concentrations, the distribution of the heavy isotopes (^{15}N and ^{18}O) was also modeled (Table 1, Fig 8). The ^{15}N atoms were treated the same as the concentrations except with each rate constant multiplied by a fractionation factor ($^{15}\alpha_{NO}$, $^{15}\alpha_{NAR}$, $^{15}\alpha_{NIR}$), which describes the ratio of rate constants for the light and isotopes defined as $^{15}\alpha = {}^{14}k/{}^{15}k$, such that normal fractionation will be greater than 1 and inverse fractionation will be less than 1. The fractionation factor is related to an isotope effect by the equation: $\varepsilon = (\alpha-1)*1000$, such that a normal isotope effect is positive and an inverse isotope effect is negative.

The treatment of $\delta^{18}O$ is more complicated for nitrite oxidation to nitrate and nitrate reduction to nitrite, because oxygen atoms are gained or lost during these processes. In the case of nitrite oxidation, there is an ^{18}O fractionation ($^{18}\alpha_{NO}$) for the selection of the nitrite molecule and another ^{18}O fractionation factor ($^{18}\alpha_{H2O}$) for the selection of a water molecule. In nitrate reduction there is an ^{18}O fractionation ($^{18}\alpha_{NAR}$) on the nitrate molecule as well as a branching isotope effect for the selection of which

oxygen molecule is removed ($^{18}\alpha_b$). Lastly, for the nitrite oxygen isotopes, we included a rate constant for abiotic exchange (k_{EXCH}) with an equilibrium fractionation factor that describes the unequal partitioning of ^{18}O between water and nitrite during this process ($^{18}\alpha_{eq}$). The values for these parameters used are shown in Table 1.

Table 1. Terms used in the Secondary Nitrite Maximum1D model

Process	**Term**	**Value**	**References**
Advection	A	6 m/y	(Anderson et al. 1982)
Diffusion	D	3000 m^2/y	(Anderson et al. 1982)
Nitrite oxidation	$^{15}\alpha_{NO}$	0.985	(Buchwald and Casciotti 2010; Casciotti 2009)
	$^{18}\alpha_{NO}$	0.997	(Buchwald and Casciotti 2010)
	$^{18}\alpha_{H2O}$	1.010	(Buchwald and Casciotti 2010)
Nitrate Reduction	$^{15}\alpha_{NAR}$	1.025	(Granger et al. 2008)
	$^{18}\alpha_{NAR}$	1.025	(Granger et al. 2008)
	$^{18}\alpha_b$	0.975	(Casciotti and McIlvin 2007)
Nitrite Reduction	$^{15}\alpha_{NIR}$	1.015	(Casciotti et al. 2002)
	$^{18}\alpha_{NIR}$	1.015	(Sigman et al. 2005)
Abiotic Nitrite Exchange	$^{18}\alpha_{eq}$	1.013	(Casciotti et al. 2007b)

Table 2. Rate constants for 5 different model runs

Model Run	k_{NAR}	k_{NIR}	k_{NO}	k_{EXCH}
1	0.015 d^{-1}	0	0	0
2	0.015 d^{-1}	0.5 d^{-1}	0	0
3	0.015 d^{-1}	0.5 d^{-1}	0	10 d^{-1}
4	0.015 d^{-1}	0.25 d^{-1}	0.25 d^{-1}	0
5	0.015 d^{-1}	0.25 d^{-1}	0.25 d^{-1}	10 d^{-1}

The model was initialized with nitrite concentrations set to zero throughout the profile and a nitrate profile typical for Pacific waters outside the ODZ (with minimal nitrate deficit). The model was then allowed to run until the nitrate deficit matched that of the data from cycle 5, cast 83. We parameterized the vertical distribution of rate constants such that the rate constant for nitrite oxidation did not vary with depth in the water column, but both nitrite reduction and nitrate reduction had rate constants that followed a skewed Gaussian distribution with depth within the ODZ, normalized to a maximum rate constant occurring at the peak of the nitrate deficit. This distribution in rates gave the best fit to the observed concentration and isotope profiles, rather than a Gaussian distribution with no skew. In order to illustrate the effects of nitrite oxidation, nitrite reduction, and oxygen atom exchange, five different model scenarios were analyzed (Figure 9). Finally, to determine the most likely distribution of rate constants, a cost function (equation 1) was used to evaluate the model and data comparison at a variety of maximum k values for all 4 processes (nitrite oxidation, nitrate reduction, nitrite reduction and exchange, Table 2). The cost function is the sum of the differences between the data and model for the number of data points (N) and for each of the 6 variables (i = $[NO_2^-]$, $[NO_3^-]$, $\delta^{15}N_{NO2}$, $\delta^{18}O_{NO2}$, $\delta^{15}N_{NO3}$, $\delta^{18}O_{NO3}$). The W represents a chosen weight for each variable, so that even when the absolute numbers are smaller they have equal weighting in the cost. The weights were determined by using the mean of the data points and some were adjust by a factor of ten until the all had an approximately equal cost value.

$$(1)\ \text{cost} = \sqrt{\sum_{i=1}^{6}\left(\sum_{j=1}^{N}\frac{\left(x_i - x_i^{obs}\right)^2}{NW}\right)}$$

In the first of the five scenarios, we only allowed nitrate reduction to occur, with no nitrite sinks. In order to obtain the correct nitrate deficit, the maximum rate constant for nitrate reduction (k_{NAR}) was set to 0.015 d^{-1}. Obviously, with no nitrite sinks, this scenario vastly overestimates the nitrite concentration, which increased to over 15 μM

(off the scale in Fig 9a). In the second scenario, nitrite reduction was added as the only sink of nitrite, with its magnitude adjusted until the amount of nitrite accumulation was more realistic. In this scenario, the nitrite profile did not follow the observed shape. The produced nitrite shape is due to the skewed Gaussian shape chosen for k_{NIR} and k_{NAR}, while this is the most likely parameterization of the nitrate reduction to create the observed nitrate deficit, if k_{NIR} was parameterized differently it may cause a more natural nitrite profile shape. In addition to the nitrite profile shape, scenario (2), with no nitrite oxidation, does not reflect the observed nitrate isotope relationship, which has deviations from the 1:1 line. The modeled relationship of $\delta^{15}N_{NO2}$ and $\delta^{18}O_{NO2}$ in the first two scenarios had a much higher slope than our data (Figure 9c). Therefore, in the 3rd scenario, we added exchange (k_{EXCH}=10), which lowers the slope of the nitrite $\delta^{18}O$ vs. $\delta^{15}N$ to a value similar to the data (Fig. 9c), although the modeled $\delta^{15}N_{NO2}$ values are too high. In these first three scenarios, where there is no nitrite oxidation, the $\delta^{15}N_{NO3}$ and $\delta^{18}O_{NO3}$ values followed a 1:1 line originating at deep water nitrate $\delta^{15}N_{NO3}$ and $\delta^{18}O_{NO3}$ values, which does not match nitrate isotope observations (Figure 9d). Since nitrite reduction does not affect nitrate isotopes, it cannot explain the observed Δ(15,18) values. The $\delta^{15}N_{NO2}$ values predicted in these scenarios are also much too high, and as discussed below, nitrite oxidation is needed to achieve the extremely negative $\delta^{15}N_{NO2}$ values. In the 4th and 5th scenarios we added nitrite oxidation to the model, which allows the data to be more closely simulated. Here, the modeled Δ(15,18) values have negative deviations (Fig. 9d), as observed. Also, the $\delta^{15}N_{NO2}$ values were lowered from the influence of nitrite oxidation, and the nitrite concentration profile had a more similar shape to the observed SNM peak. Again, allowing oxygen atom exchange more accurately simulated the range and pattern of $\delta^{18}O_{NO2}$ observed. However, not all nitrite consumption can be explained by nitrite oxidation. Clearly, from the fact that a DIN deficit is present, some nitrite reduction has to have occurred. We find that by making the sinks of nitrite equal to half nitrite oxidation (0.25 d^{-1}) and nitrite reduction (0.25 d^{-1}) we have the best fit to all the data (dark blue lines in Figure 9). Using these rate constants and observed concentrations in this location the maximum reduction and oxidation rates for nitrite

would be 220 nM d^{-1} and 450 nM d^{-1} for nitrate reduction. These nitrite oxidation rates are similar to measured rates in the Nambian ODZ ($\leq$ 372 nM d^{-1}; Füssel et al. 2012) and the Eastern Tropical South Pacific (170-600 nM d^{-1} ; Lipschulz et al. 1990), but rather high among other geochemical estimates (Devol et al., 2006).

In order to mimic the concentration profiles of nitrite and nitrate observed in the CRD, it requires rate constants for nitrate reduction equal to 0.015 d^{-1} and nitrite removal processes of 0.5 d^{-1} about 33 times greater than nitrate reduction. When neglecting nitrite oxidation as a sink the nitrite concentration profiles will produce an unexpected shape, there will be no negative deviations in the $\Delta(15,18)$ and the $\delta^{15}N_{NO2}$ values will be too high. Adding nitrite oxidation as half of the nitrite sink, the nitrite profile will be produced at a more similar shape, the $\Delta(15,18)$ will have negative deviations and the $\delta^{15}N_{NO2}$ will be at lower values. Then lastly, an added exchange term of 10 d^{-1} will lower the slope of the $\delta^{15}N_{NO2}$ and $\delta^{18}O_{NO2}$ relationship to more accurately represent the data. Our analysis agrees with the other recent studies suggesting nitrite re-oxidation as a dominant process in an ODZ (Fuessel et al. 2012). Our estimation of 50% nitrite oxidation and 50% nitrite reduction is within the range of what Anderson et al. (1982) predicted and close to what Casciotti, 2009 estimated for the ETNP. Also the interpretation that negative deviations in $\Delta(15,18)$ can be caused by nitrite re-oxidation also match the interpretation of nitrate isotopes by Sigman et al. (2005) and Casciotti and McIlvin (2007).

CONCLUSIONS

Multiple isotope tracers including $\delta^{15}N_{NO2}$, $\delta^{18}O_{NO2}$, $\delta^{15}N_{NO3}$, $\delta^{18}O_{NO3}$, $\Delta(15,18)$ and $\Delta\delta^{15}N$, along with concentration measurements of nitrite, nitrate, ammonium and oxygen, were found to be powerful tools in interpreting nitrogen cycling in the PNM and SNM in the Costa Rica Upwelling Dome. Nitrite and ammonium concentration profiles indicated that there was decoupling of ammonia oxidation and nitrite oxidation near the surface to the base of the euphotic zone, which is shallow in the CRD, indicating that

light inhibition might be a factor causing the accumulation of ammonium and nitrite. Applying nitrite isotopic analysis to the PNM, the possibility of incomplete nitrate reduction by phytoplankton was indicated by high $\delta^{18}O_{NO2}$ values. The low $\delta^{15}N_{NO2}$ values also indicated that nitrite was largely consumed by nitrite oxidation. The slow nitrification rates and low AOA and AOB abundances also support this hypothesis. Lastly, the turnover time of this nitrite was calculated to be an average of 128 days old, such that regardless of the reaction involved, the production and consumption rates were slow.

In the SNM, found deeper in the water column, nitrate concentration and isotope profiles suggested a nitrate sink by denitrification, from enrichment of $\delta^{15}N_{NO3}$ and $\delta^{18}O_{NO3}$. The nitrite isotopes, $\Delta(15,18)$ and $\Delta\delta^{15}N$, also revealed a strong influence of nitrite re-oxidation at the edges of the ODZ. Using these isotope tracers and concentration profiles in a 1D reaction diffusion model, we found that nitrite oxidation is required to reproduce the observed isotope profiles., The best fit occured when the nitrite sink was split between nitrite re-oxidation and nitrite reduction (50% each). This study adds a new observation that nitrite re-oxidation is a dominant process in ODZs. This has implications for determining the fate of nitrate in ODZs, if 50% of nitrite is re-oxidized, then twice as much nitrate is reduced as is released as N_2. Also using the stoichiometry of nitrate and nitrite reduction there would be 1.4 times increase in the amount of organic matter is remineralized when including re-oxidation. This recycling also supports a chemoautotrophic community that can remove some additional CO_2 from the water column. Our model also shows that nitrite oxygen exchange is affecting the $\delta^{18}O_{NO2}$, because the rates of the production and consumption processes are comparable to abiotic isotope exchange, and this process is important to include in future interpretation of nitrite and nitrate isotopes in the ocean.

ACKNOWLEDGEMENTS

We are grateful to Mike Landry (Chief Scientist) and the Captain and Crew of the R/V Melville for enabling the collection of the samples. We thank James Moffett and Dreux Chappell, participants on the cruise, for useful discussion and insight on the CRD. Also

we thank Jessica Tsay for helping measure [NO_2^-] and Matt McIlvin for help analyzing isotope samples. We would like to thank Jeffery Kaeli for his help construction of the 1D model. This research was funded by the National Science Foundation grants OCE 05-26277 and OCE 09-610998 to KLC.

References

Anderson, J. J., A. Okubo, A. S. Robbins and F. A. Richards. 1982. A Model for Nitrite and Nitrate Distributions in Oceanic Oxygen Minimum Zones. **29:** , doi:10.1016/0198-0149(82)90031-0.

Bohlke, J. K., S. J. Mroczkowski and T. B. Coplen. 2003. Oxygen isotopes in nitrate: new reference materials for O-18 : O-17 : O-16 measurements and observations on nitrate-water equilibration. **17:** , doi:10.1002/rcm.1123.

Brandes, J. A. and A. H. Devol. 2002. A global marine-fixed nitrogen isotopic budget: Implications for Holocene nitrogen cycling. Global Biogeochem. Cycles. **16:** 1120, doi:10.1029/2001GB001856.

Brandhorst, W. 1959. Nitrification and denitrification in the Eastern Tropical North Pacific. **25:** 2-20.

Broenkow, W. W. 1965. The distribution of nutrients in the Costa Rica Dome in the eastern tropical Pacific Ocean. **10:** 40-52.

Buchwald, C., A. E. Santoro, M. R. McIlvin and K. L. Casciotti. 2012. Oxygen isotopic composition of nitrate and nitrite produced by nitrifying cocultures in and natural marine assemblages. **57:** 1361-1375.

Buchwald, C. and K. L. Casciotti. 2010. Oxygen isotopic fractionation and exchange during bacterial nitrite oxidation. Limnol. Oceanogr. **55:** 1064-1074, doi:10.4319/lo.2010.55.3.1064.

Casciotti, K. L. and M. R. McIlvin. 2007. Isotopic analyses of nitrate and nitrite from reference mixtures and application to Eastern Tropical North Pacific waters. Mar. Chem. **107:** 184-201, doi:10.1016/j.marchem.2007.06.021.

Casciotti, K. L., D. M. Sigman, M. G. Hastings, J. K. Bohlke and A. Hilkert. 2002. Measurement of the oxygen isotopic composition of nitrate in seawater and freshwater using the denitrifier method. Anal. Chem. **74:** 4905-4912, doi:10.1021/ac020113w.

Casciotti, K. L. 2009. Inverse kinetic isotope fractionation during bacterial nitrite oxidation. Geochim. Cosmochim. Acta. **73:** 2061-2076, doi:10.1016/j.gca.2008.12.022.

Casciotti, K. L., J. K. Boehlke, M. R. McIlvin, S. J. Mroczkowski and J. E. Hannon. 2007a. Oxygen isotopes in nitrite: Analysis, calibration, and equilibration. Anal. Chem. **79:** 2427-2436, doi:10.1021/ac061598h.

Casciotti, K. L., J. K. Boehlke, M. R. McIlvin, S. J. Mroczkowski and J. E. Hannon. 2007b. Oxygen isotopes in nitrite: Analysis, calibration, and equilibration. Anal. Chem. **79:** 2427-2436, doi:10.1021/ac061598h.

Casciotti, K. L., M. McIlvin and C. Buchwald. 2010. Oxygen isotopic exchange and fractionation during bacterial ammonia oxidation. Limnol. Oceanogr. **55:** 753-762, doi:10.4319/lo.2009.55.2.0753.

Codispoti, L. A., J. A. Brandes, J. P. Christensen, A. H. Devol, S. W. A. Naqvi, H. W. Paerl and T. Yoshinari. 2001. The oceanic fixed nitrogen and nitrous oxide budgets: Moving targets as we enter the anthropocene? **65:** .

Collos, Y. 1998. Nitrate uptake, nitrite release and uptake, and new production estimates. **171:** .

Deutsch, C., D. M. Sigman, R. C. Thunell, A. N. Meckler and G. H. Haug. 2004. Isotopic constraints on glacial/interglacial changes in the oceanic nitrogen budget. Global Biogeochem. Cycles. **18:** GB4012, doi:10.1029/2003GB002189.

Dore, J. E. and D. M. Karl. 1996. Nitrification in the euphotic zone as a source for nitrite, nitrate, and nitrous oxide at Station ALOHA. Limnol. Oceanogr. **41:** 1619-1628.

Francis, C. A., K. J. Roberts, J. M. Beman, A. E. Santoro and B. B. Oakley. 2005. Ubiquity and diversity of ammonia-oxidizing archaea in water columns and sediments of the ocean. Proc. Natl. Acad. Sci. U. S. A. **102:** 14683-14688, doi:10.1073/pnas.0506625102.

Franck, V. M., K. W. Bruland, D. A. Hutchins and M. A. Brzezinski. 2003. Iron and zinc effects on silicic acid and nitrate uptake kinetics in three high-nutrient, low-chlorophyll (HNLC) regions. **252:** , doi:10.3354/meps252015.

Fuessel, J., P. Lam, G. Lavik, M. M. Jensen, M. Holtappels, M. Guenter and M. M. M. Kuypers. 2012. Nitrite oxidation in the Namibian oxygen minimum zone. **6:** , doi:10.1038/ismej.2011.178.

Granger, J., D. M. Sigman, J. A. Needoba and P. J. Harrison. 2004. Coupled nitrogen and oxygen isotope fractionation of nitrate during assimilation by cultures of marine phytoplankton. Limnol. Oceanogr. **49:** 1763-1773.

Granger, J. and D. M. Sigman. 2009. Removal of nitrite with sulfamic acid for nitrate N and O isotope analysis with the denitrifier method. **23:** , doi:10.1002/rcm.4307.

Granger, J., D. M. Sigman, M. F. Lehmann and P. D. Tortell. 2008. Nitrogen and oxygen isotope fractionation during dissimilatory nitrate reduction by denitrifying bacteria. Limnol. Oceanogr. **53:** 2533-2545, doi:10.4319/lo.2008.53.6.2533.

Gruber, N. and J. L. Sarmiento. 1997. Global patterns of marine nitrogen fixation and denitrification. Global Biogeochem. Cycles. **11:** , doi:10.1029/97GB00077.

Gruber, N. and J. N. Galloway. 2008. An Earth-system perspective of the global nitrogen cycle. Nature. **451:** , doi:10.1038/nature06592.

Guerrero, M. A. and R. D. Jones. 1996. Photoinhibition of marine nitrifying bacteria .1. Wavelength-dependent response. **141:** , doi:10.3354/meps141183.

Holmes, R. M., A. Aminot, R. Kerouel, B. A. Hooker and B. J. Peterson. 1999. A simple and precise method for measuring ammonium in marine and freshwater ecosystems. Can. J. Fish. Aquat. Sci. **56:** , doi:10.1139/cjfas-56-10-1801.

Hooper, A. B. and K. R. Terry. 1974. Photoinactivation of Ammonia Oxidation in Nitrosomonas. J. Bacteriol. **119:** .

Kiefer, D. A., R. J. Olson and O. Holmhansen. 1976. Another Look at Nitrite and Chlorophyll Maxima in Central North Pacific. Deep-Sea Res. **23:** , doi:10.1016/0011-7471(76)90895-0.

Lam, P., M. M. Jensen, A. Kock, K. A. Lettmann, Y. Plancherel, G. Lavik, H. W. Bange and M. M. M. Kuypers. 2011. Origin and fate of the secondary nitrite maximum in the Arabian Sea. **8:** , doi:10.5194/bg-8-1565-2011.

Lam, P., G. Lavik, M. M. Jensen, J. van de Vossenberg, M. Schmid, D. Woebken, D. Gutierrez, R. Amann, M. S. M. Jetten and M. M. M. Kuypers. 2009. Revising the nitrogen cycle in the Peruvian oxygen minimum zone. Proc. Natl. Acad. Sci. U. S. A. **106:** , doi:10.1073/pnas.0812444106.

Lipschultz, F., S. C. Wofsy, B. B. Ward, L. A. Codispoti, G. Friedrich and J. W. Elkins. 1990. Bacterial Transformations of Inorganic Nitrogen in the Oxygen-Deficient Waters of the Eastern Tropical South-Pacific Ocean. **37:** , doi:10.1016/0198-0149(90)90060-9.

Lomas, M. W. and F. Lipschultz. 2006. Forming the primary nitrite maximum: Nitrifiers or phytoplankton? Limnol. Oceanogr. **51:** 2453-2467.

Mackey, K. R. M., L. Bristow, D. R. Parks, M. A. Altabet, A. F. Post and A. Paytan. 2011. The influence of light on nitrogen cycling and the primary nitrite maximum in a seasonally stratified sea. Prog. Oceanogr. **91:** , doi:10.1016/j.pocean.2011.09.001.

McIlvin, M. R. and M. A. Altabet. 2005. Chemical conversion of nitrate and nitrite to nitrous oxide for nitrogen and oxygen isotopic analysis in freshwater and seawater. Anal. Chem. **77:** 5589-5595, doi:10.1021/ac050528s.

McIlvin, M. R. and K. L. Casciotti. 2011. Technical Updates to the Bacterial Method for Nitrate Isotopic Analyses. Anal. Chem. **83:** , doi:10.1021/ac1028984.

Merbt, S. N., D. A. Stahl, E. O. Casamayor, E. Marti, G. W. Nicol and J. I. Prosser. 2012. Differential photoinhibition of bacterial and archaeal ammonia oxidation. FEMS Microbiol. Lett. **327:** , doi:10.1111/j.1574-6968.2011.02457.x.

Milligan, A. J. and P. J. Harrison. 2000. Effects of non-steady-state iron limitation on nitrogen assimilatory enzymes in the marine diatom Thalassiosira weissflogii (Bacillariophyceae). J. Phycol. **36:** , doi:10.1046/j.1529-8817.2000.99013.x.

Mincer, T. J., M. J. Church, L. T. Taylor, C. Preston, D. M. Kar and E. F. DeLong. 2007. Quantitative distribution of presumptive archaeal and bacterial nitrifiers in Monterey Bay

and the North Pacific Subtropical Gyre. Environ. Microbiol. **9:** , doi:10.1111/j.1462-2920.2007.01239.x.

Olson, R. J. 1981. Differential Photoinhibition of Marine Nitrifying Bacteria - a Possible Mechanism for the Formation of the Primary Nitrite Maximum. J. Mar. Res. **39:** .

Rotthauwe, J. H., K. P. Witzel and W. Liesack. 1997. The ammonia monooxygenase structural gene amoA as a functional marker: Molecular fine-scale analysis of natural ammonia-oxidizing populations. Appl. Environ. Microbiol. **63:** .

Saito, M. A., G. Rocap and J. W. Moffett. 2005. Production of cobalt binding ligands in a Synechococcus feature at the Costa Rica upwelling dome. Limnol. Oceanogr. **50:** .

Santoro, A. E., K. L. Casciotti and C. A. Francis. 2010. Activity, abundance and diversity of nitrifying archaea and bacteria in the central California Current. Environ. Microbiol. **12:** 1989-2006, doi:10.1111/j.1462-2920.2010.02205.x.

Sigman, D. M., K. L. Casciotti, M. Andreani, C. Barford, M. Galanter and J. K. Bohlke. 2001. A bacterial method for the nitrogen isotopic analysis of nitrate in seawater and freshwater. Anal. Chem. **73:** , doi:10.1021/ac010088e.

Sigman, D. M., J. Granger, P. J. DiFiore, M. M. Lehmann, R. Ho, G. Cane and A. van Geen. 2005. Coupled nitrogen and oxygen isotope measurements of nitrate along the eastern North Pacific margin. Global Biogeochem. Cycles. **19:** GB4022, doi:10.1029/2005GB002458.

Strickland, J. D. H. and Parsons T. R. 1972. A practical handbook of seawater analysis. **167:** 1-310.

Thomas, W. H. 1966. Surface Nitrogenous Nutrients and Phytoplankton in Northeastern Tropical Pacific Ocean. Limnol. Oceanogr. **11:** .

Vaccaro, R. and J. Ryther. 1960. Marine phytoplankton and the distribution of nitrite in the sea. **25:** 260-271.

Wada, E. and A. Hattori. 1971. Nitrite Metabolism in Euphotic Layer of Central North Pacific Ocean. Limnol. Oceanogr. **16:** 766-772.

Ward, B. B., R. J. Olson and M. J. Perry. 1982. Microbial Nitrification Rates in the Primary Nitrite Maximum Off Southern-California. **29:** , doi:10.1016/0198-0149(82)90112-1.

Waser, N. A. D., P. J. Harrison, B. Nielsen, S. E. Calvert and D. H. Turpin. 1998. Nitrogen isotope fractionation during the uptake and assimilation of nitrate, nitrite, ammonium, and urea by a marine diatom. Limnol. Oceanogr. **43:** 215-224.

Wyrtki, K. 1962. The Oxygen Minima in Relation to Ocean Circulation. Deep-Sea Res. **9:** , doi:10.1016/0011-7471(62)90243-7.

Wyrtki, K. 1964. Upwelling in the Costa Rica Dome. **63:** 355-372.

Figures

Figure 1. Nitrite and nitrate cycling in the oxic and anoxic water column

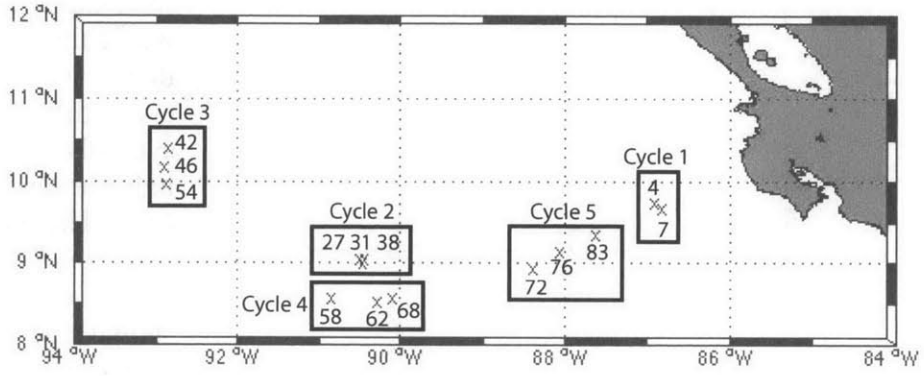

Figure 2. Map of cycle and cast locations during the cruise MV1008

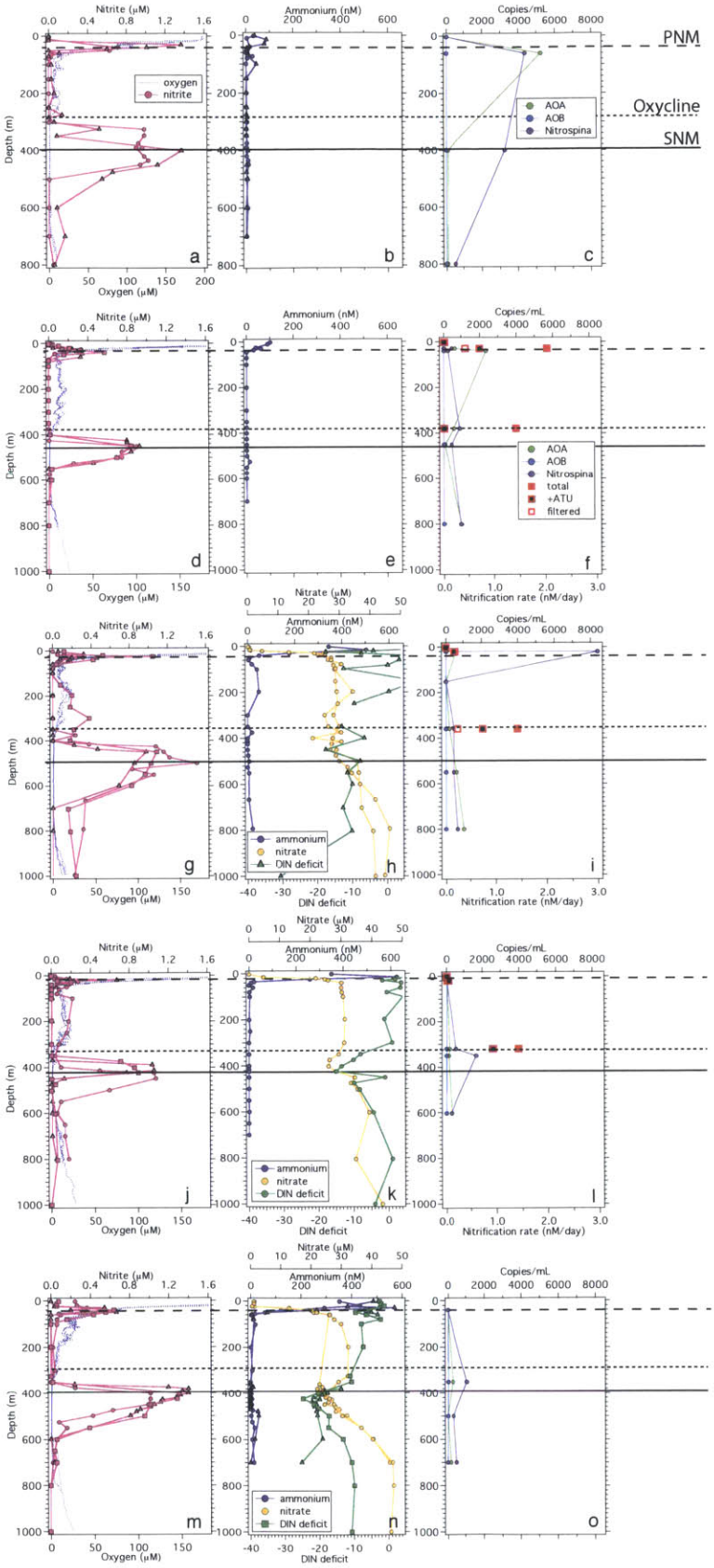

Figure 3. Oxygen and nitrite concentrations (a,d,g,j,m), ammonium, nitrate and DIN deficits (b,e,h,k,n). In cases where there was more than one cast per cycle, different symbols were used to indicate separate casts. The *amoA* and *Nitrospina* 16S rRNA gene abundance are shown with the nitrification rates at three depths during cycles 2, 3 and 4 (c,f,i,l,o). The different nitrification rate symbols indicate the three types of experiments: uninhibited whole water (filled square), ATU treatment (black filled square) and a filtered control (open square). The horizontal lines indicate where the PNM (big dash), oxycline (small dash), and SNM (solid) are located. Each row indicates a different cycle; cycle 1 (a,b,c), cycle 2 (d,e,f), cycle 3 (g,h,i), cycle 4 (j,k,l) and cycle 5 (m,n,o).

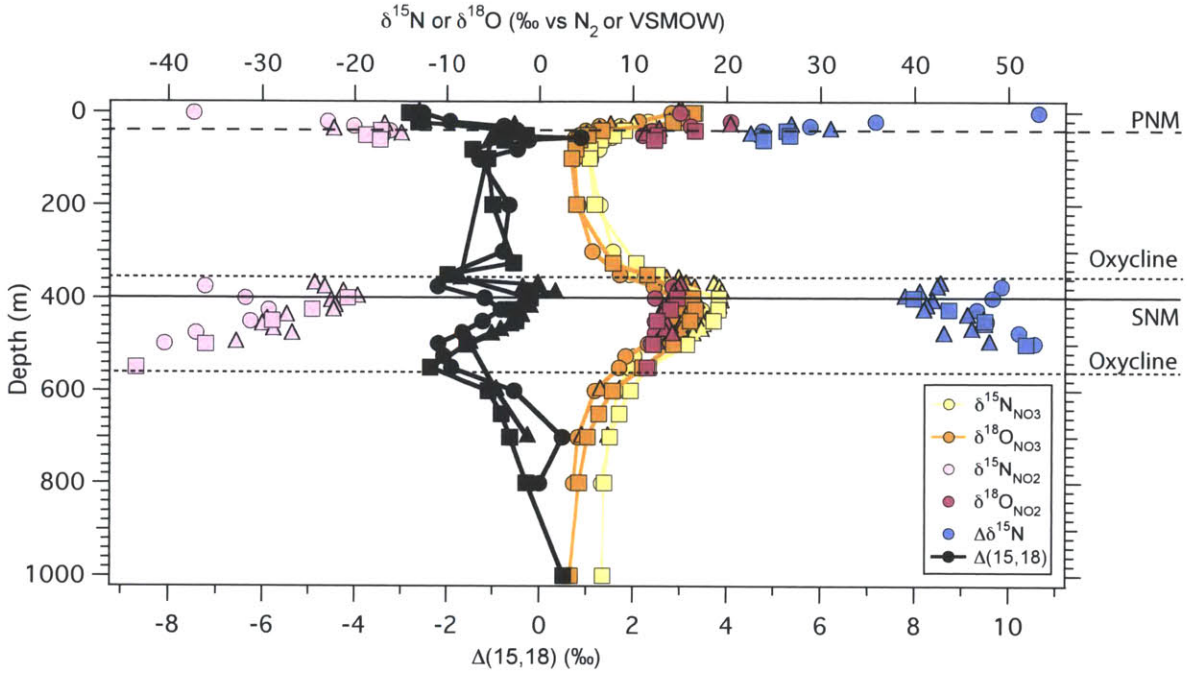

Figure 4. Isotope profiles of nitrite ($\delta^{15}N_{NO2}$ and $\delta^{18}O_{NO2}$), nitrate ($\delta^{15}N_{NO3}$ and $\delta^{18}O_{NO3}$), $\Delta(15,18)$ and $\Delta\delta^{15}N_{NO2}$ from casts 72 (circle), 76 (square) and 83 (triangle) in cycle 5 in the CRD. Dashed line indicates the location of the PNM, dotted lines indicate the top and bottom oxycline and the solid line is the location of the SNM. Different symbols indicated different casts from the same station.

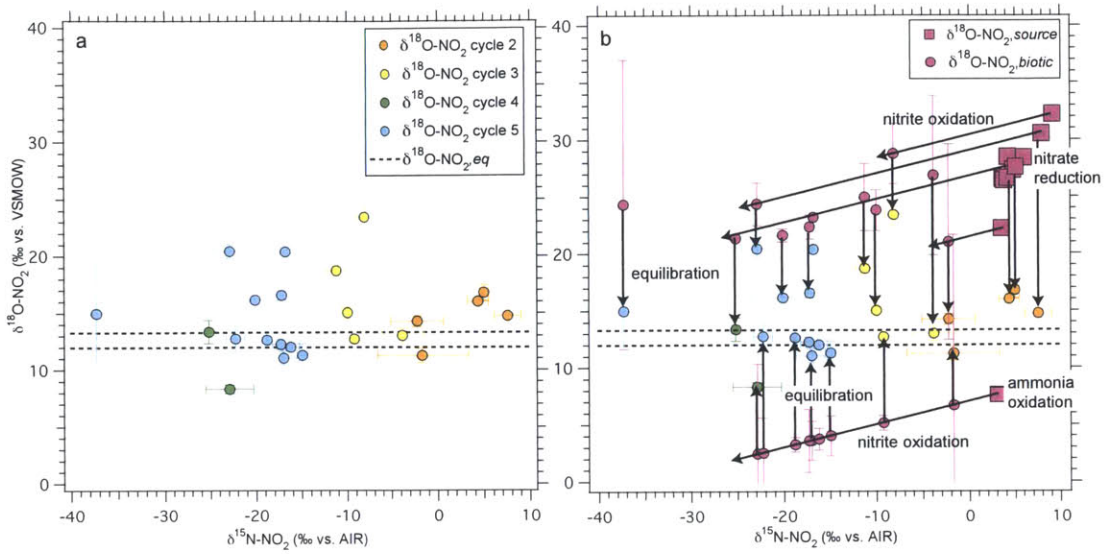

Figure 5. The $\delta^{18}O_{NO2}$ and $\delta^{15}N_{NO2}$ in nitrite samples from the PNM (a) and the possible sources and sinks to predict the pre-equilibrated nitrite $\delta^{18}O_{NO2,b}$, shown in pink circles in (b).

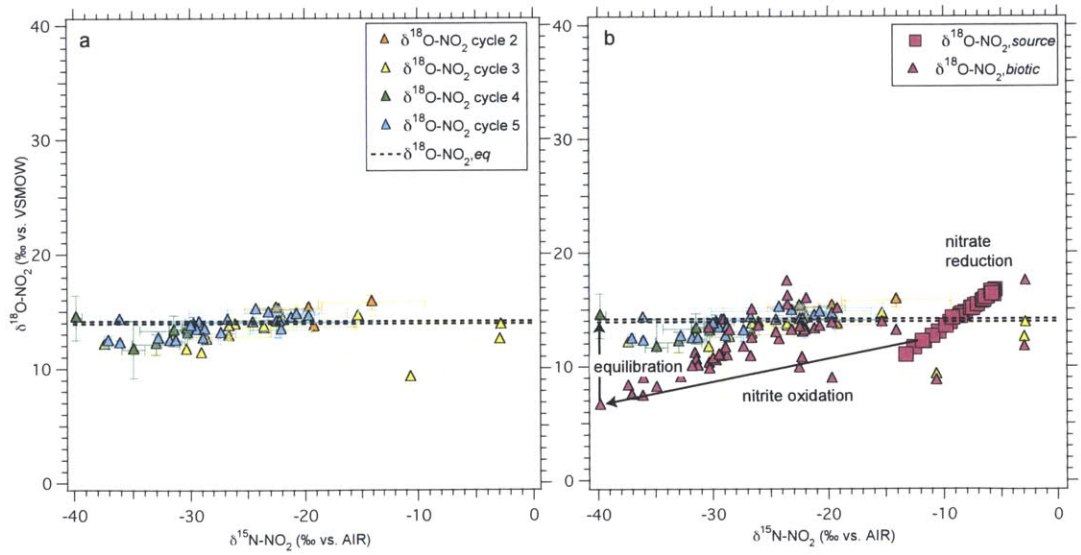

Figure 6. The $\delta^{18}O_{NO2}$ and $\delta^{15}N_{NO2}$ in nitrite samples from the SNM (a) and the possible sources and sinks to predict the pre-equilibrated nitrite $\delta^{18}O_{NO2,b}$, shown in pink triangles in (b).

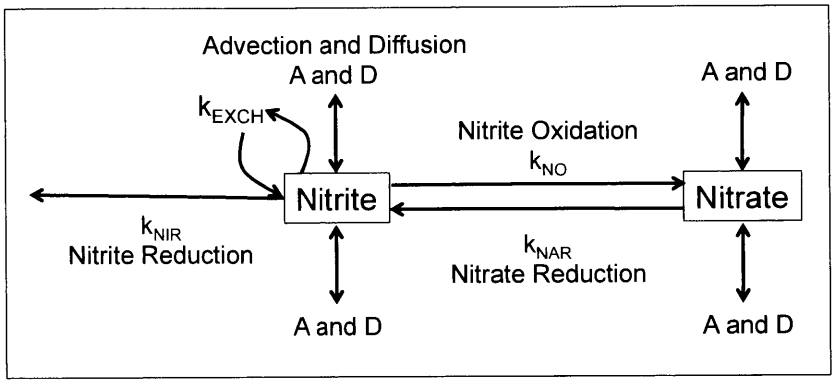

Figure 7. Depiction of system described by 1D model used to analyze the SNM. Main processes considered were nitrite oxidation (NO), nitrate reduction (NAR), nitrite reduction (NIR), advection (A) and diffusion (D). Biological processes were treated as first order rate equation with rate constants (k_{NO}, k_{NAR} and k_{NIR}).

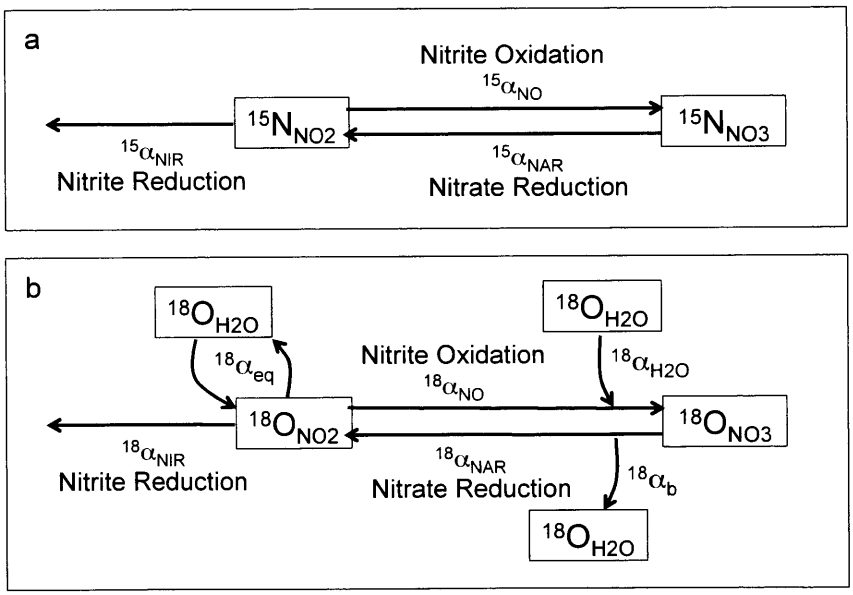

Figure 8. Depiction of the ^{15}N (a) and ^{18}O (b) isotope system described by 1D model used to analyze the SNM. Main processes considered were nitrite oxidation (NO), nitrate reduction (NAR), nitrite reduction (NIR), advection (A) and diffusion (D). Biological processes were treated as first order rate equation with rate constants (k_{NO}, k_{NAR} and k_{NIR}) with isotope fractionation factors ($^{15}\alpha_{NO}$, $^{18}\alpha_{NO}$, $^{15}\alpha_{NIR}$, $^{18}\alpha_{NIR}$, $^{15}\alpha_{NAR}$, $^{18}\alpha_{NAR}$, $^{18}\alpha_{H2O}$, $^{18}\alpha_b$ and $^{18}\alpha_{eq}$).

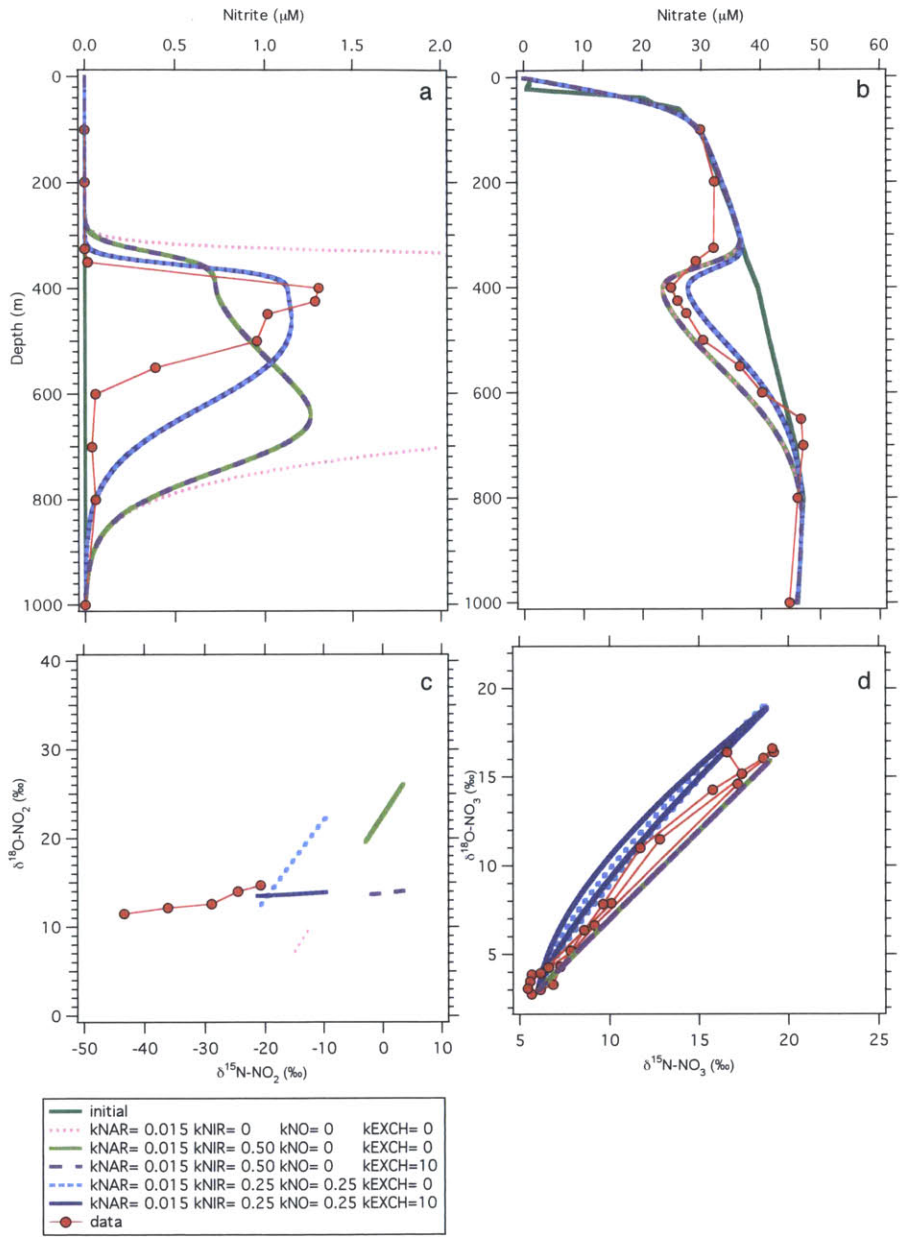

Figure 9. Nitrite profiles (a), nitrate profiles (b), nitrite isotopes (c) and nitrate isotopes (d) plotted for 5 different model runs with different rate constants used for nitrate reduction, nitrite reduction, nitrite oxidation and exchange (Table 2).

Chapter 6

Conclusions

Conclusions

Fixed nitrogen in the forms of NO_3^-, NO_2^-, and NH_4^+ are important ocean nutrients and can limit the amount of primary production throughout much of the ocean. The cycling of these nutrients, in particular the balance of inputs (nitrogen fixation, atmospheric deposition, and continental runoff) and outputs (denitrification and anammox), has been an area of research for decades (Gruber and Sarmiento 1997; Brandes et al. 1998; Codispoti et al. 2001). The delicate balance of nitrogen in the ocean determines the ocean's ability to act as a sink for CO_2 from the atmosphere and therefore, has important implications for controlling ongoing global climate change.

At the same time that scientists are beginning to understand how the fixed nitrogen budget in the ocean is mediated naturally, humans are changing the equation by creating vast amounts of fixed nitrogen to use as fertilizer in order to grow more food. The majority of this newly fixed nitrogen is then washed into our oceans (Gruber and Galloway 2008). It is estimated that humans have doubled the amount of fixed nitrogen that enters the ocean each year, and this will only increase as the earth's population increases (Gruber and Galloway 2008). It is important to understand the impact that this increased source of fixed nitrogen will have on the chemistry of the ocean and its ability to absorb CO_2 and thereby influencing our climate.

There are large areas of the ocean in which new nutrients are brought to the surface during natural upwelling processes. These nutrients stimulate the growth of phytoplankton, which die and sink through the water column. As these particles sink they are re-mineralized by bacteria that consume oxygen from the mid-water column. As waters age, the oxygen concentrations steadily decrease. In some regions, known as oxygen deficient zones (ODZs), oxygen concentrations in very old water can drop to levels insufficient to support aerobic respiration. These ODZs are hot spots for nitrogen removal since the process of converting nitrate to gaseous nitrogen occurs in the absence of oxygen. Understanding the mechanisms and control of this removal will help us predict the potential sinks for nitrogen in the ocean and can be used as analogue to anthropogenically induced oxygen deficiency.

Tracking the inputs and outputs of nitrogen in the ocean is a challenge. Previous studies have attempted to quantify the rates of addition and removal of nitrogen by conducting incubation experiments (Lam et al. 2011; Ward et al. 2009). These experiments have had many drawbacks, for example, it is nearly impossible to mimic oceanic conditions when removing seawater and placing it in a contained bottle. Specifically, in ODZs it is difficult to avoid oxygen contamination during sampling, which could cause drastically different rates of removal. Also, often these rates are patchy due to geographic and temporal heterogeneity and would require a much larger sampling effort in order to capture the full picture of what is going on. These limitations have led scientists to rely on stable isotopes. Isotopes are natural tracers, which record the history of processes that have previously occurred in the water column.

In this thesis, I have proven that nitrogen and oxygen isotopes in nitrite and nitrate are powerful tools in predicting what processes, including where and at what rates, are occurring in ODZs. This utility can only be realized by using the large body of research on the isotope systematics of each process involved.

Chapters 2 and 3 of this thesis provide the determination of the much needed isotope systematics for nitrification, which were previously unknown to isotope geochemists and oceanographers.

Chapter 4 presents the discovery of a unique property in nitrite oxygen isotope systematics, which can be used to interpret the sources sinks and age of nitrite in oceanic, terrestrial, and groundwater systems. Nitrite oxygen isotopes are now one of the few isotope systems that can quantify rates of processes from one static measurement.

Combining the findings from the three previous chapters, Chapter 5 provides the first example of the quantification of the relative rates of nitrate and nitrite removal from isotope profiles. A one-dimensional model was constructed that can predict the relative rates of nitrate and nitrite production and consumption to mimic the concentration and dual isotope ($\delta^{15}N$ and $\delta^{18}O$) of nitrite and nitrate profiles in a water column. The results of this model showed that, in addition to nitrate reduction and nitrite reduction removing fixed N, there was a large proportion of nitrite re-oxidation of up to 50% throughout the

ODZ. This means that the system will support more organic matter remineralization and CO_2 fixation that previously predicted, neglecting this recycling.

Future Research

Overall this thesis has provided a significant contribution to understanding how to use stable isotopes to interpret nitrogen cycling in the ocean. The second and third chapters measured the much needed oxygen isotope effects for nitrification. These values will be useful for future research including, creating a global fixed nitrogen budget using oxygen isotopes and interpreting the new tracer for coupled nitrate isotopes $\Delta(15,18)$. Providing a new fixed nitrogen budget using different tracer will add to the building debate on the balance of fixed nitrogen in the ocean.

The fourth chapter has provided the foundation for a new technique of analyzing nitrite isotopes to not only determine the sources and sinks, but also the age of nitrite. This technique can now easily be applied to samples from new locations, such as the PNM throughout the ocean and in the SNM other ODZs not examined within this thesis. Also, this technique was limited most by knowing the isotope effects for each nitrite transformation process. These isotope effects are needed to accurately predict the biotic end member ($\delta^{18}O_{NO2,b}$). Particularly, there should be future work measuring the isotope effects associated with nitrate reduction during nitrate assimilation and nitrite assimilation. The estimates for the isotope effects for nitrite assimilation assumed that the ^{15}N and ^{18}O were equal, although this has not been tested. Also, many of these isotope effects are limited to a few culture incubations, and could benefit measuring a wider variety of cultures, as well as natural population isotope effects.

Lastly, the fifth chapter has demonstrated how to use stable isotope profiles to predict rates of processes in an ODZ. The 1D model created can now be used in other ODZs, specifically to test whether same amount of nitrite re-oxidation is occurring in all ODZs. In addition to applying this model to other locations, there is still much more work that can be done to improve this model. Similarly to the fourth chapter, having a greater confidence in the isotope effects would increase the certainty in the model. Also,

future work in measuring the isotope effects of anammox may allow us to separate anammox from denitrification within the model. Lastly, one of the most surprising finding in this chapter was that nitrite re-oxidation was happening with in the ODZ, where there was no oxygen. Future research experimenting with the possibility of nitrite oxidizers using other electron acceptors, such as Fe (III) and Mn (IV), would help understand what they are doing in the anoxic water column.

This thesis has proved the utility of using stable isotope profiles of nitrite and nitrate to interpret rates of nitrogen cycling processes in the ocean, and has also uncovered unexpected processes stimulating new questions to be tested in the future.

References

Brandes, J. A., A. H. Devol, T. Yoshinari, D. A. Jayakumar and S. W. A. Naqvi. 1998. Isotopic composition of nitrate in the central Arabian Sea and eastern tropical North Pacific: A tracer for mixing and nitrogen cycles. Limnol. Oceanogr. **43:** 1680-1689.

Codispoti, L. A., J. A. Brandes, J. P. Christensen, A. H. Devol, S. W. A. Naqvi, H. W. Paerl and T. Yoshinari. 2001. The oceanic fixed nitrogen and nitrous oxide budgets: Moving targets as we enter the anthropocene? **65:** 85-105.

Gruber, N. and J. L. Sarmiento. 1997. Global patterns of marine nitrogen fixation and denitrification. Global Biogeochem. Cycles. **11:** 235-266, doi:10.1029/97GB00077.

Gruber, N. and J. N. Galloway. 2008. An Earth-system perspective of the global nitrogen cycle. Nature. **451:** 293-296, doi:10.1038/nature06592.

Lam, P., M. M. Jensen, A. Kock, K. A. Lettmann, Y. Plancherel, G. Lavik, H. W. Bange and M. M. M. Kuypers. 2011. Origin and fate of the secondary nitrite maximum in the Arabian Sea. **8:** 4752-4757, doi:10.5194/bg-8-1565-2011.

Ward, B. B., A. H. Devol, J. J. Rich, B. X. Chang, S. E. Bulow, H. Naik, A. Pratihary and A. Jayakumar. 2009. Denitrification as the dominant nitrogen loss process in the Arabian Sea. Nature. **461:** 78-82, doi:10.1038/nature08276.